

GALAXIES

Lecture 5-6

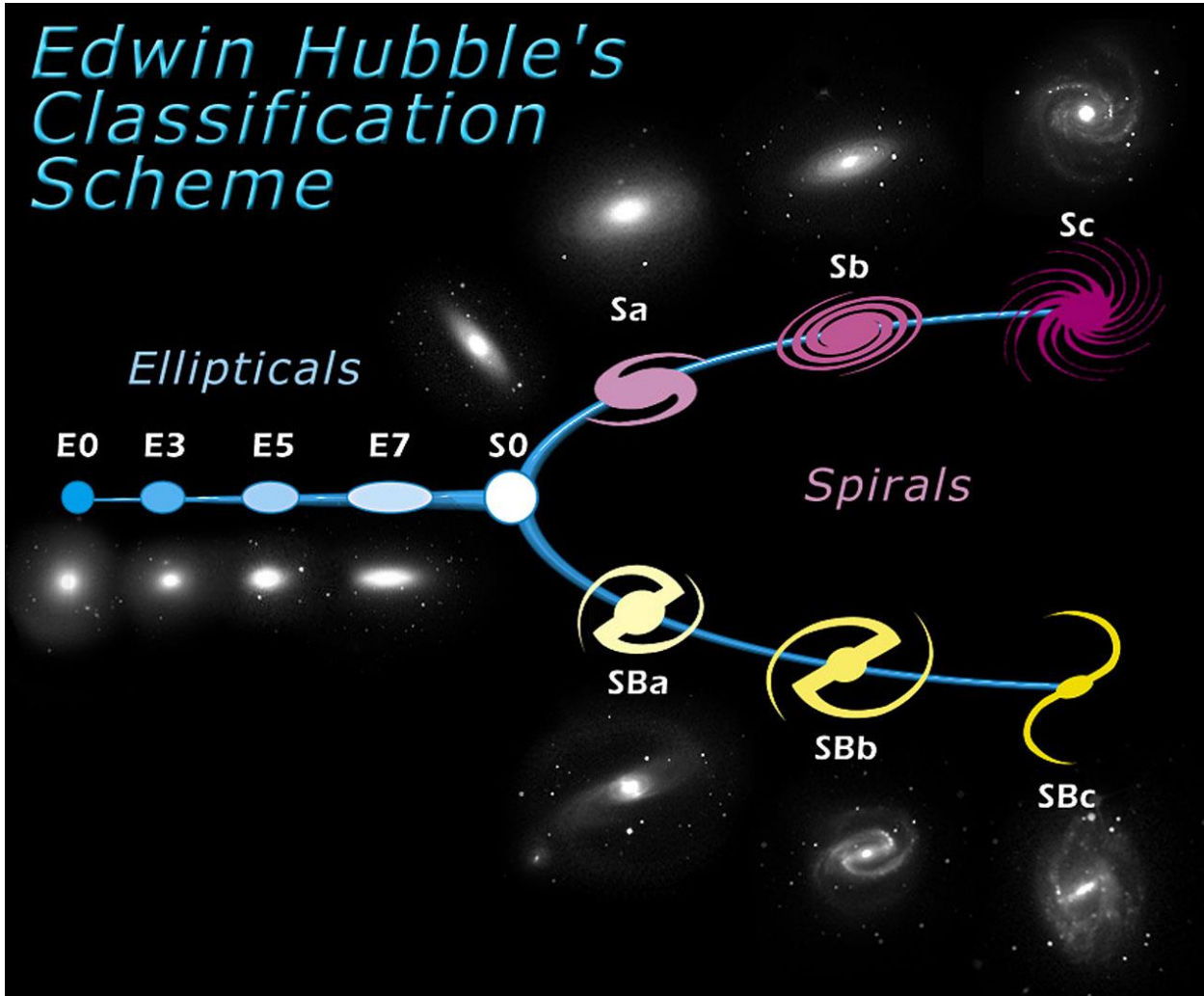
Ewa L. Łokas

Copernicus Center, Warsaw

Plan

1. Structure of galaxies: haloes and disks, circular velocities, NFW profile, exponential disk, Sersic profile
2. The Milky Way and galaxies of the Local Group
3. Orbits of stars in different potentials
4. Distribution functions, Jeans modeling, orbit-superposition models
5. Bars in galaxies: formation, evolution, orbital structure, dependence on environment
6. Spiral structure: geometry of spiral arms, formation scenarios
7. Interactions: tidal evolution and mergers, properties of merger remnants
8. Galaxy formation in cosmological context, cold and hot dark matter scenarios, top hat model, problems of theory on small scales

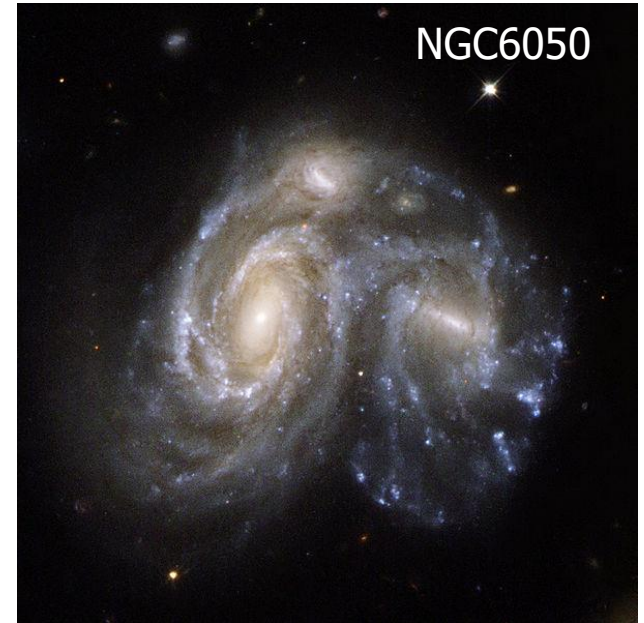
Morphological classification



Barred galaxies constitute a substantial fraction of spiral galaxies

Bars in galaxies

- Bars are quite common in the universe
- About 30% of spirals have strong bars
- The fraction of barred spirals increases to 50-70% if we count weak bars
- Bar fraction depends on environment



Dependence on type

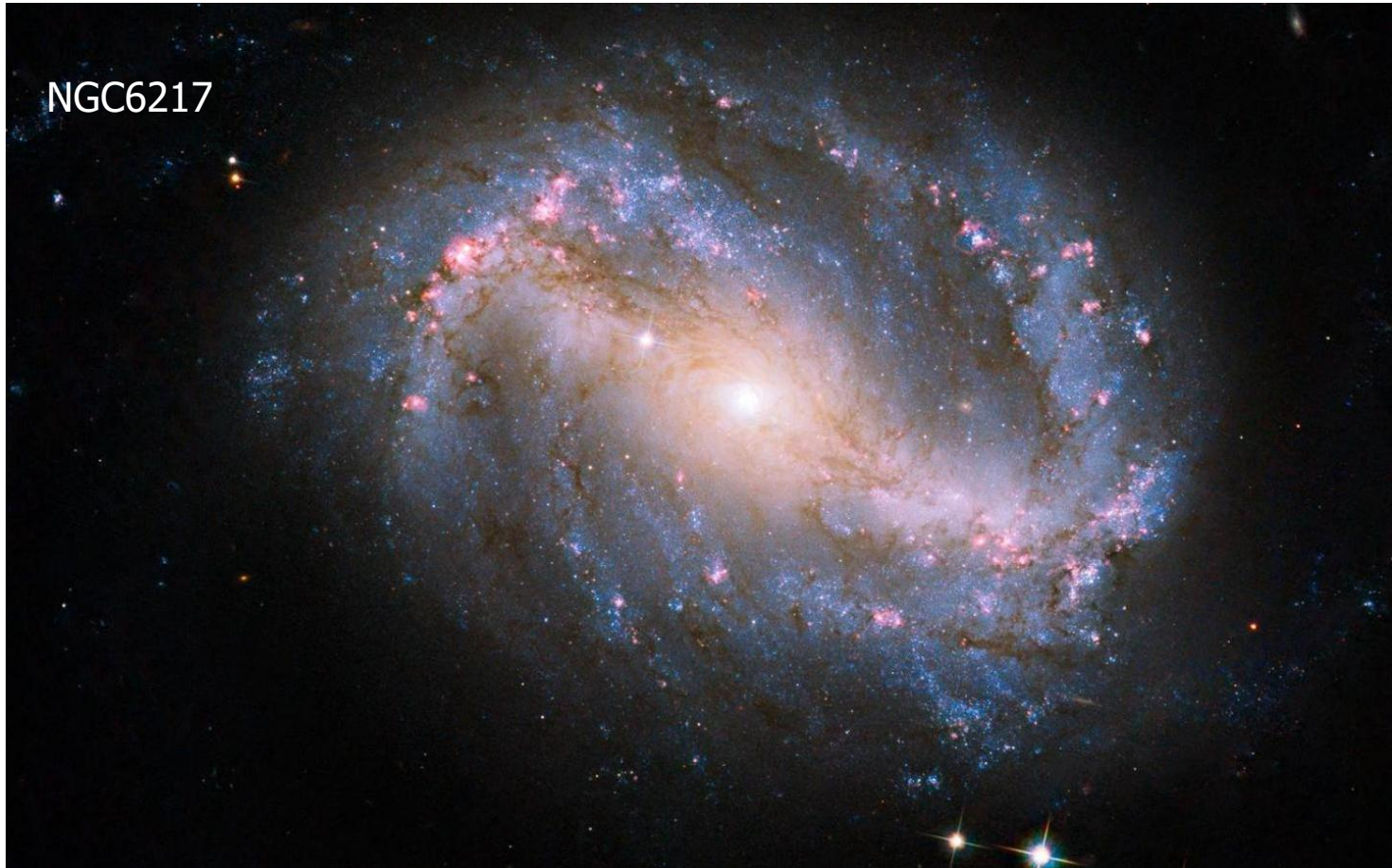
- Earlier type spirals SBab have flatter surface brightness distribution along the bar than later types SBcd which have exponential profiles
- The bars in earlier types are larger relative to the size of the disk, containing up to 1/3 of the total luminosity
- The isophotes of bars are not elliptical, they are intermediate between ellipses and rectangles
- Bars are rather elongated with axis ratios 2:1 or even 3:1

Examples of bars



Galaxy of type SBb in the Fornax cluster, at a distance of 18 Mpc, discovered in 1826 by James Dunlop

Examples of bars



Galaxy of type SBbc, actively forming stars, at a distance of 1.8 Mpc, discovered in 1797 by William Herschel

Examples of bars



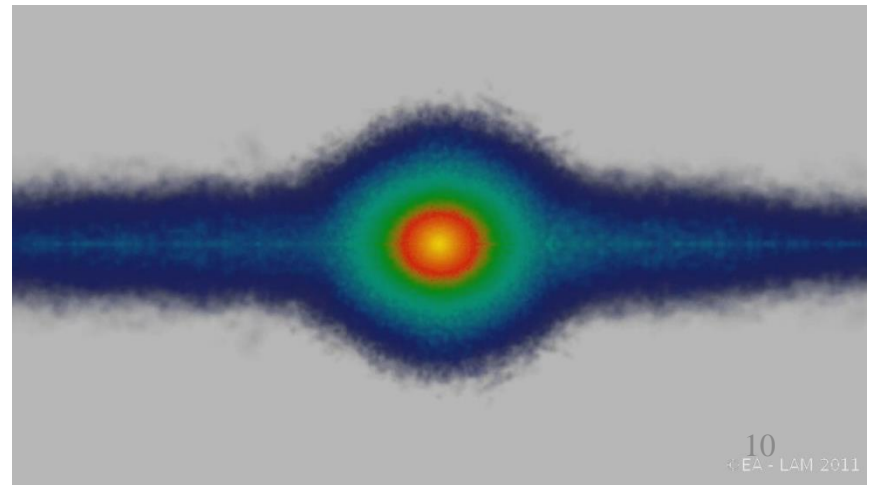
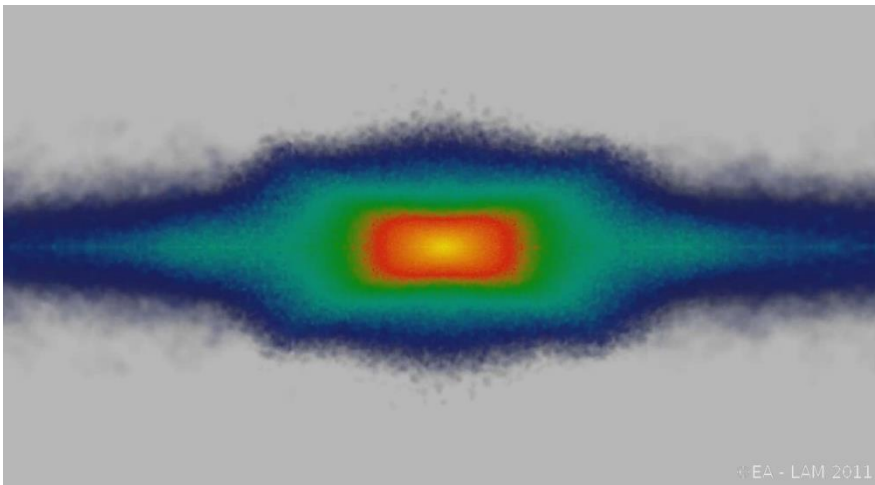
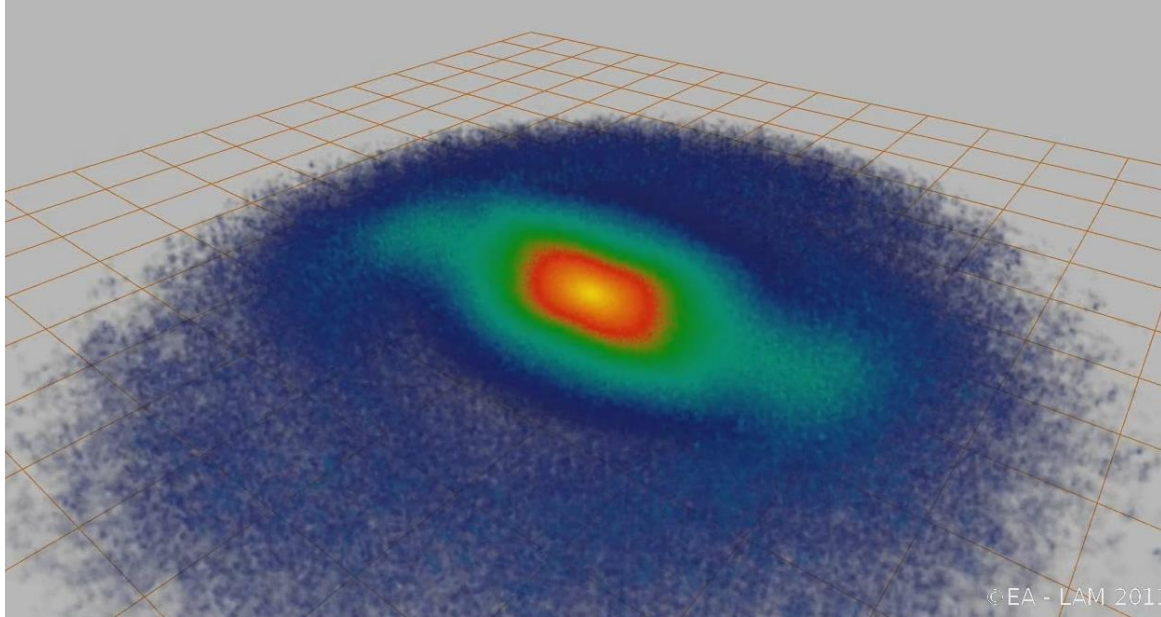
Galaxy of type SBc at a distance of 4.6 Mpc, in the galaxy group M83, discovered in 1752 by Nicolas de Lacaille

The bar in the Milky Way



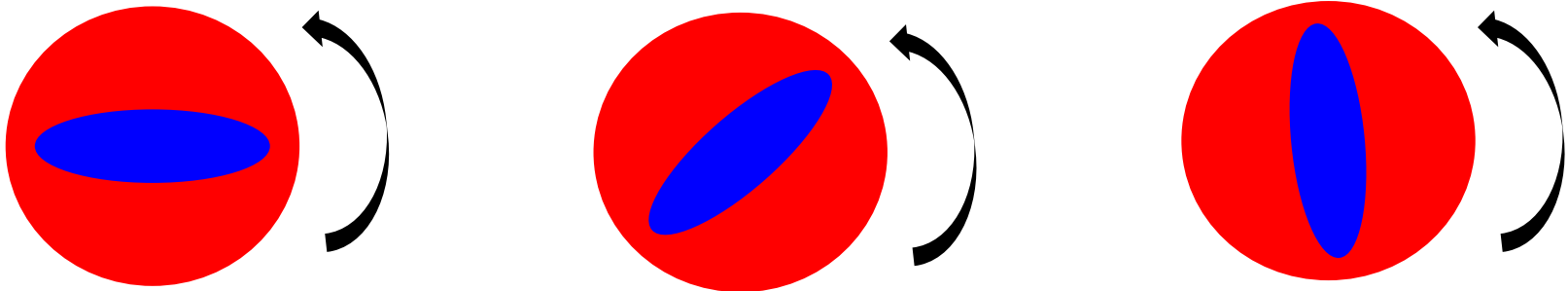
- First suggestions in 1950s
- First evidence in 1990s
- A bar was difficult to distinguish from the bulge
- Precise measurements of the distribution and kinematics of the stars were necessary

Simulations of the MW bar



Basic properties

- The bar constitutes a major non-axisymmetric component of the mass distribution
- The bar pattern tumbles rapidly about the axis normal to the disc plane
- The observed motions are consistent with material within the bar streaming along highly elongated orbits aligned with the rotating major axis



Description of motion

- We assume that the potential rotates steadily with a constant pattern speed Ω_p
- The equation of motion is then

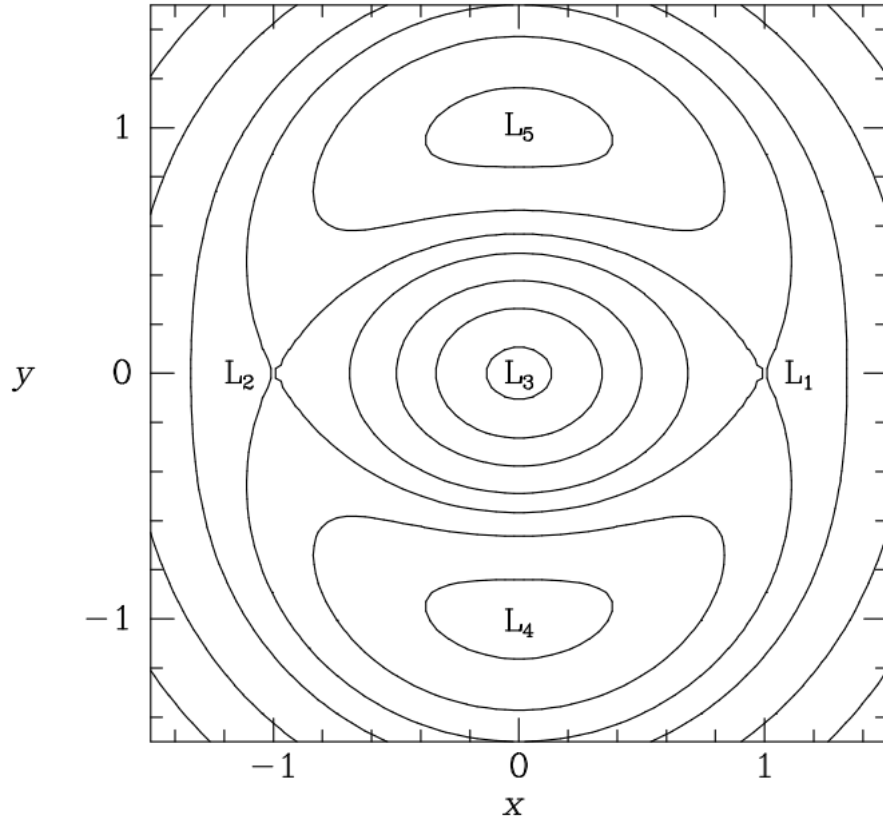
$$\ddot{\mathbf{r}} = -\nabla\Phi_{\text{eff}} - 2(\Omega_p \times \dot{\mathbf{r}}) \quad \text{Coriolis term}$$

- The effective potential is $\Phi_{\text{eff}} = \Phi - \frac{1}{2}\Omega_p^2 r^2$
- The energy and angular momentum of a star are not conserved but the Jacobi integral is conserved

$$E_J = \frac{1}{2}|\dot{\mathbf{r}}|^2 + \Phi_{\text{eff}}$$

- The zero velocity surface is at $\Phi_{\text{eff}} = E_J$

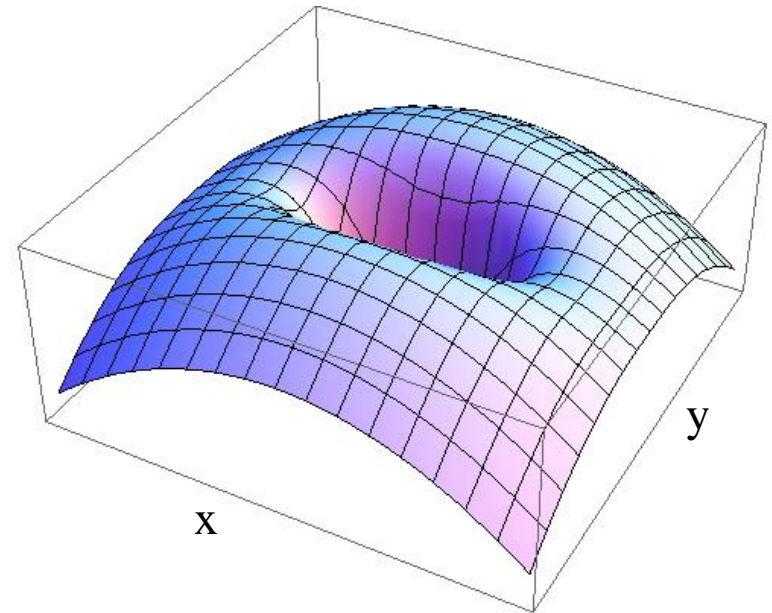
Effective potential



Lagrange points:

where $\nabla\Phi_{\text{eff}} = 0$

„volcano”, x – along the bar



L_3 - minimum

$L_{1,2}$ - saddle points

$L_{4,5}$ - maxima

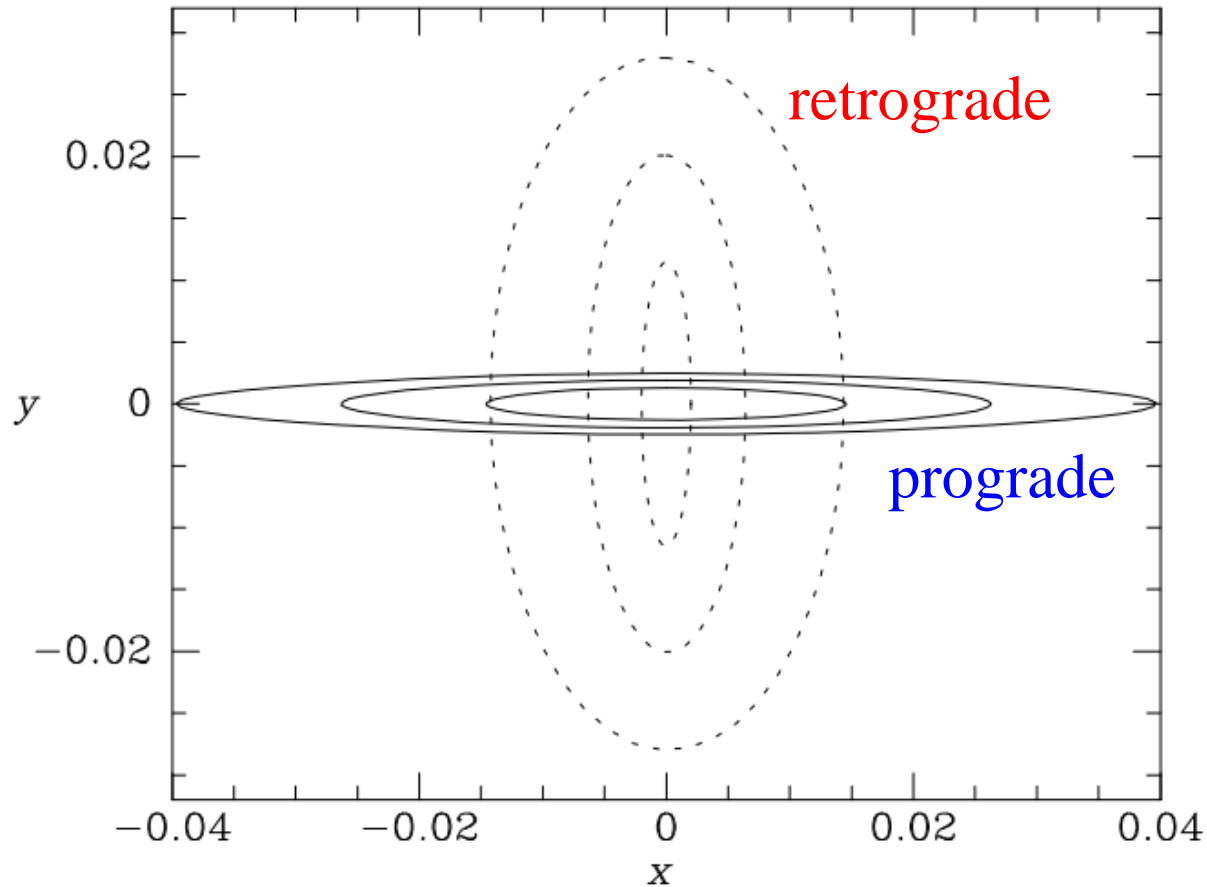
Lagrange points

- The central stationary point L_3 is a minimum and this region is dominated by gravity
- At points $L_{1,2,4,5}$ a star can travel on a circular orbit with $\Omega = \Omega_p$ so that it appears stationary in the rotating frame – it **corotates** with the potential
- Stars with $E_J < \Phi_{\text{eff}}$ at points $L_{1,2}$ are confined to remain either inside corotation or outside it
- Only stars with $E_J > \Phi_{\text{eff}}$ at the points $L_{4,5}$ (the absolute maxima of effective potential) are free energetically to explore all space

Motion near Lagrange points

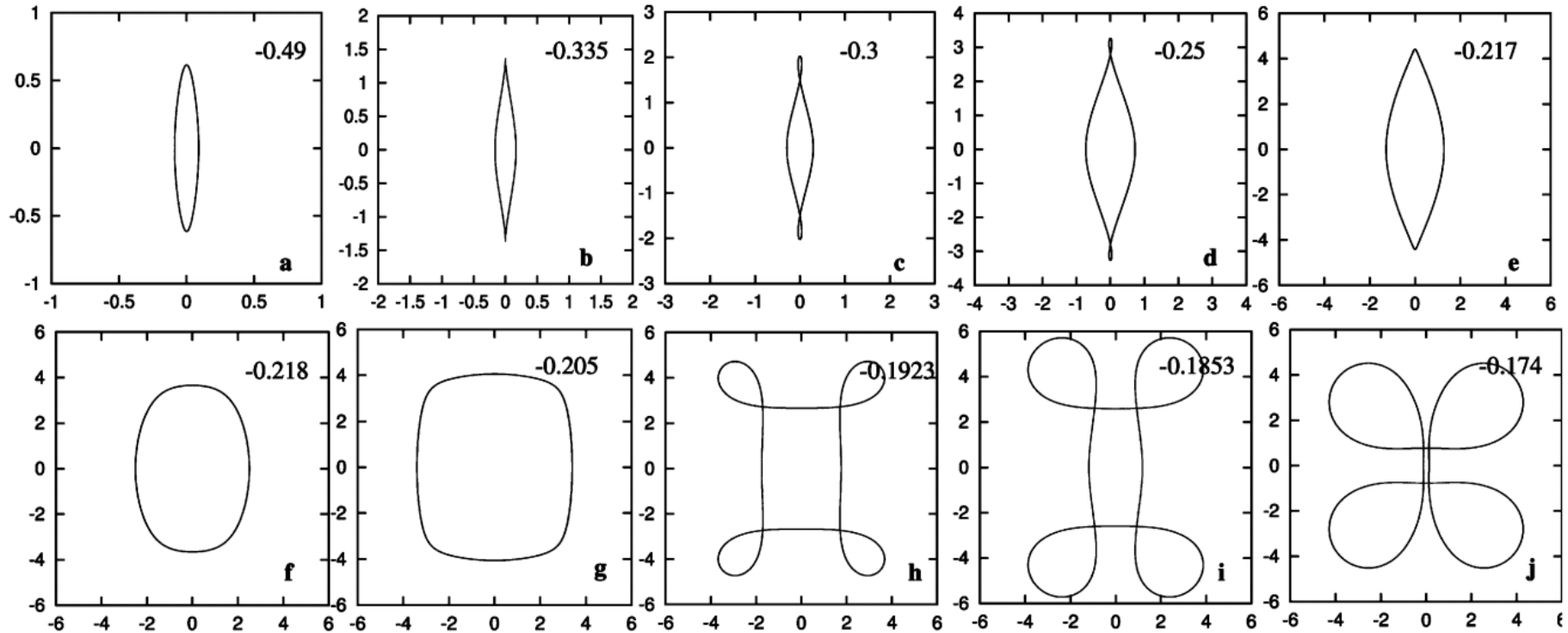
- The motion near Lagrange points can be studied by expanding the effective potential near the points
- Solutions of the equations of motion in this approximation allow us to determine if Lagrange points are stable (solutions oscillate) or not (solutions grow infinitely)
- The general conclusion is that the minimum point L_3 is always stable, the saddle points $L_{1,2}$ are always unstable while the stability of the maximum points $L_{4,5}$ depends on the details of the potential

Examples of orbits



Typical orbits near the L_3 point, prograde orbits are elongated along the bar (x axis)

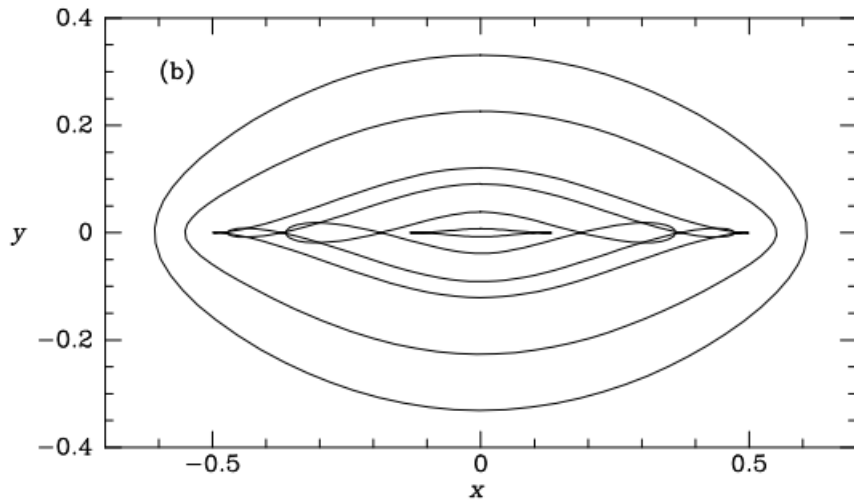
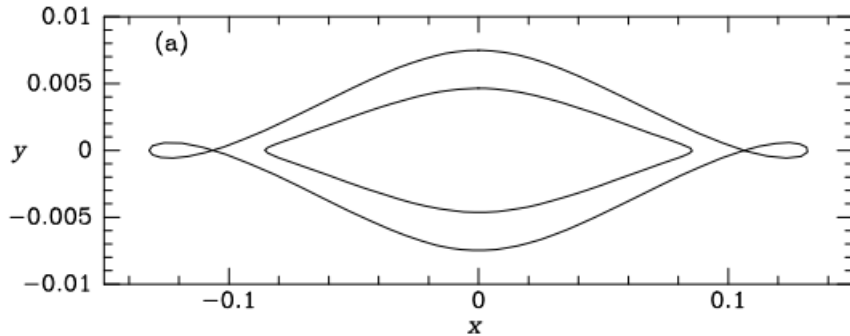
Orbits of different energies



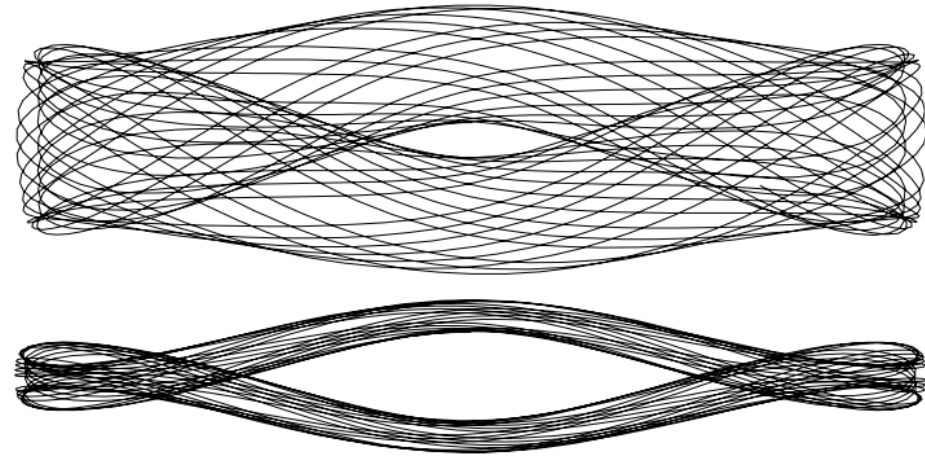
Orbits belonging to the family elongated with the potential

Skokos et al. 2002

Examples of orbits



Closed orbits of
different energies



Non-closed orbits

In general, the mass distribution has to be elongated as potential, so most orbits must keep stars close to the long axis

Weak bars

- If the bar is weak the orbits can be studied using the perturbative approach, similar to epicycle approximation

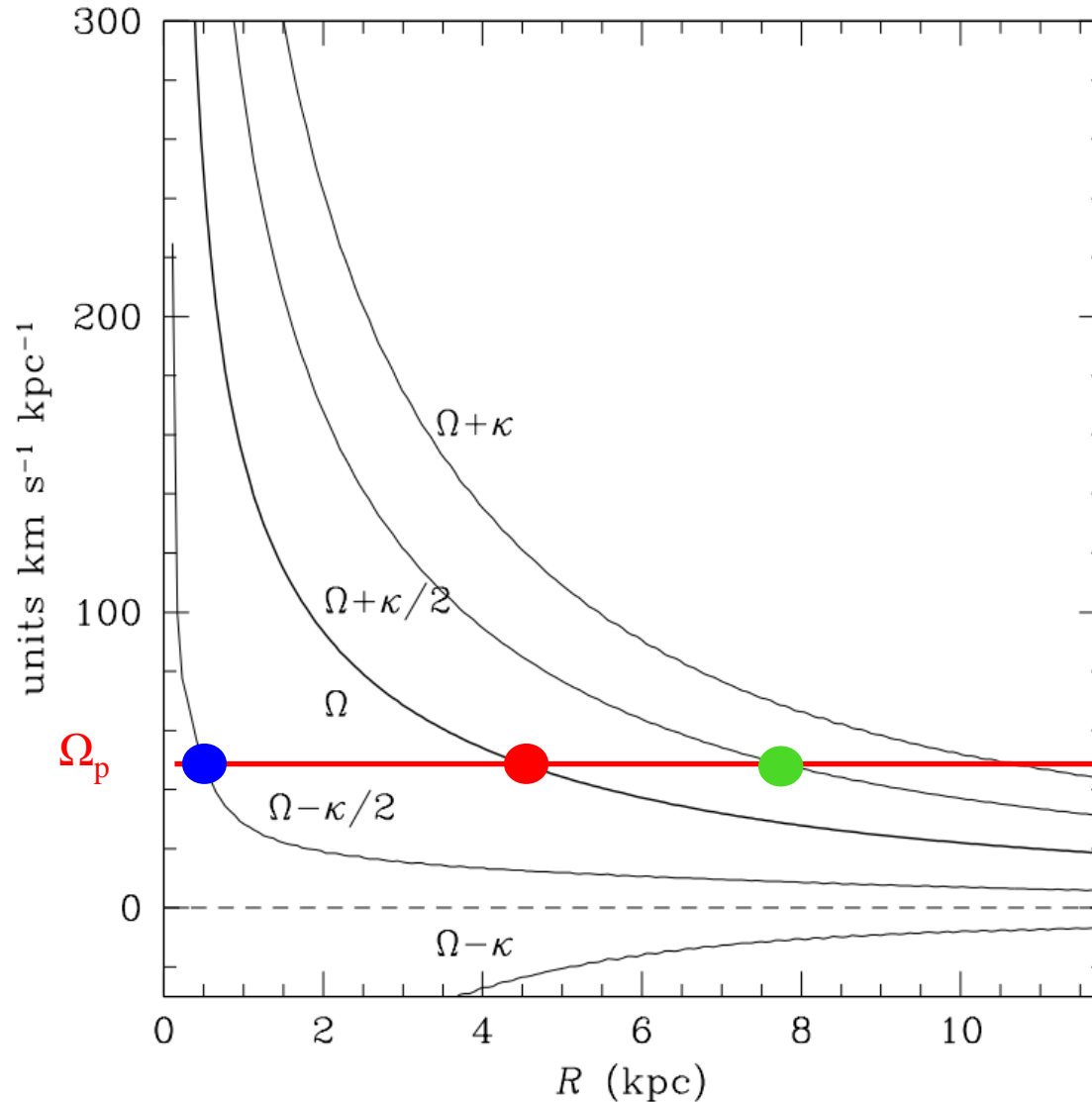
$$\Phi(R, \varphi) = \Phi_0(R) + \Phi_1(R, \varphi) \quad R(t) = R_0 + R_1(t)$$

- The solution for R_1 with $\Phi_1(R, \varphi) = \Phi_b(R) \cos(m\varphi)$ singular at

$$\Omega_0 = \Omega_b \quad \text{corotation resonance (circular frequency equal to pattern speed)}$$

$$m(\Omega_0 - \Omega_b) = \pm \kappa_0 \quad \text{Lindblad resonance (forcing frequency seen by a star coincides with its epicycle frequency)}$$

Lindblad resonances

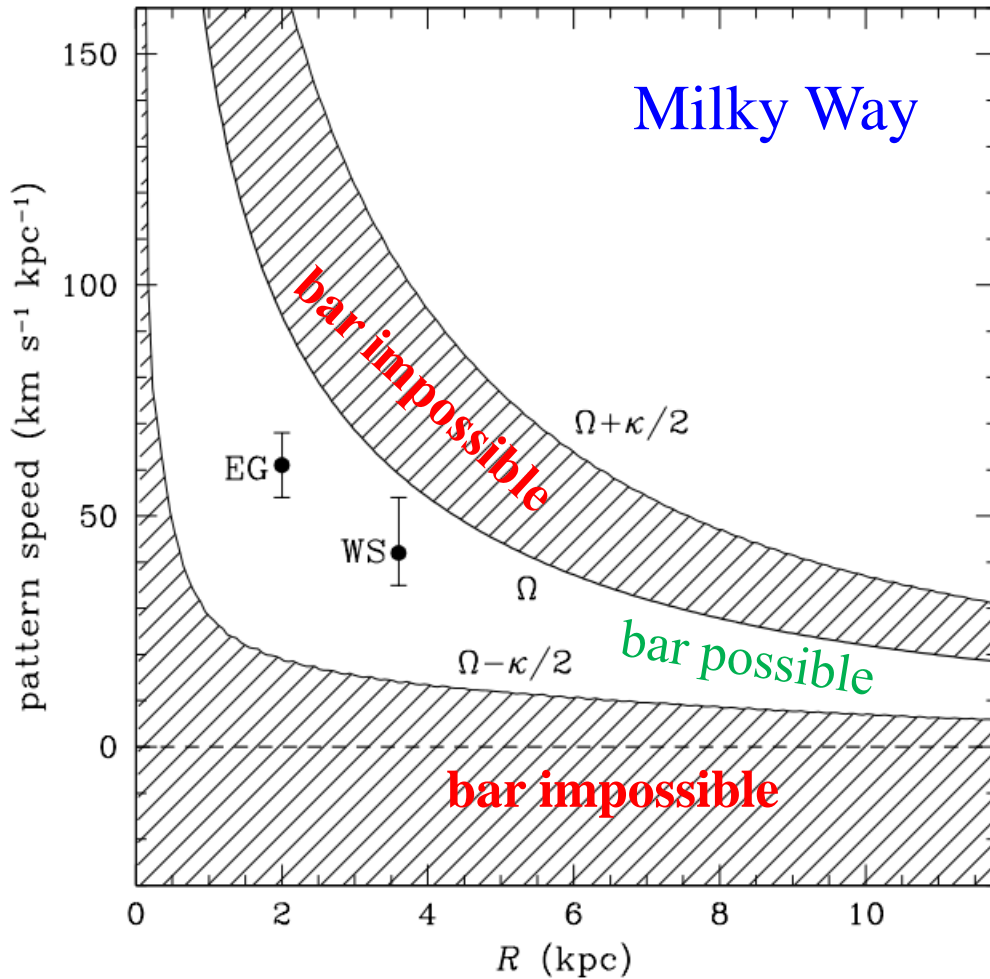


Frequencies for a typical galaxy potential, such as the one of the Milky Way

$m=2$ for a bar

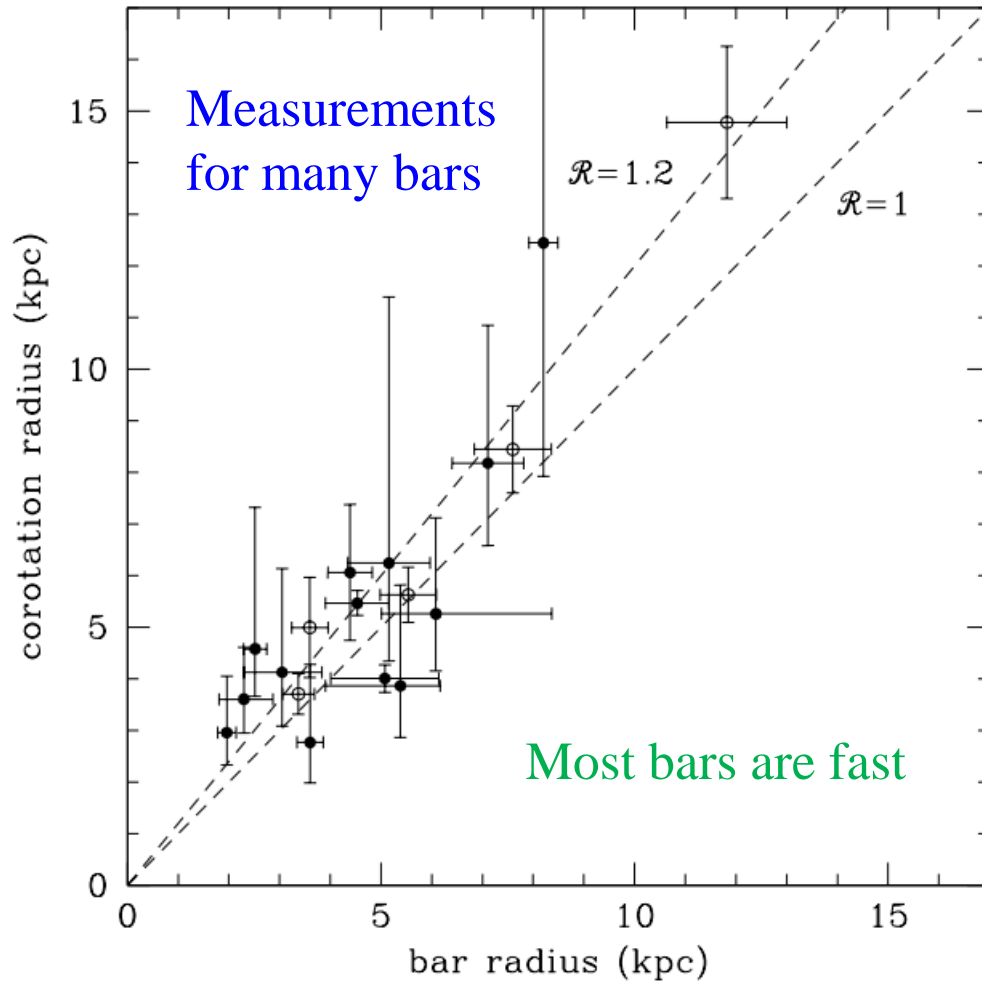
- inner Lindblad resonance
- corotation
- outer Lindblad resonance

Bar region



- The existence of a bar is only allowed between the inner Lindblad resonance and corotation
- Measurements confirm that the properties of the Milky Way bar fall in the allowed region

Speed of bars



The measure of the speed of the bar

$$R = R_{CR}/a_b$$

R_{CR} – corotation radius

a_b - bar semi-major axis

All bars have $R > 1$

$R \approx 1$ fast bars

$R \gg 1$ slow bars

Formation of bars

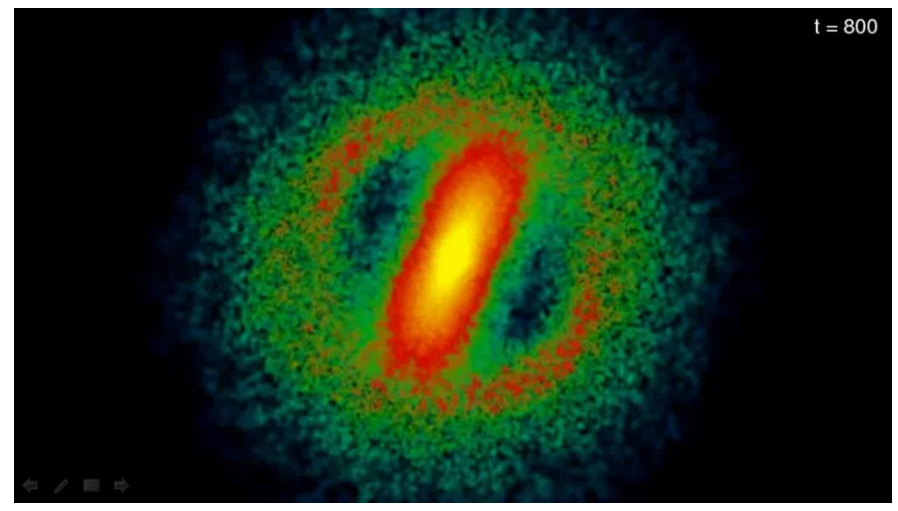
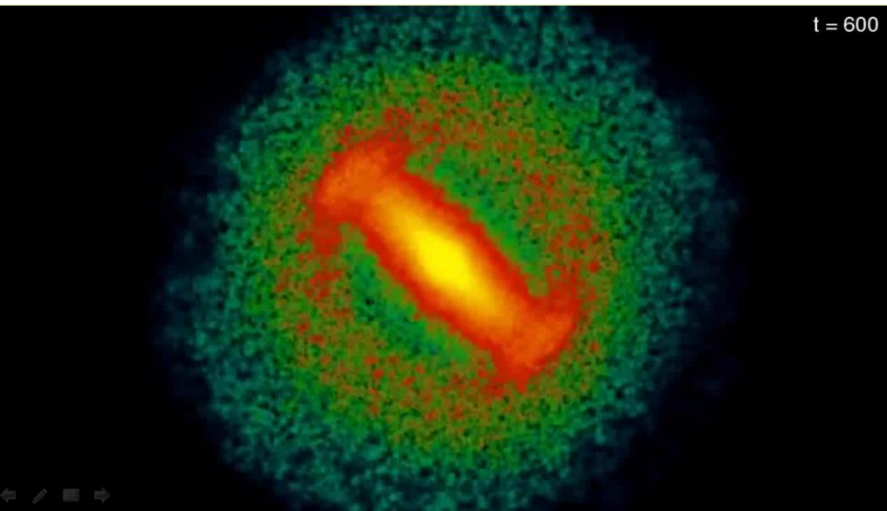
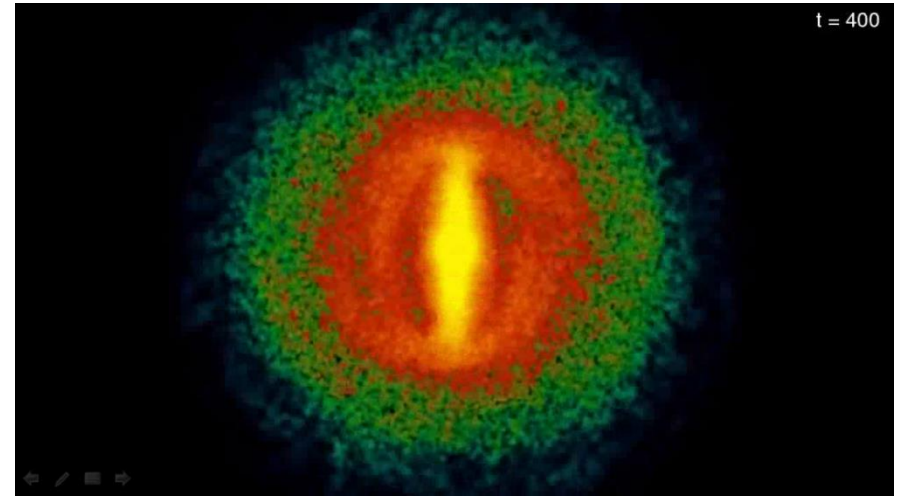
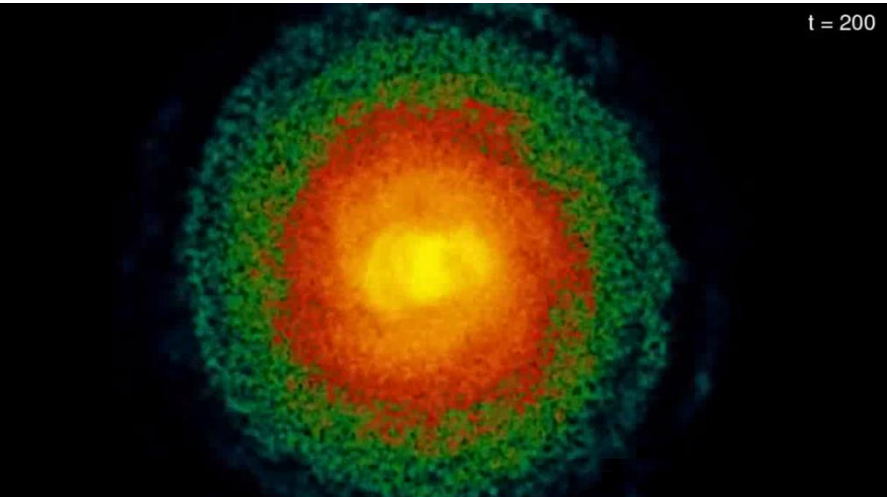
- The exact mechanism for the formation of a bar is not known
- Generally it is believed that the formation of the bar is related to the disk instability
- The disk is believed to be stable if it fulfills the Toomre stability criterion

$$Q \equiv \frac{\sigma_R \kappa}{3.36 G \Sigma} > 1$$

- Bars can also form as a result of interactions between galaxies

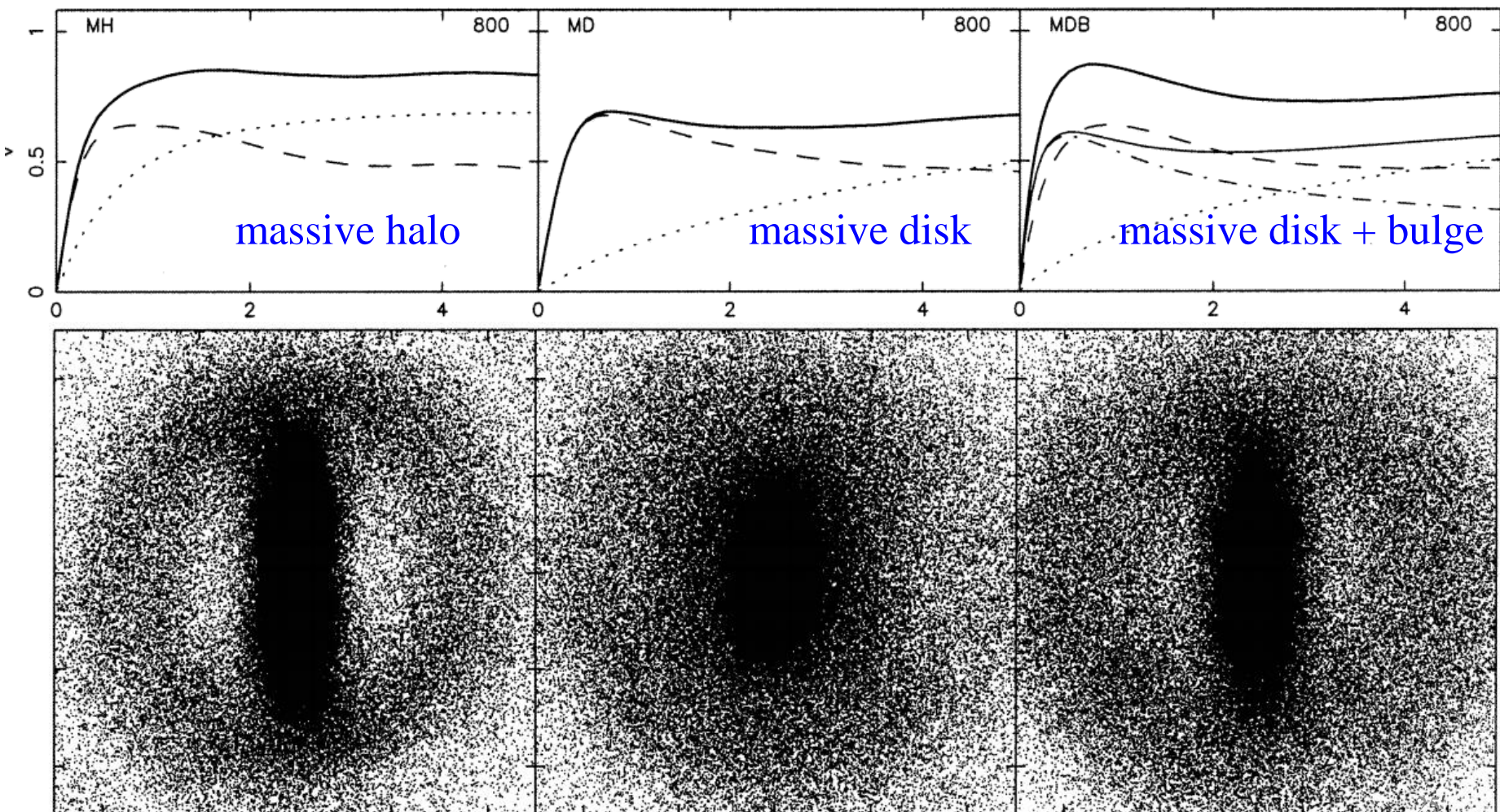
Formation of a bar

Total evolution time: 11 Gyr

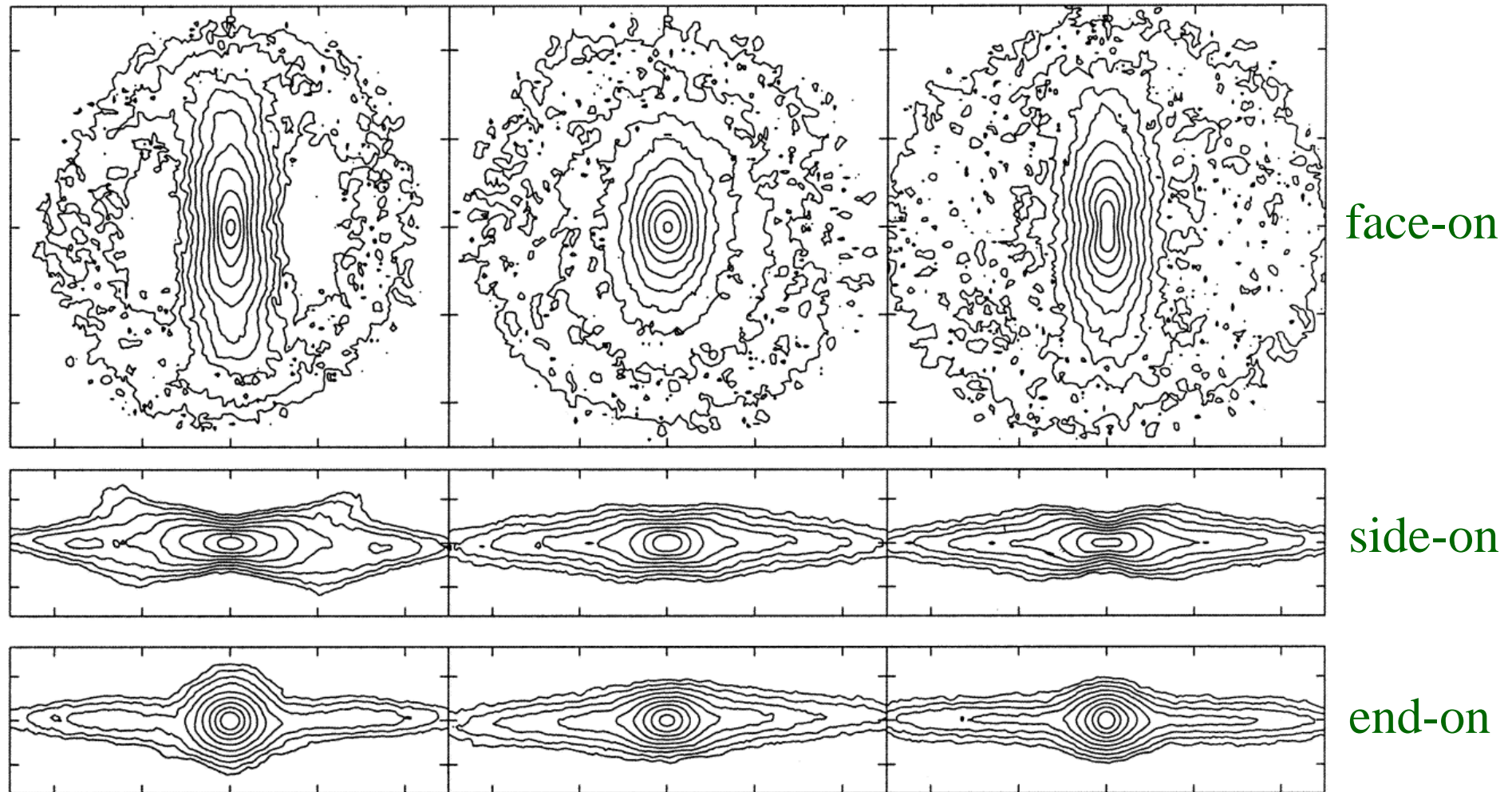


Three simulated bars

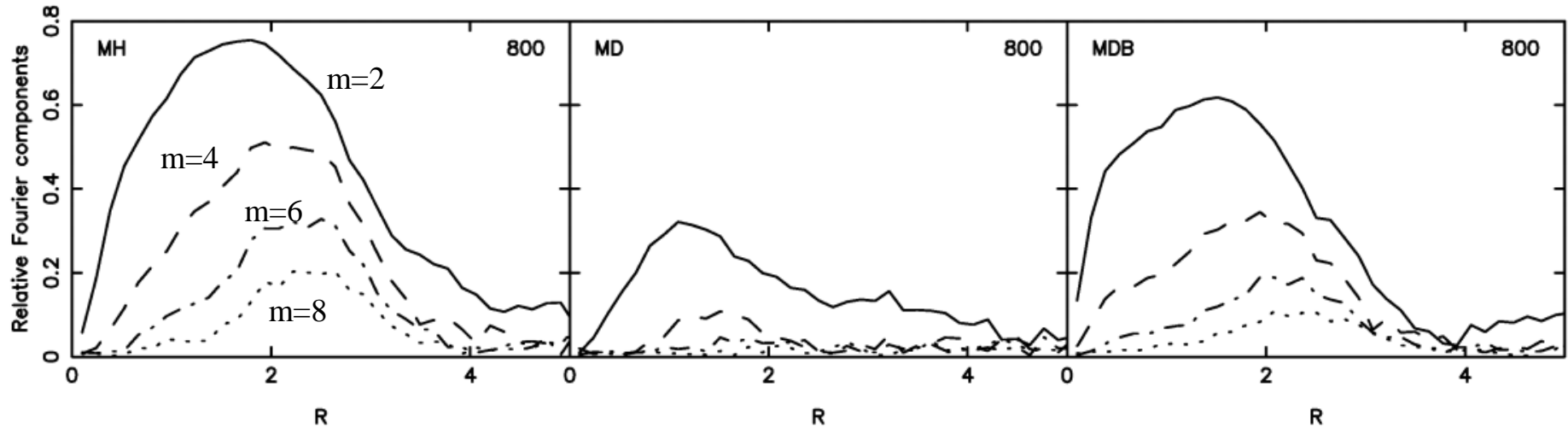
Formation of a bar in 3 models



Surface density



Fourier modes



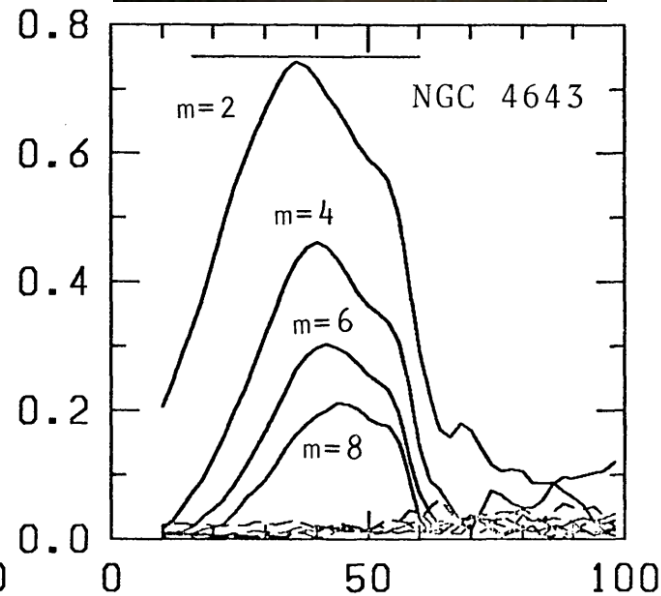
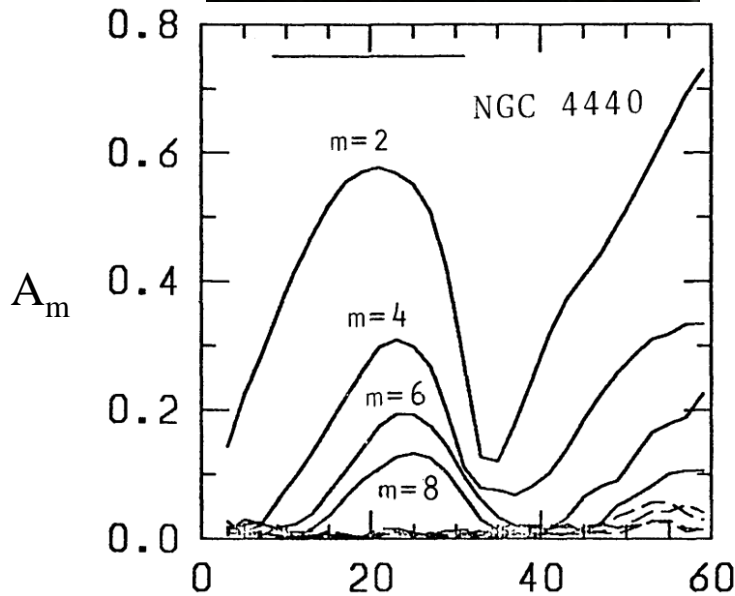
A customary way to quantify the properties of the bar is to calculate the Fourier modes in the disk plane

$$A(m) = \frac{1}{N} \sum_{j=1}^N \exp[im\varphi_j]$$

Athanassoula
& Misiriotis 2002

$$A(m = 2) = A_2 e^{2i\varphi}$$

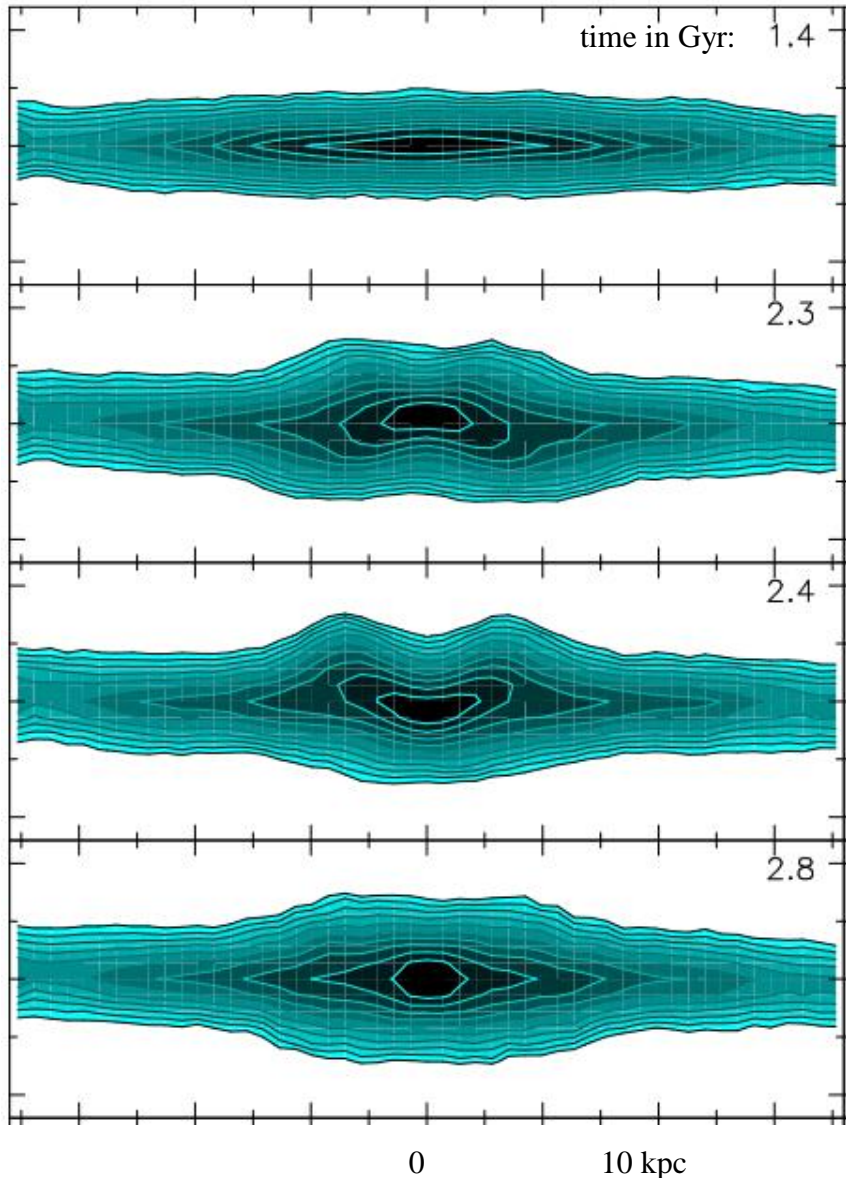
Comparison with real galaxies



Ohta et al.
1990

radius [arcsec]

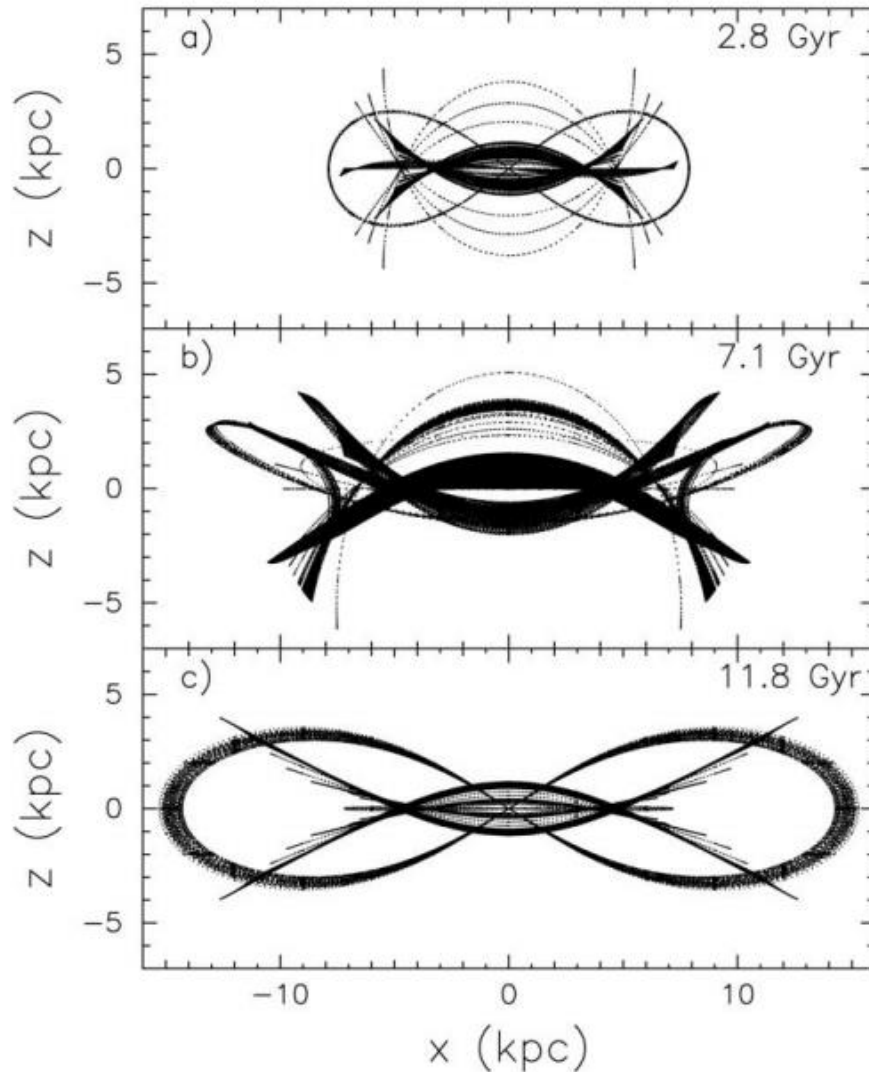
Buckling



- Some bars undergo buckling instability
- The bar is then distorted with respect to the disk plane
- The instability is probably related to vertical orbital resonances

Martinez-Valpuesta et al. 2006

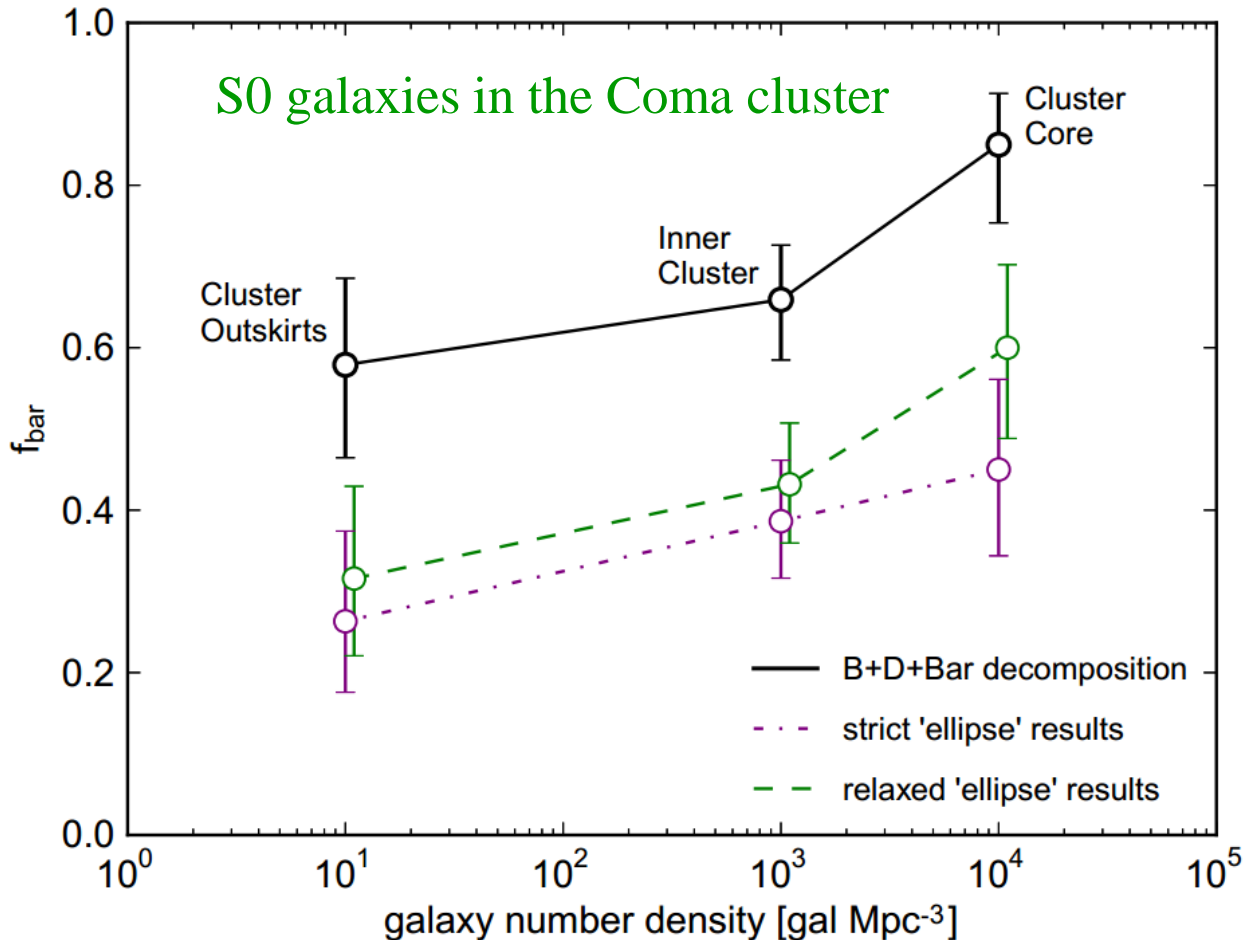
Orbits of stars in a buckling bar



- Examples of stellar orbits in a bar
- Lack of symmetry with respect to the $z=0$ plane signifies buckling
- The size of the orbits increases with time so the bar grows in the direction of the x axis

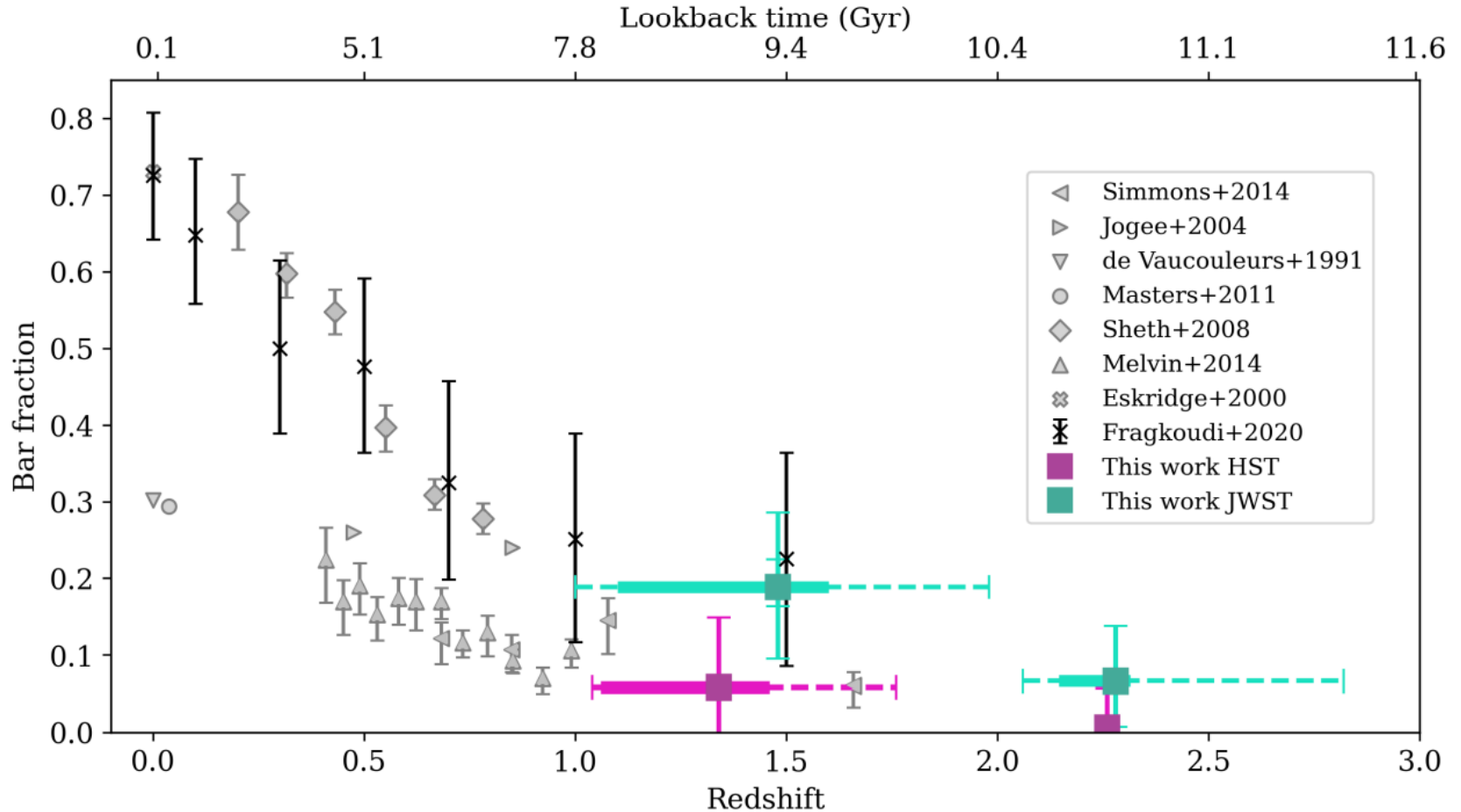
Martinez-Valpuesta et al. 2006

Dependence on environment



- Bars seem to form more efficiently in high-density environments
- Bar fraction increases in the centers of galaxy clusters

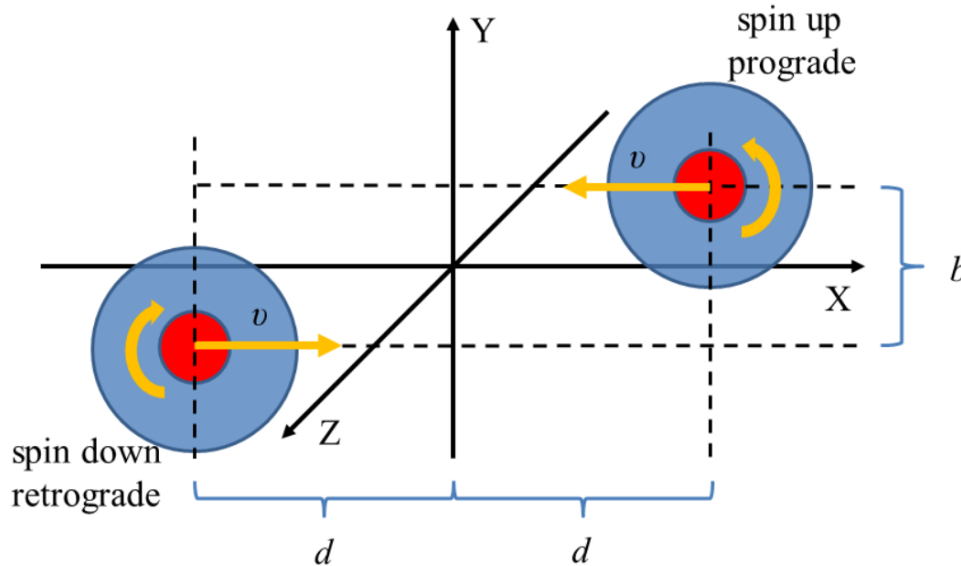
Dependence on time



Le Conte et al. 2023

Bar fraction increases in time

Controlled simulations of flybys

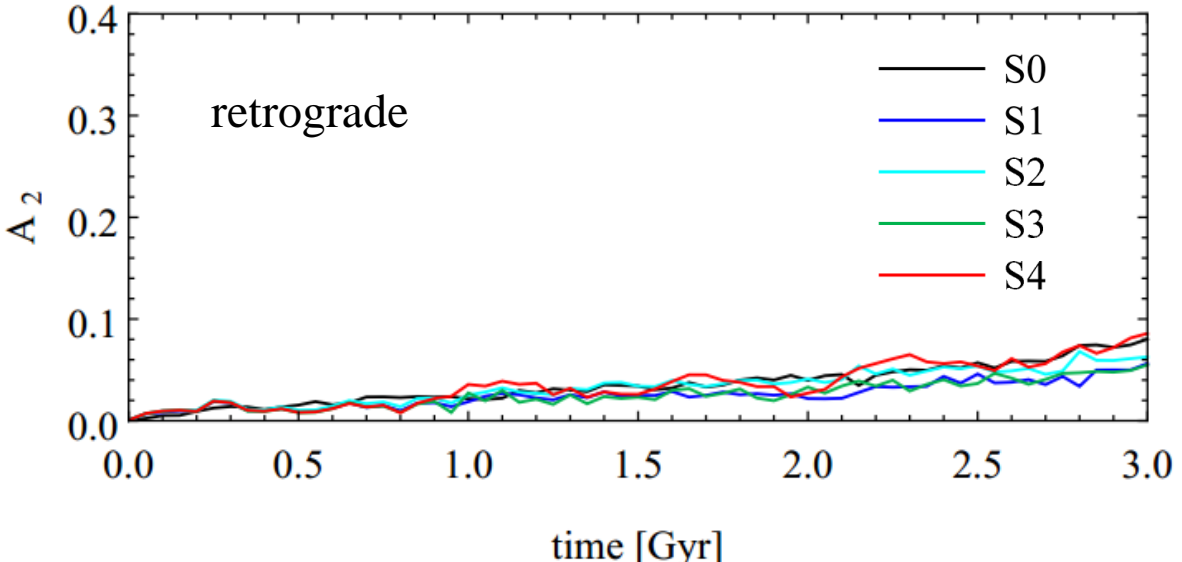
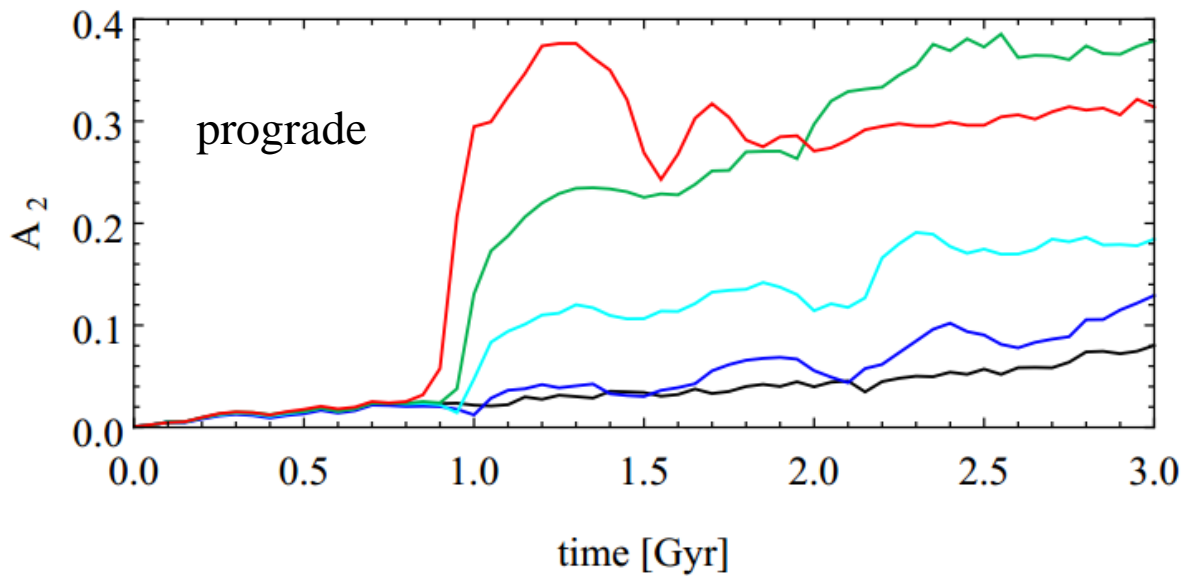
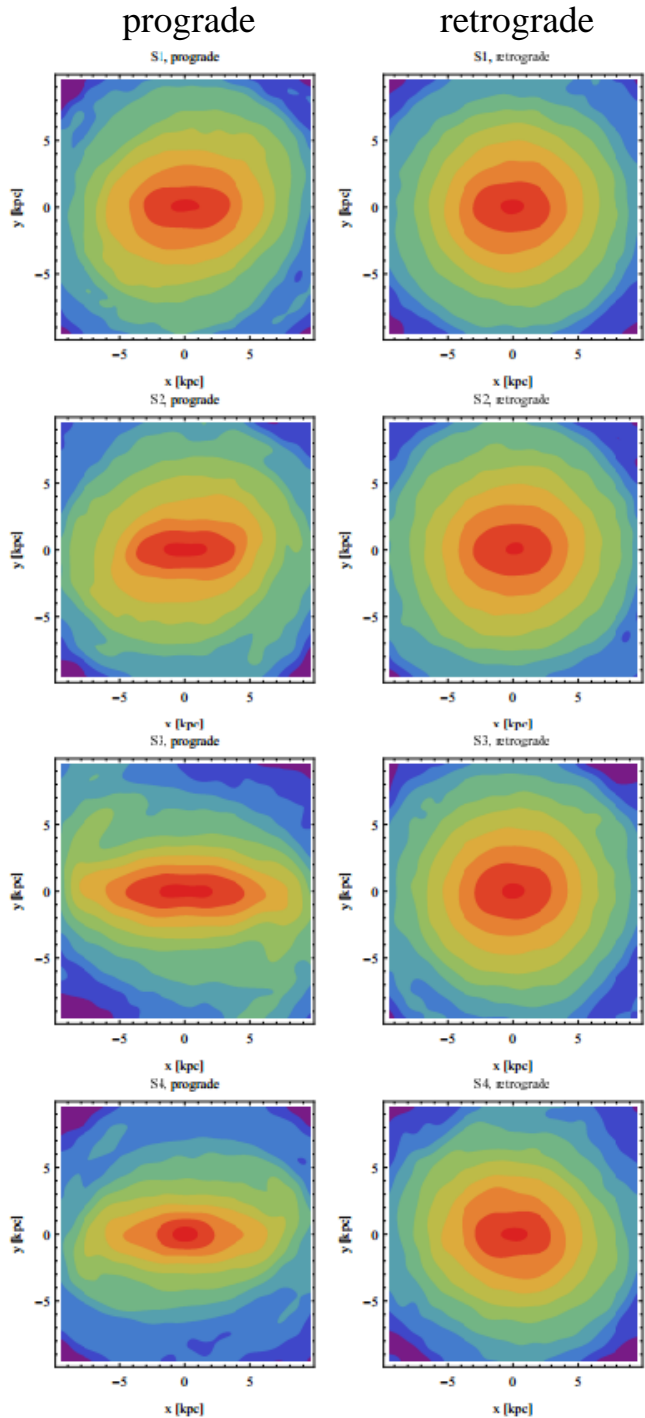


The disks of both galaxies lie in the orbital plane but they rotate in opposite directions

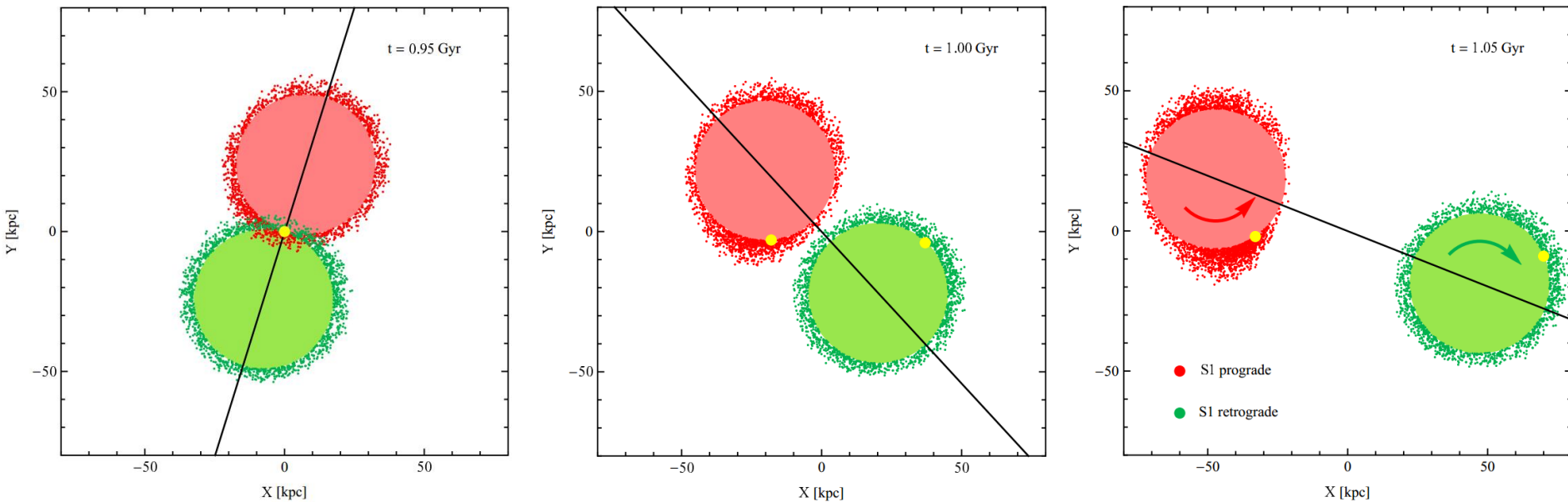
Simulation	d (kpc)	b (kpc)	v (km s^{-1})	S	Line Color
S0	black
S1	500	50	500	0.02	blue
S2	500	25	500	0.07	cyan
S3	350	25	350	0.15	green
S4	250	25	250	0.26	red

- The effect of the interaction depends strongly on whether the spin of the galaxy disk has the same orientation as the orbital spin
- The bars form only when the spin orientations are similar

Tidally induced bars

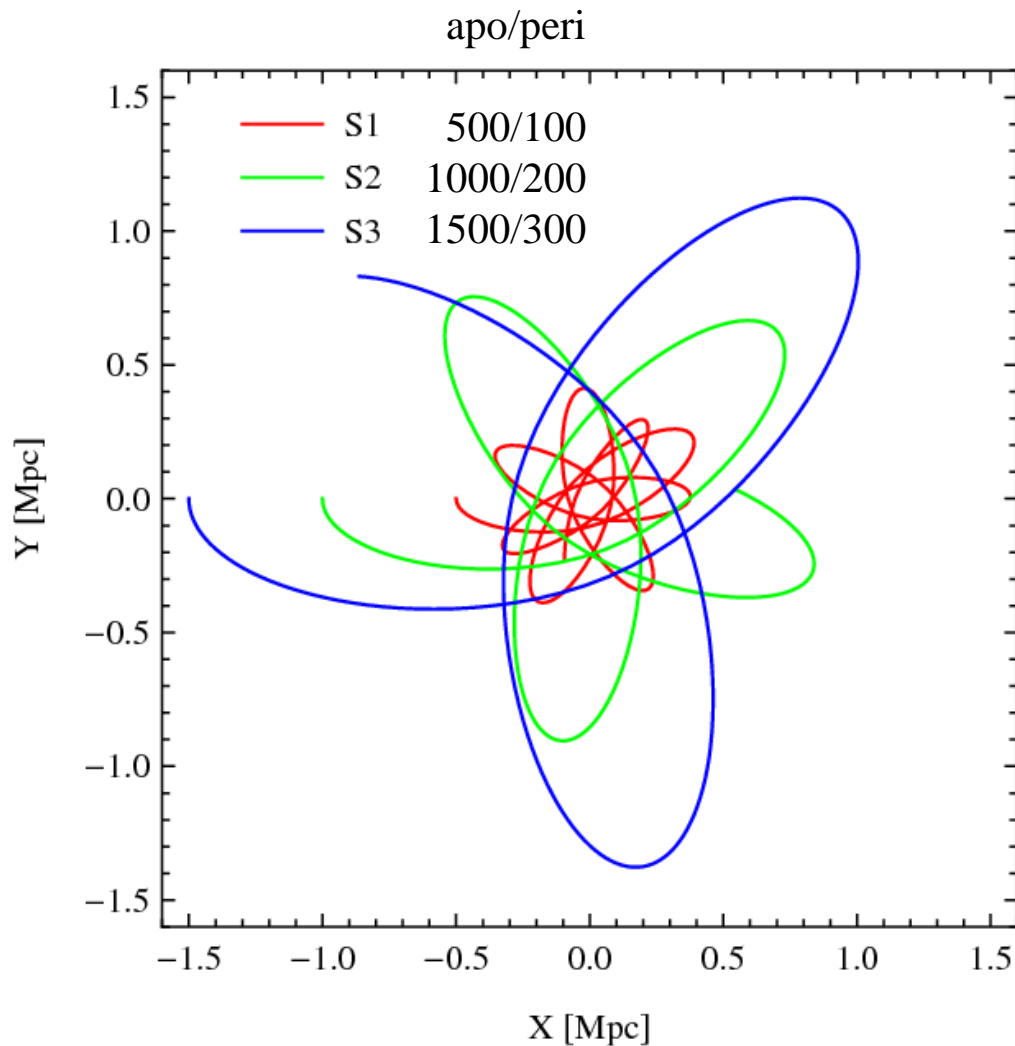


Dependence on the spin orientation



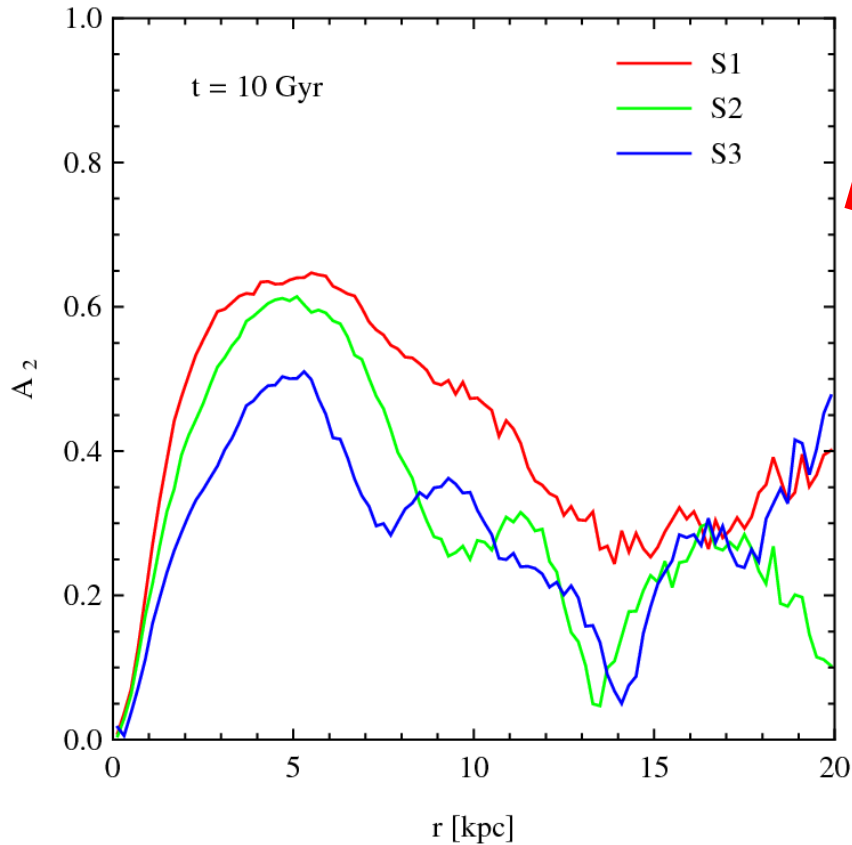
- The star in the prograde galaxy remains longer under the influence of the tidal forces from the other galaxy
- The effect of the interaction is stronger when the rotation velocity of the star in the disk is more similar to the relative velocity of the two galaxies

Galaxies in clusters



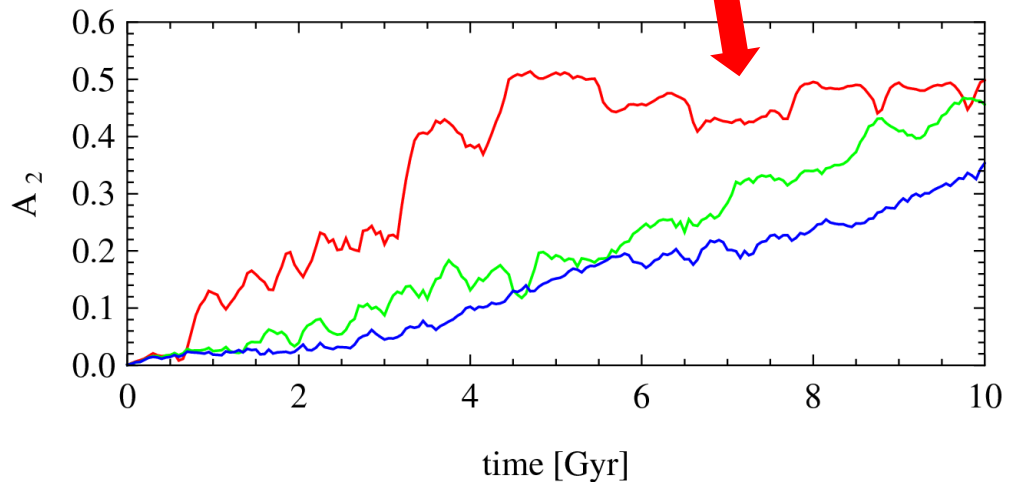
- A Milky Way-like galaxy was placed on different orbits in a Virgo-like cluster
- The Milky Way model was stable against bar formation in isolation
- The evolution was followed for 10 Gyr

Bar mode



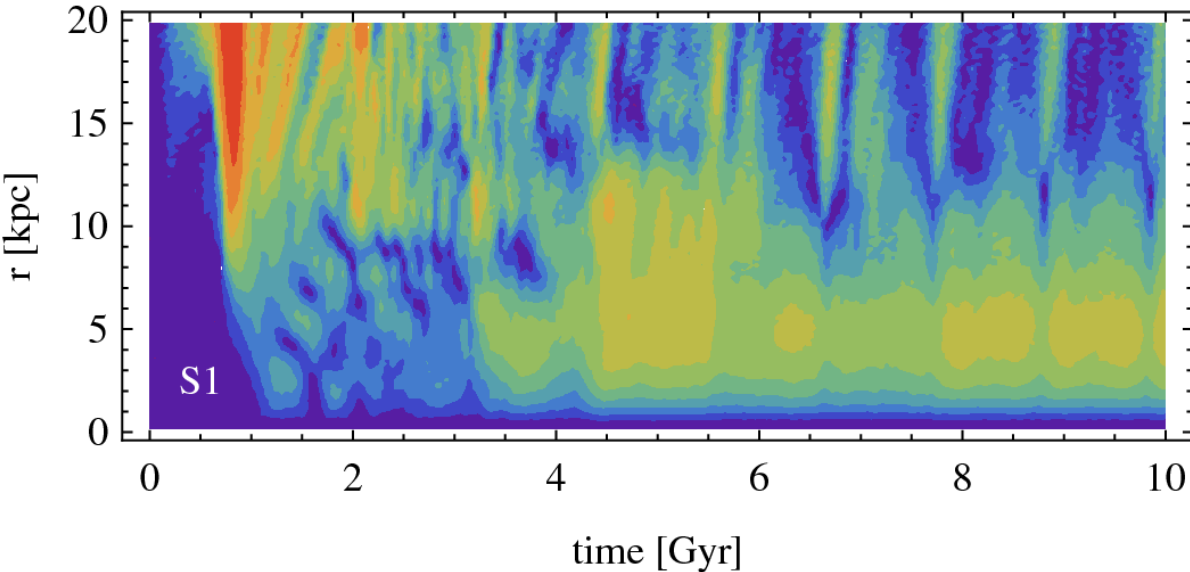
As a function of radius, at the final stage

As a function of time, for stars within a fixed radius of 7 kpc

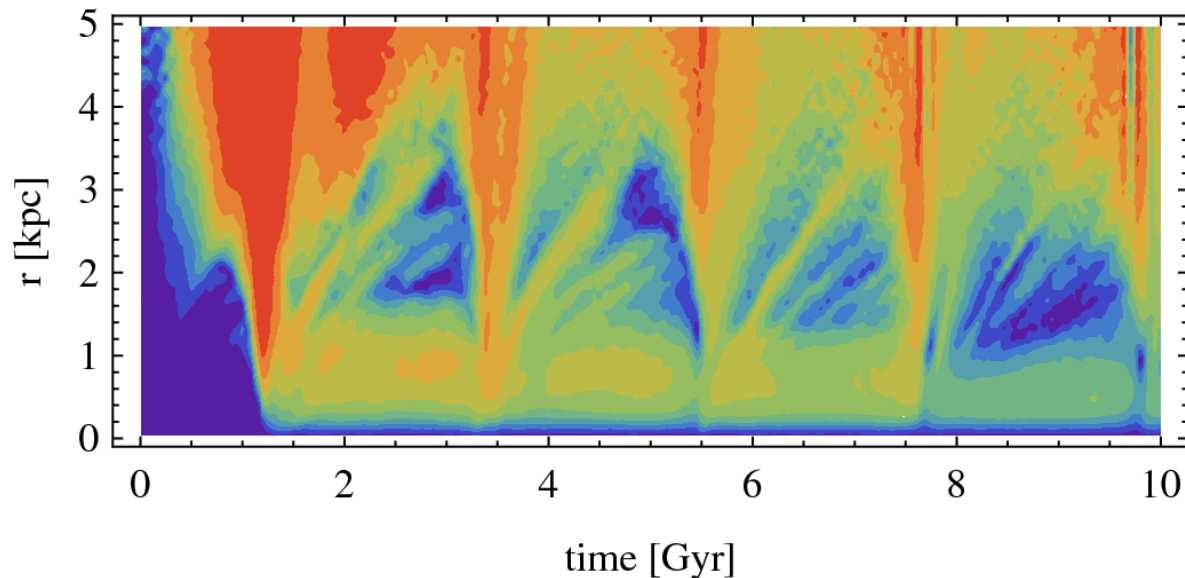


Bar mode in big and small

Łokas et al. 2016



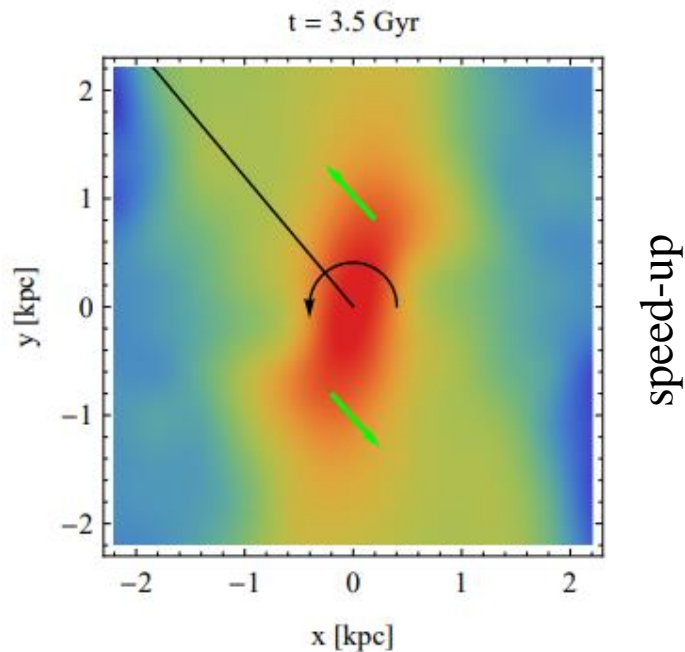
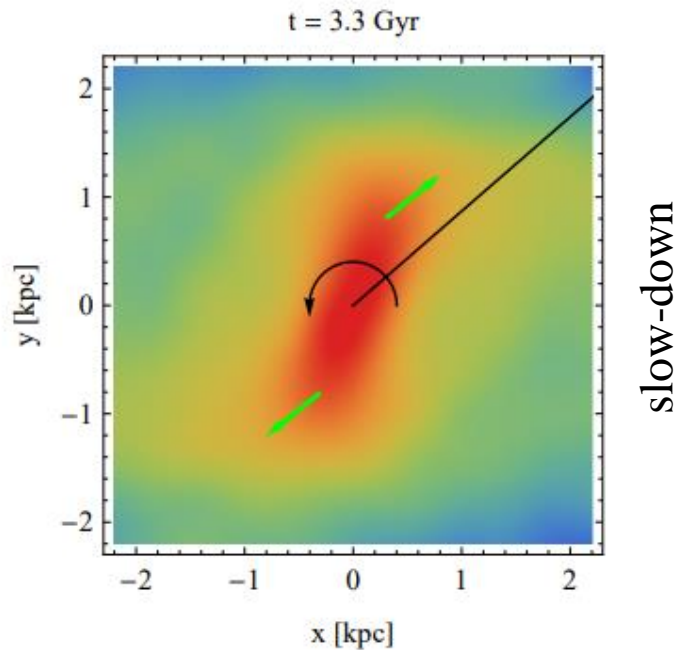
Normal-size disk
galaxy orbiting a
cluster



Dwarf disk galaxy
orbiting the Milky
Way

Łokas et al. 2014, Gajda et al. 2017

Tidal torque acting on bar

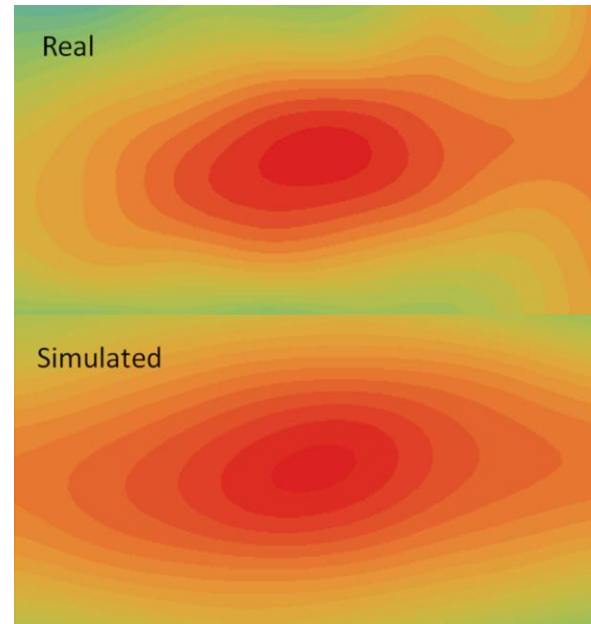
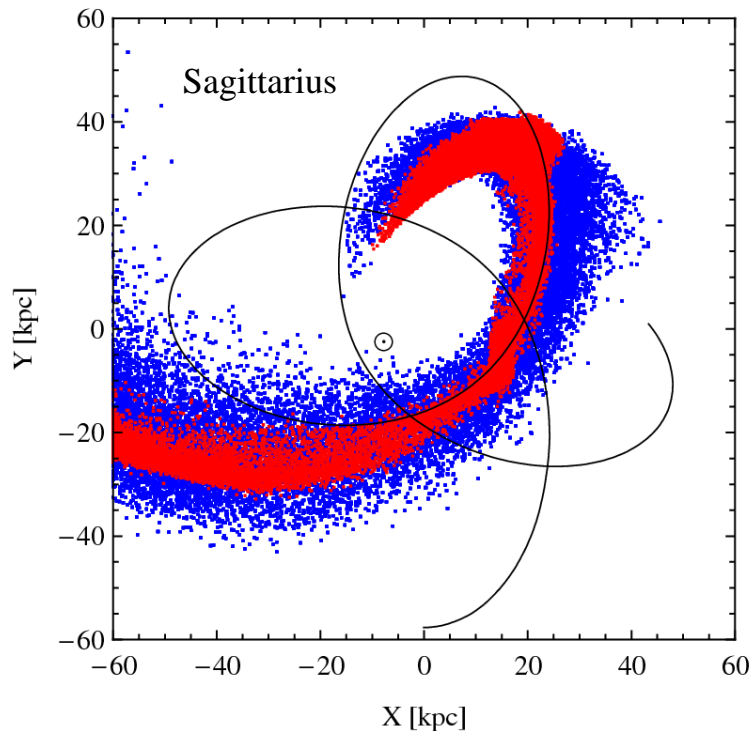


After formation at first pericenter the bar can slow down or speed up at subsequent pericenters depending on the orientation of the bar with respect to the tidal torque from the bigger structure

slow-down \rightarrow stronger bar

speed-up \rightarrow weaker bar

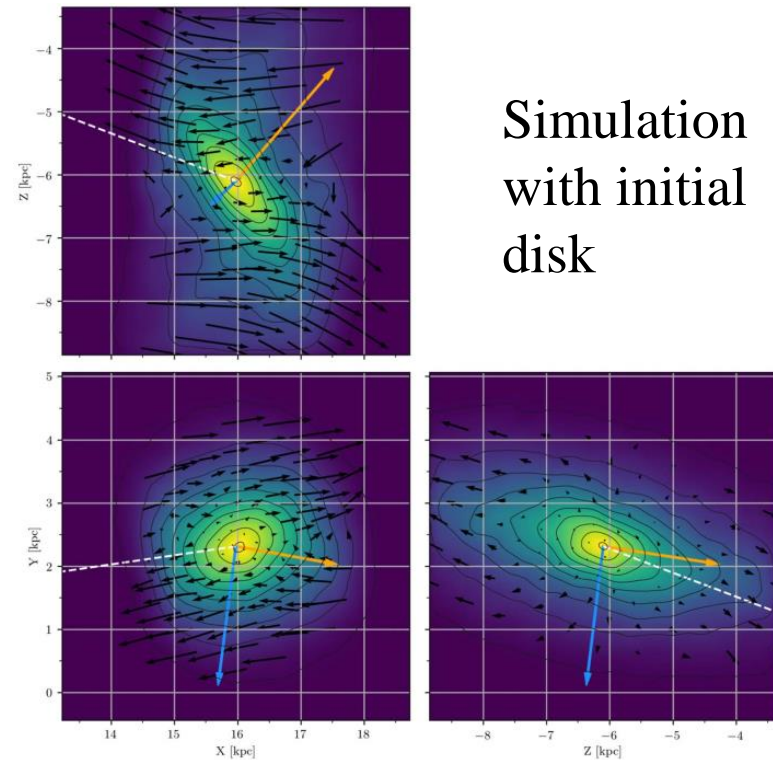
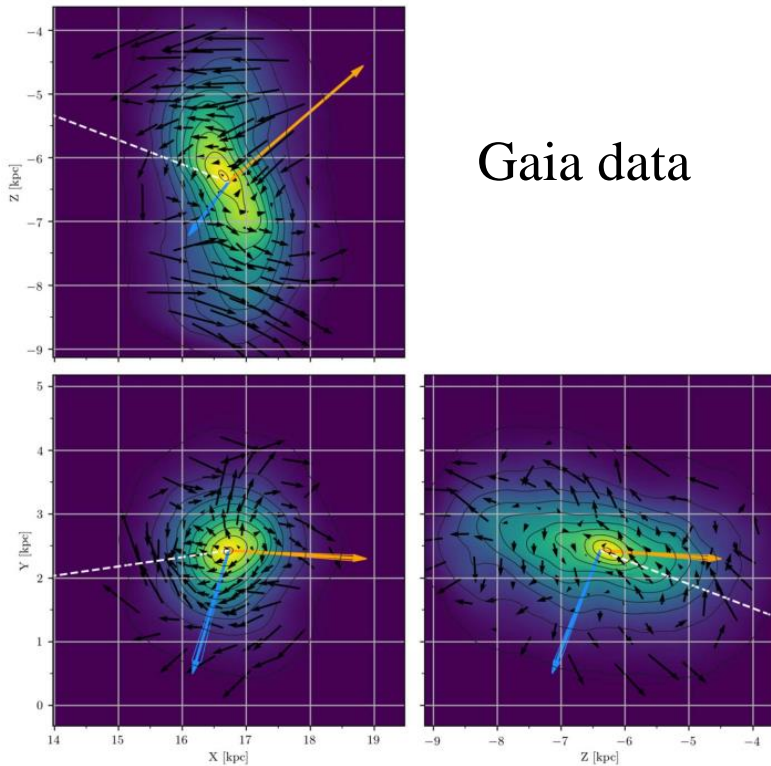
Candidates for tidally induced bars in dwarfs



Many properties of the Sagittarius dwarf can be reproduced by a disk dwarf that passed the second pericenter on a tight orbit

Sagittarius

→ velocity
→ angular momentum



Surface density and kinematics in galactocentric coordinates

Cosmological simulations IllustrisTNG

The coupled dynamics of DM and gas is followed using the Arepo code with adaptive mesh by solving the equations of ideal magnetohydrodynamics

Key physical processes included in addition to gravitational force:

- Microphysical gas radiative mechanisms, including primordial and metal-line cooling and heating with an evolving background radiation field
- Star formation in the dense interstellar medium
- Stellar population evolution and chemical enrichment following supernovae Ia, II, and AGB stars, individually tracking some elements
- Stellar feedback driven galactic-scale outflows
- The formation, merging, and accretion of nearby gas by supermassive black holes
- Multi-mode blackhole feedback different for high and low accretion states
- Amplification of cosmic magnetic fields from a minute primordial seed field at early times

<https://www.tng-project.org/>

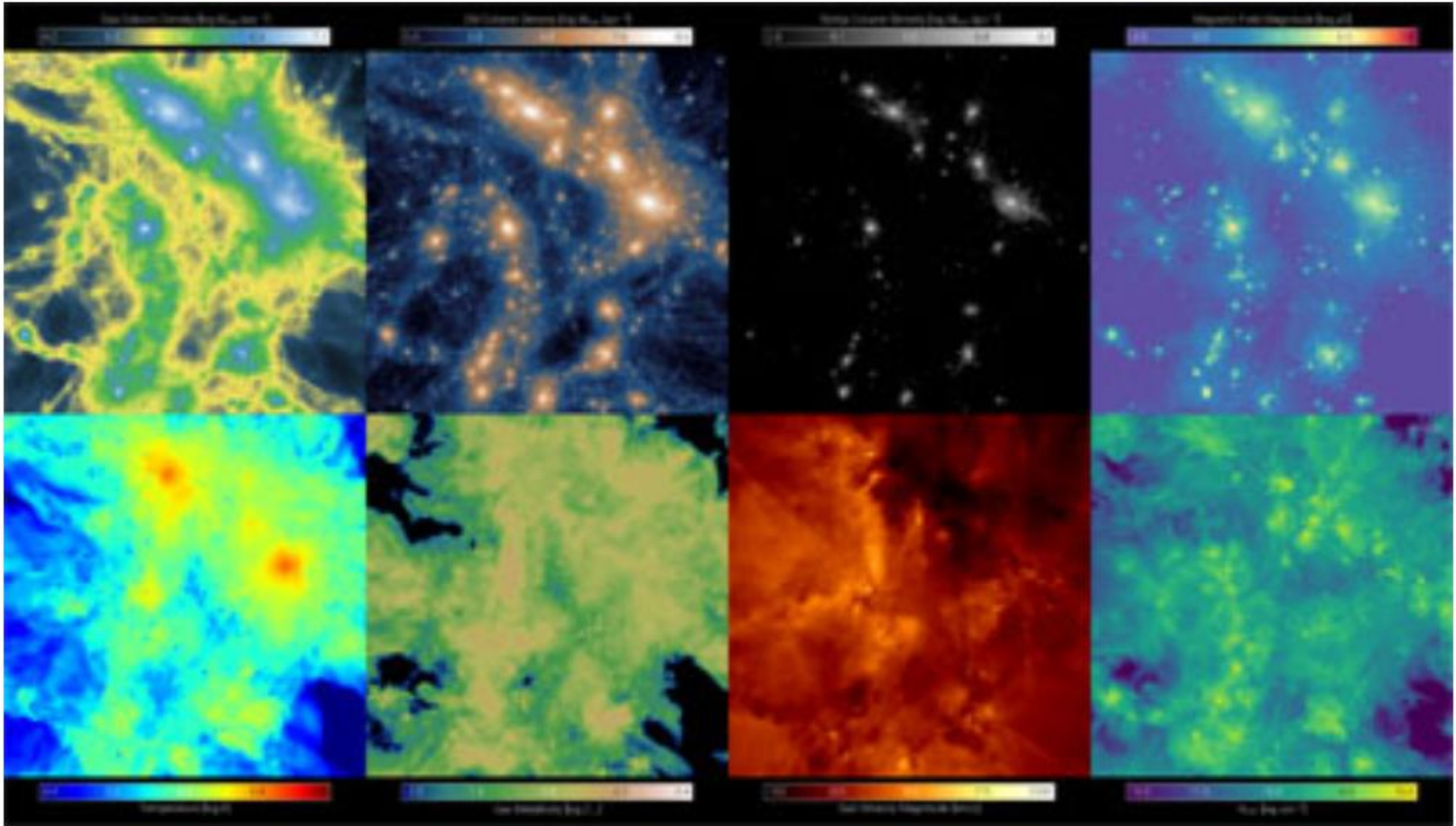
IllustrisTNG simulations

gas density

dark matter density

stellar mass

magnetic field strength



gas temperature

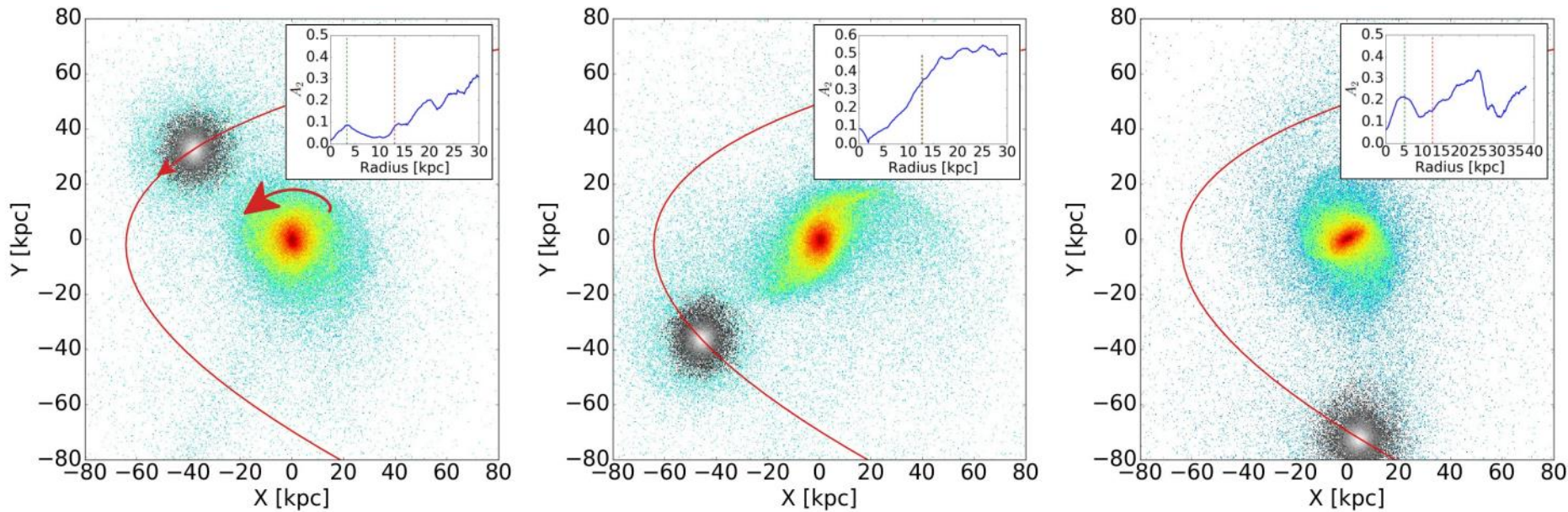
gas metallicity

gas velocity

column density of OVI

10 Mpc region from IllustrisTNG-100

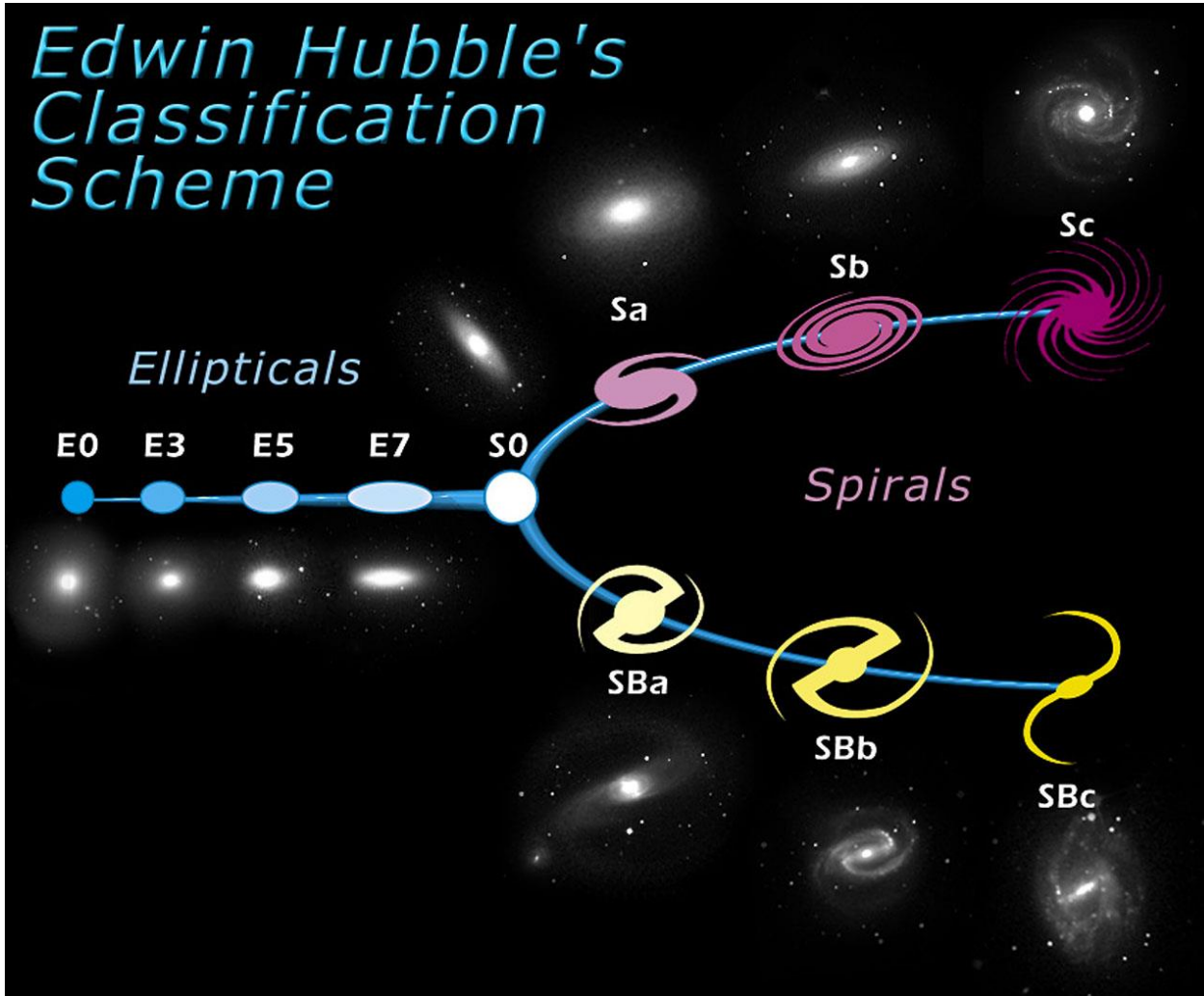
Tidally induced bars in Illustris



Example of the formation of a tidally induced bar by a perturber passing on a prograde orbit

Most of bars in massive disks are formed by interactions

Morphological classification



Spiral galaxies constitute a majority of all galaxies

Spiral galaxies

- Spiral galaxies make up about 2/3 of all massive galaxies according to Galaxy Zoo project
- All of the spiral types may or may not have bars
- Around 60% of spirals exhibit some grand design structure, either in the inner or entire part of the disc
- Star formation occurs mainly in the spiral arms
- Understanding the nature of spiral arms is essential for theory of galaxy evolution and star formation

Spiral arms

Elmegreen (1990) classified galaxies according to the type of spiral arms into 3 types:

- flocculent spiral galaxies
(with many short arms,
such as NGC2841)



- multi-armed spirals (e.g. M33)



- grand design galaxies
(with two main spiral
arms, e.g. M51).



From early to late types

Transition Sa \rightarrow Sd means:

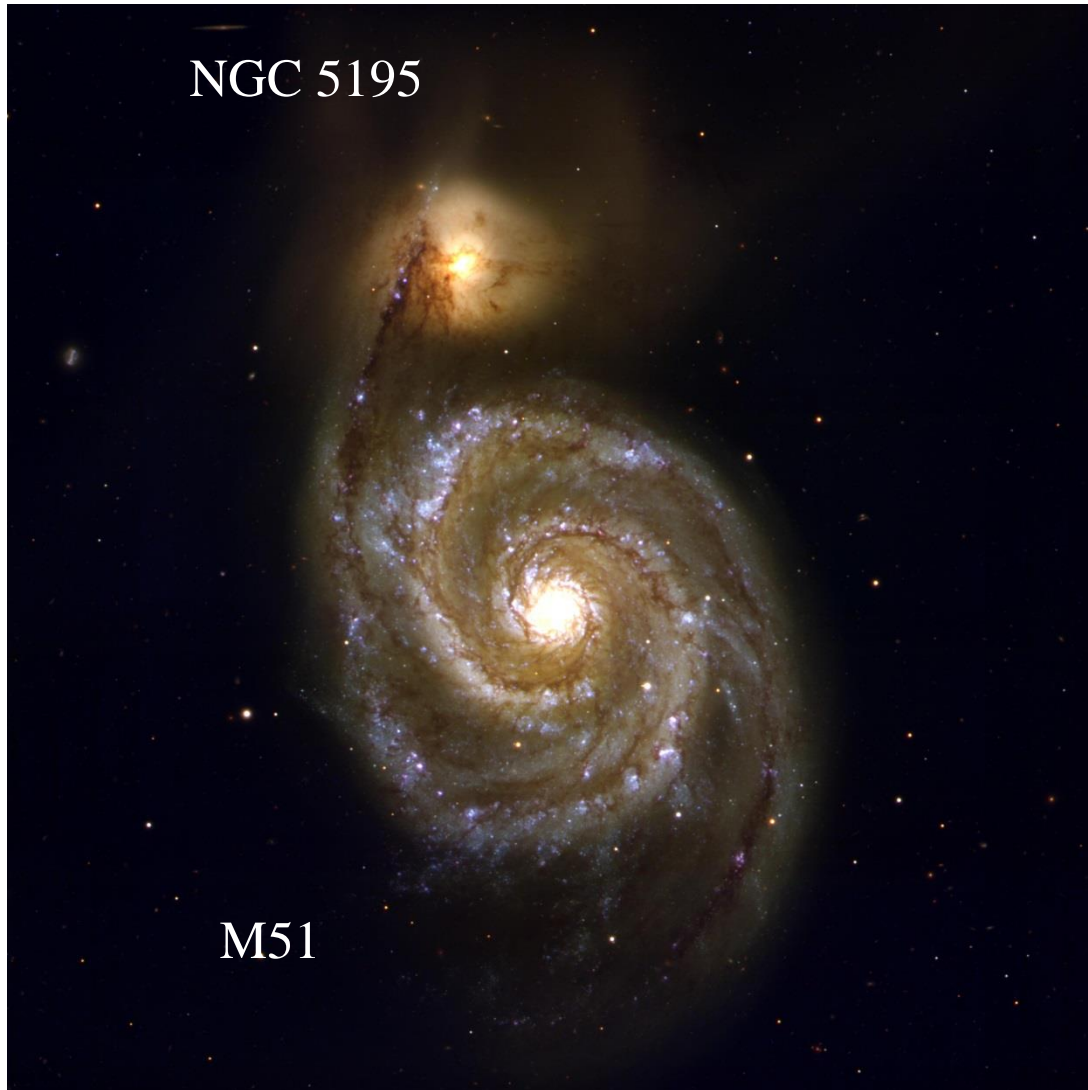
- More open spiral arms
- Decrease in the size and luminosity of the bulge
- Increase in gas content
- Spiral arms become more clumpy

Examples of spirals



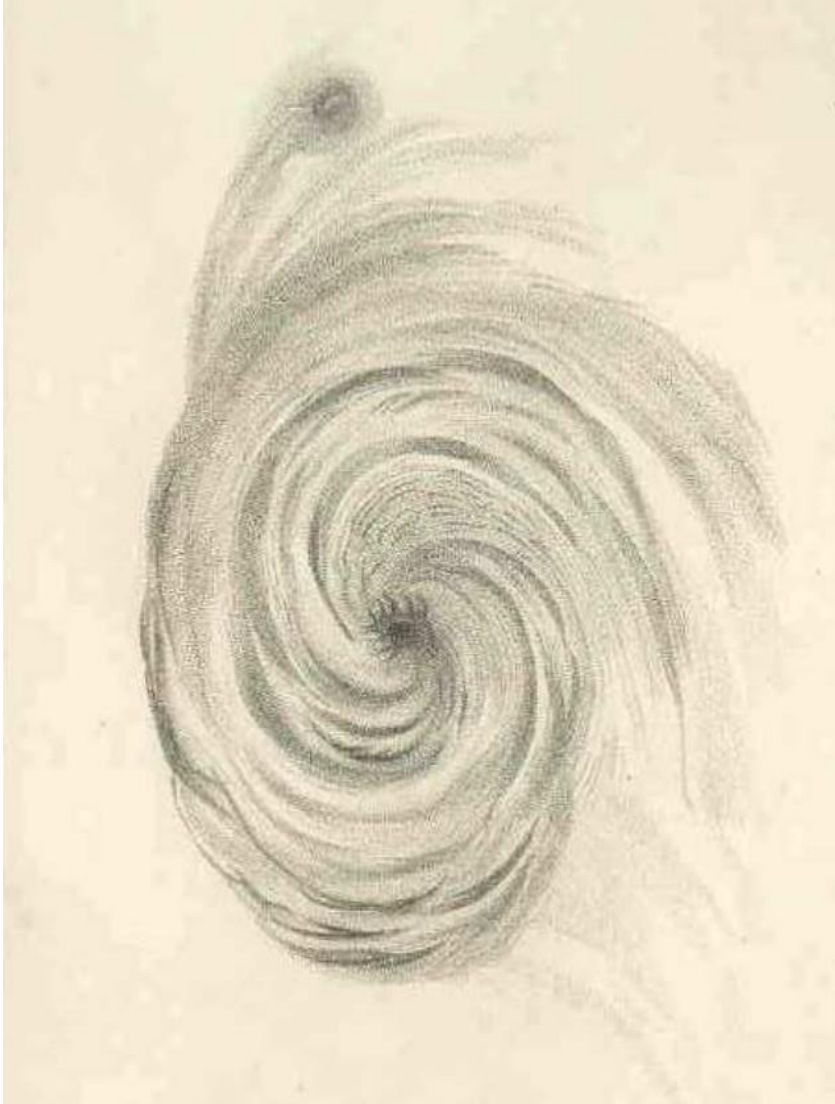
A grand design spiral galaxy of type Sbc, one of the brightest galaxies in the Virgo cluster, at a distance of 17 Mpc, discovered in 1781 by Pierre Mechain

Examples of spirals



The Whirlpool Galaxy of type Sbc, one of nearby galaxies, at a distance of 7 Mpc, discovered in 1773 by Charles Messier

The first spiral nebula



M51 was the first object to show the spiral structure (drawing by William Parsons, 1845)

Examples of spirals



The Pinwheel galaxy, a spiral of type Scd, with more shorter spiral arms, at distance of 6.4 Mpc, discovered in 1781 by Pierre Mechain

Examples of spirals



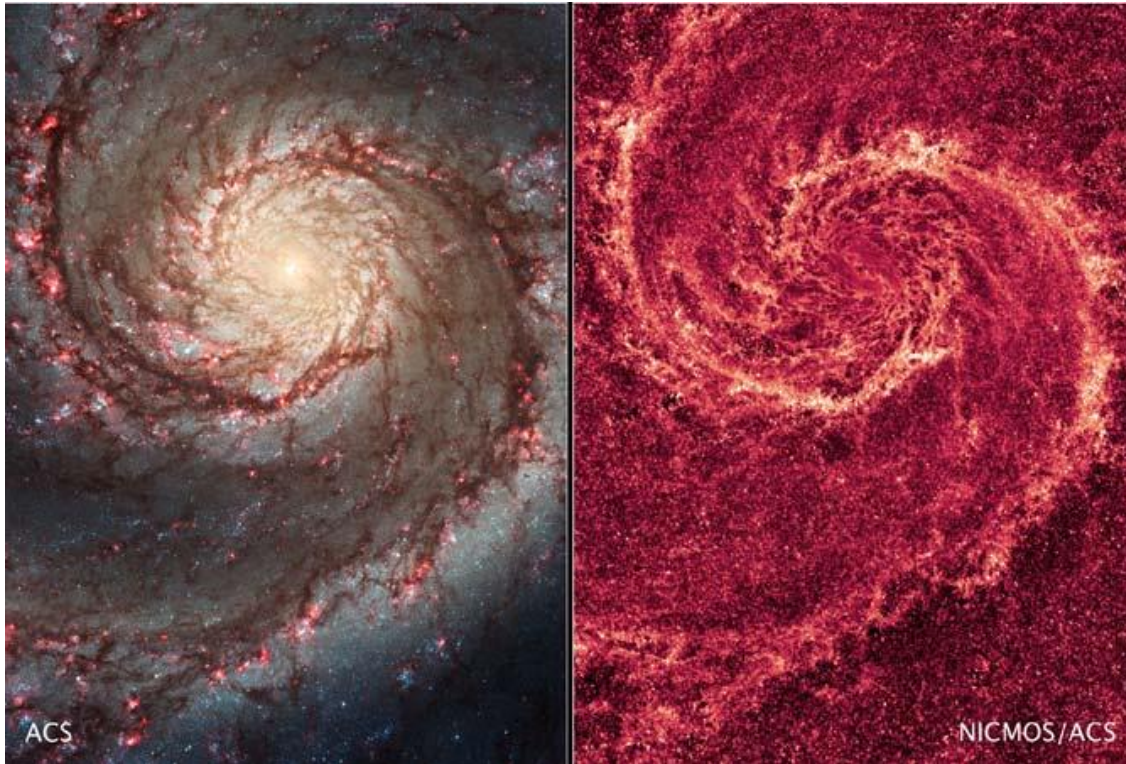
M33, the third largest galaxy of the Local Group, has less pronounced spiral structure with multiple spiral arms

Examples of spirals



M63, the Sunflower Galaxy, of type Sbc, part of the M51 group, an example of flocculent spiral structure

Spiral arms at different wavelenghts



Spiral structure of M51 is seen in optical (left), infrared (right), but also radio and molecular and atomic gas

This means that the spiral structure must be long-lived and is not only due to young stars that formed and were wound up

The importance of gas content

- Spirals differ from S0s by: higher density of cold interstellar gas, presence of young stars, the presence of spiral arms
- Only a small fraction of gas-poor disk galaxies exhibit spiral arms and these may have been stripped of gas only recently
- Thus, although spiral structure is present in the old disk stars, it seems that the interstellar gas is essential for persistent spiral structure

presence of gas \Leftrightarrow spiral structure

Geometry of spiral arms

- The strength and number of arms
- Leading versus trailing arms
- The pitch angle
- The pattern speed

The strength and number of arms

- If the surface brightness distribution remains unchanged under rotation by $2\pi/m$

$$I(R, \phi + 2\pi/m) = I(R, \phi)$$

the galaxy has m -fold rotational symmetry and m arms

- The strength of the spiral structure can be parametrized by the amplitude of the Fourier components in the expansion

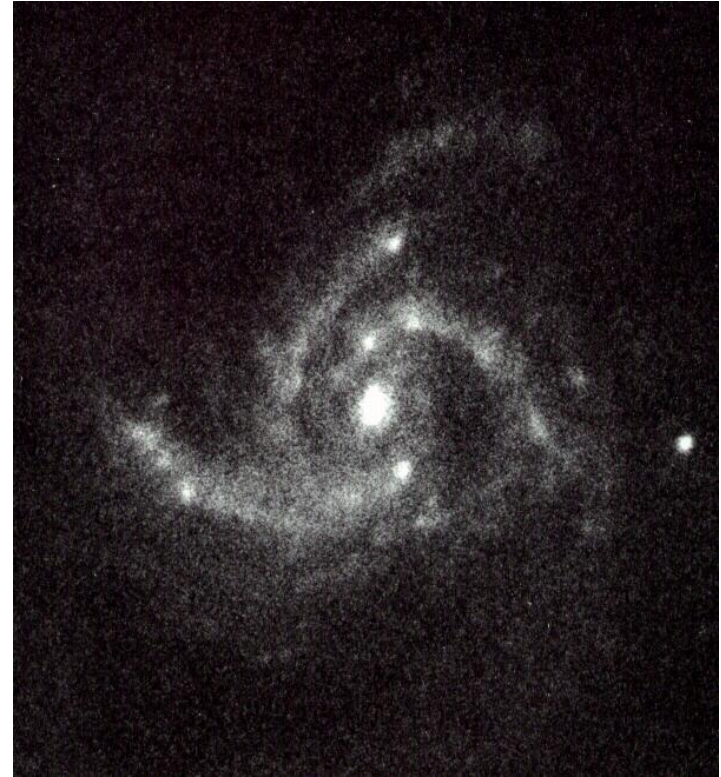
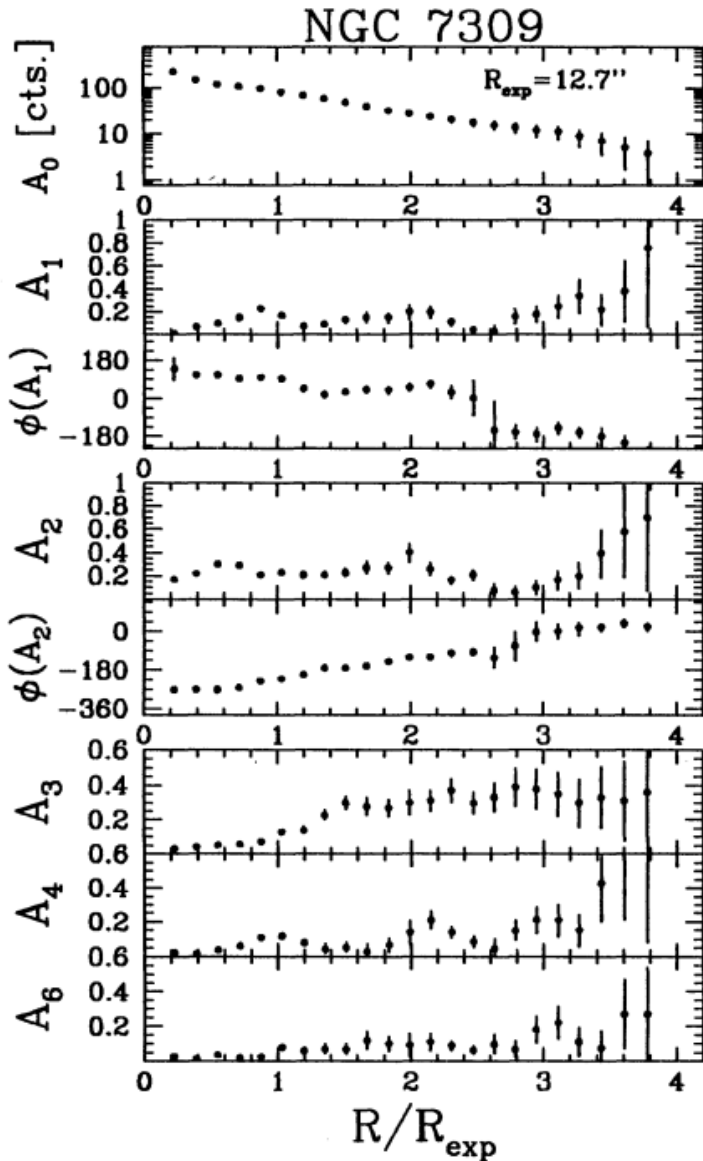
$$\frac{I(R, \phi)}{\bar{I}(R)} = 1 + \sum_{m=1}^{\infty} A_m(R) \cos m[\phi - \phi_m(R)]$$

$$\bar{I}(R) \equiv (2\pi)^{-1} \int_0^{2\pi} d\phi I(R, \phi)$$

Two-armed spirals

- Most grand-design spirals are two-armed with $0.15 < A_2 < 0.6$
- Grand-design spirals with $m \neq 2$ are rare
- Some spirals show asymmetric distortions (lopsidedness) with $A_1 > 0.2$
- The dominance of two-armed spirals needs to be explained theoretically

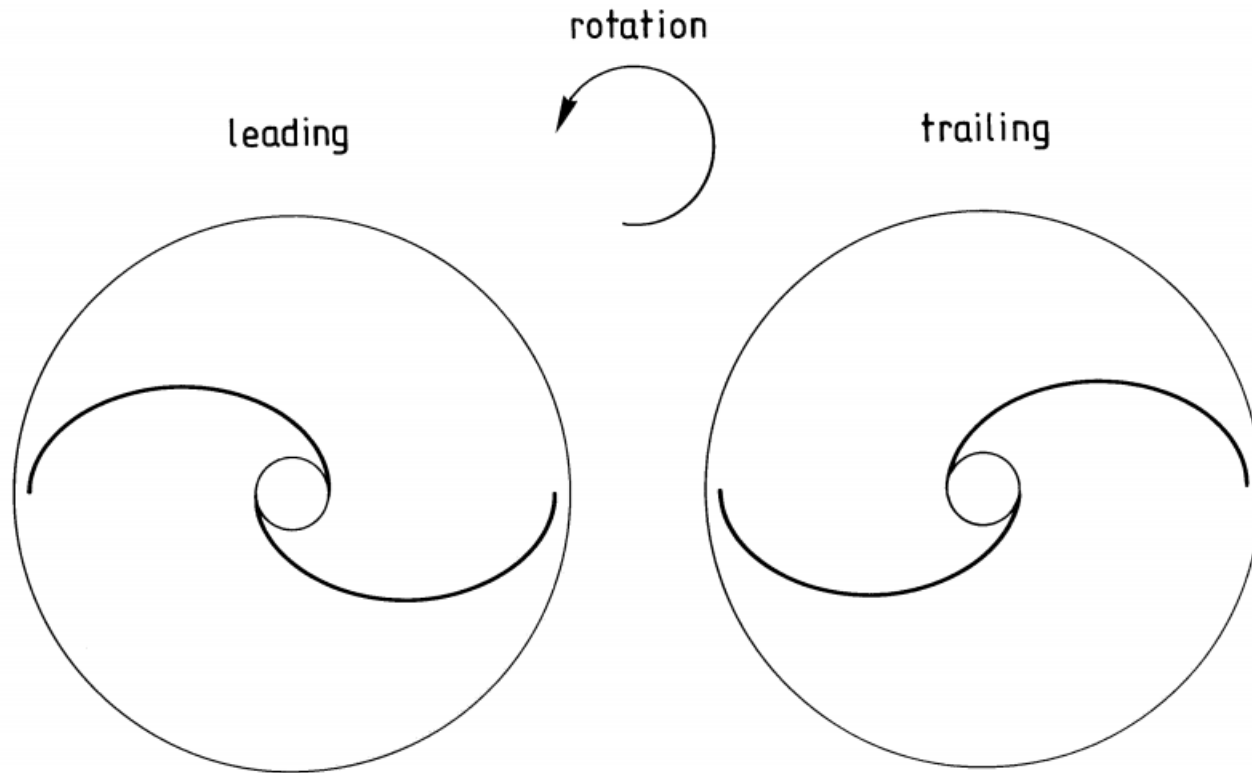
Example of Fourier decomposition



Asymmetry: $A_1 > 0, A_3 > 0$

Rix & Zaritsky 1995

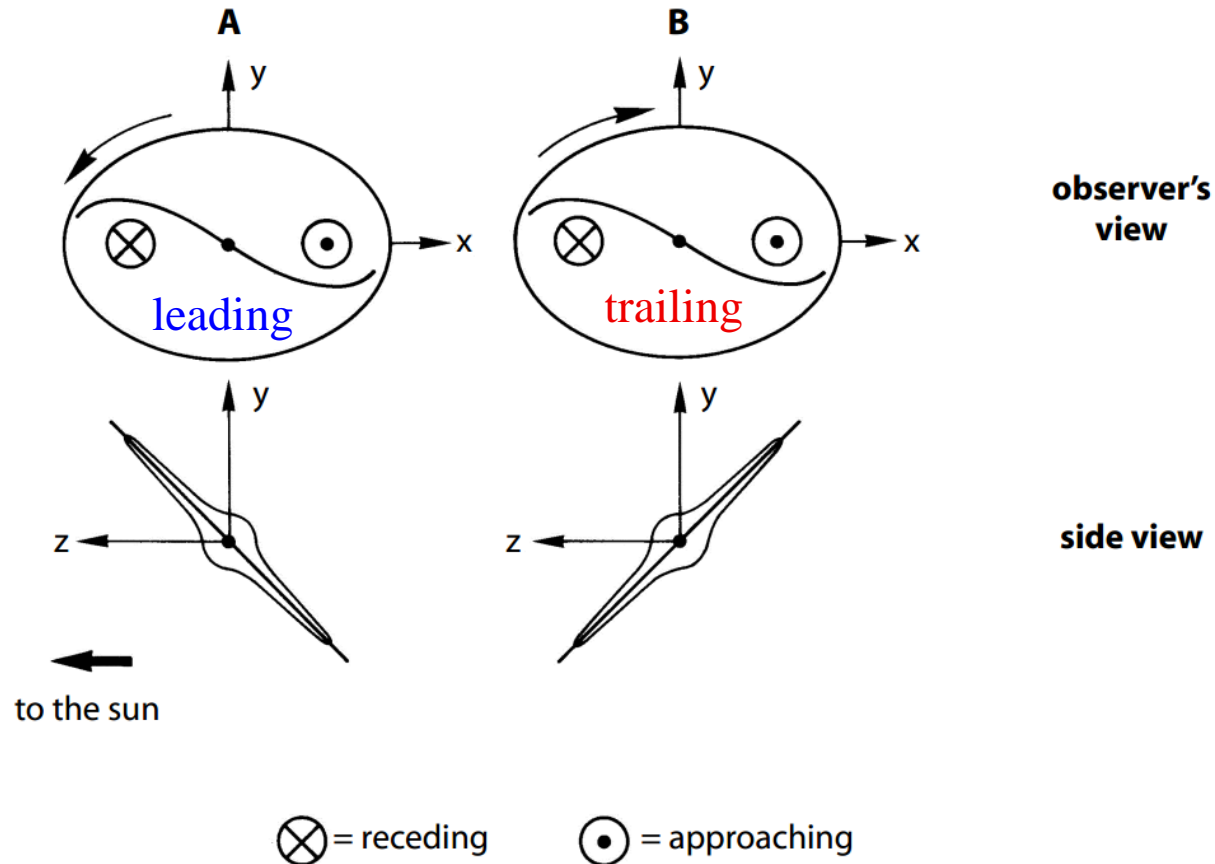
Leading and trailing arms



A leading arm points in the direction of the galaxy rotation

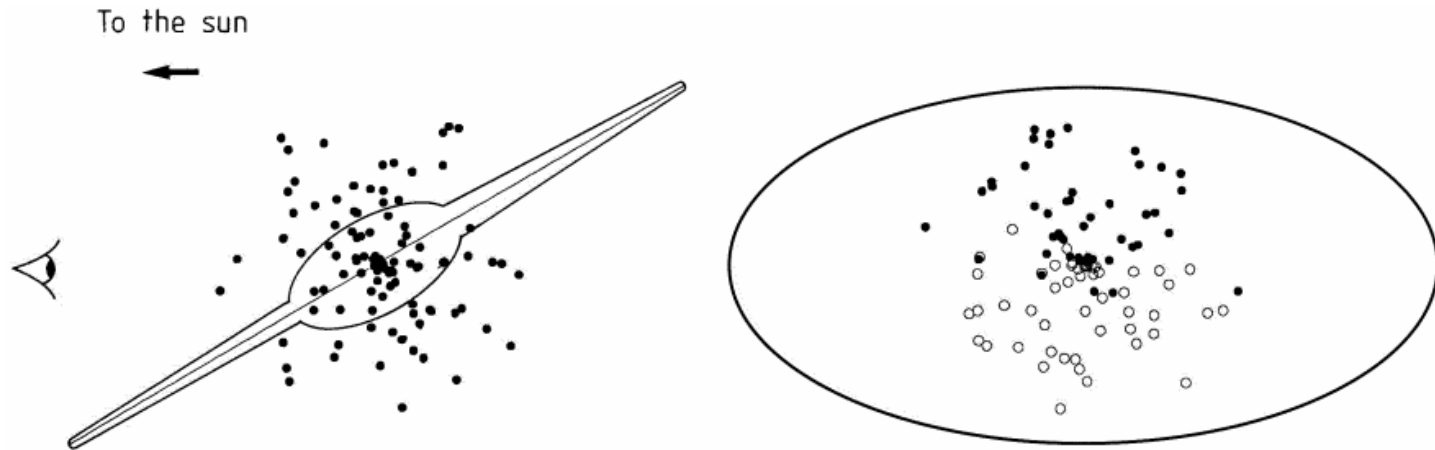
A trailing arm points in the direction opposite to the galaxy rotation

Observing leading and trailing arms



It is difficult to distinguish the leading and trailing arms observationally

Trailing arms dominate



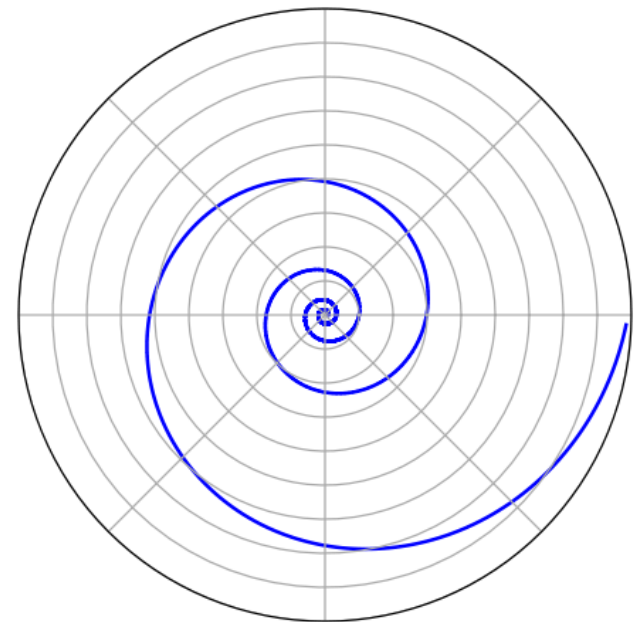
- The velocity measurements themselves do not allow us to distinguish leading and trailing arms
- We can tell which galaxy side is closer to us if there is additional information available (e.g. fainter objects on one side of the galaxy)
- In all well-studied cases (including the Milky Way) the spiral arms were found to trail

The logarithmic spiral

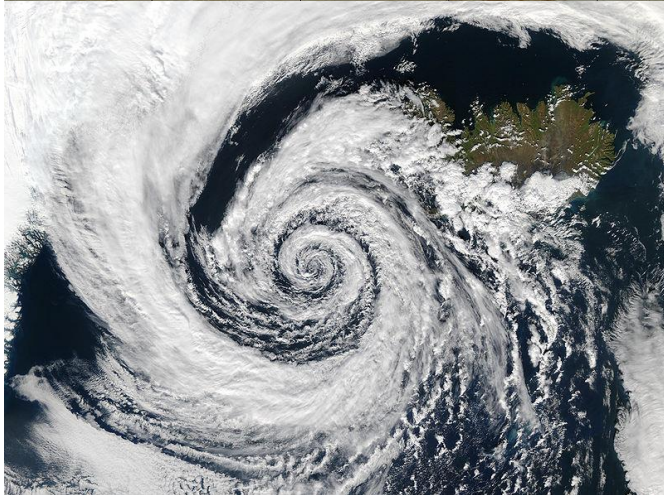
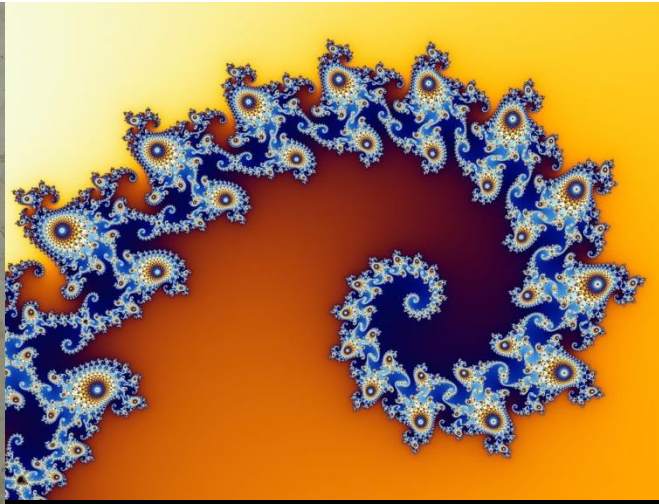
- The spiral arms in many galaxies can be described as logarithmic spirals
- The logarithmic spiral is given in polar coordinates (R, ϕ) by the relation

$$R = a e^{b\phi}$$

- The spiral has the property that the angle between the tangent and radial line at any point is constant

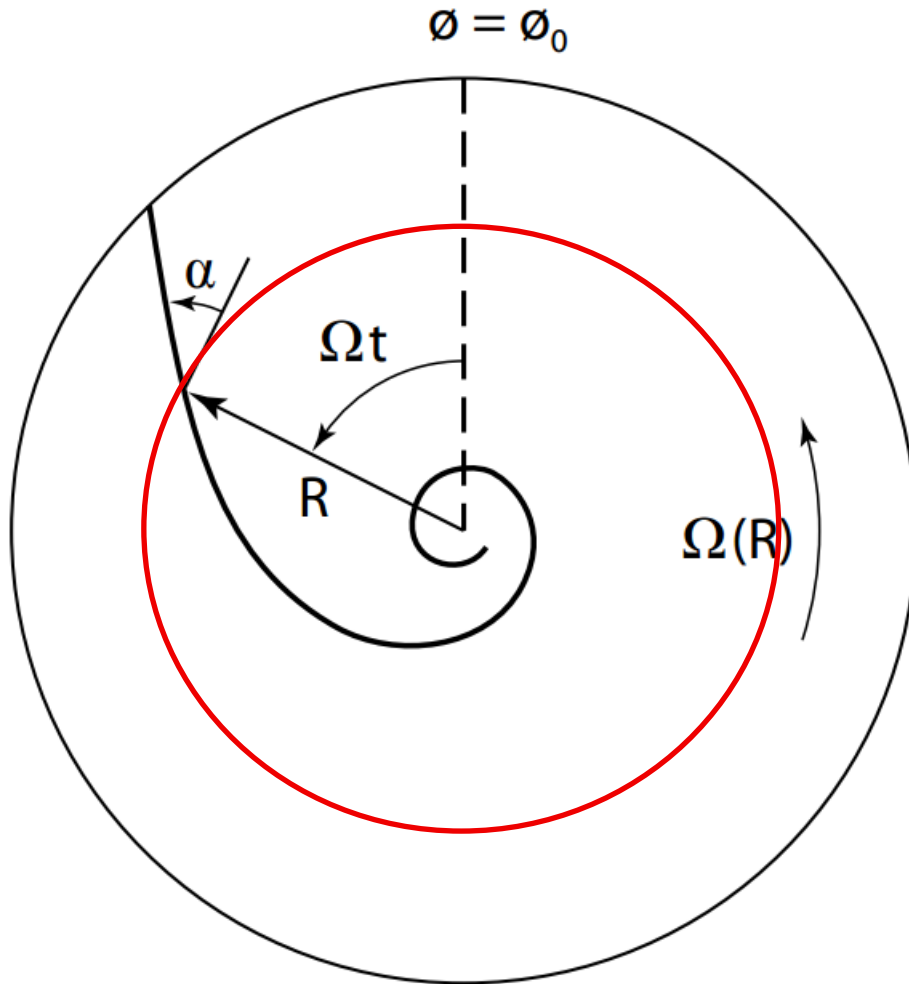


Logarithmic spirals in nature



shells
fractals
cyclons
plants
...

The pitch angle

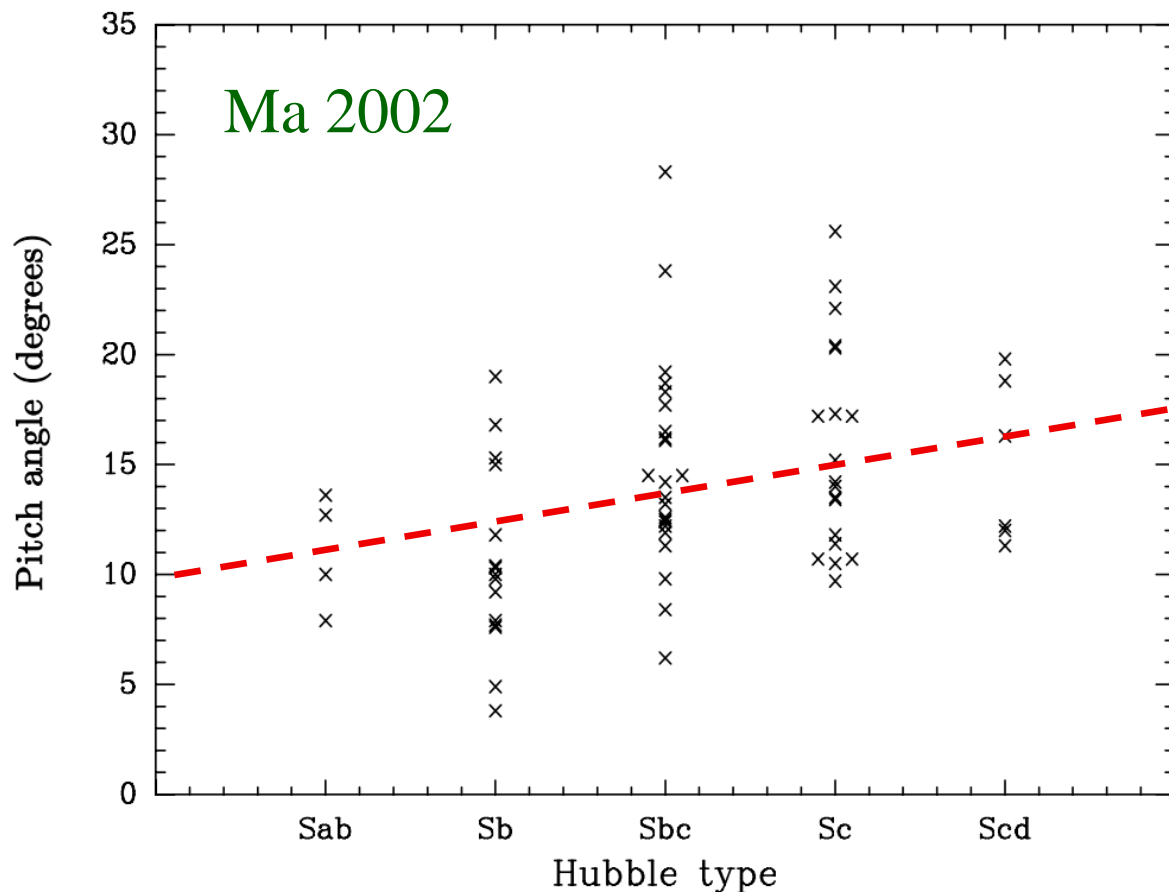


Pitch angle α is the angle between the tangent to the spiral arm and the circle $R = \text{const}$

$$0 < \alpha < 90 \text{ deg}$$

The angle is a measure of how tightly wound are the spiral arms

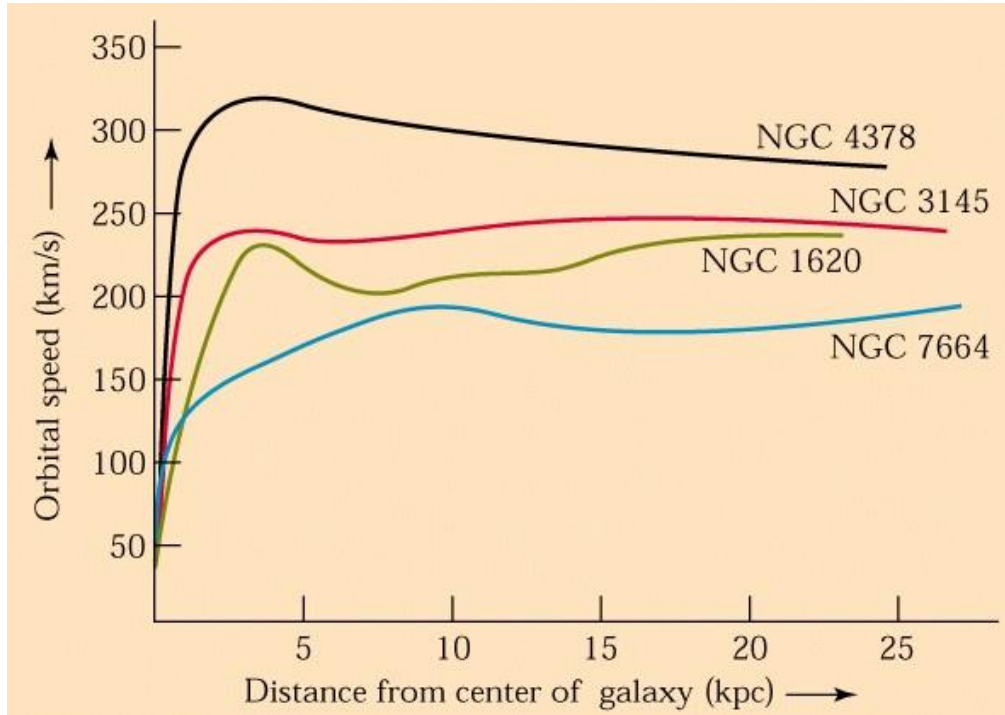
Pitch angle depends on type



The value of the pitch angle is a function of the Hubble type of the galaxy: later types have more open spiral arms

Typical values of the pitch angle are of the order of $\alpha = 10-15$ deg

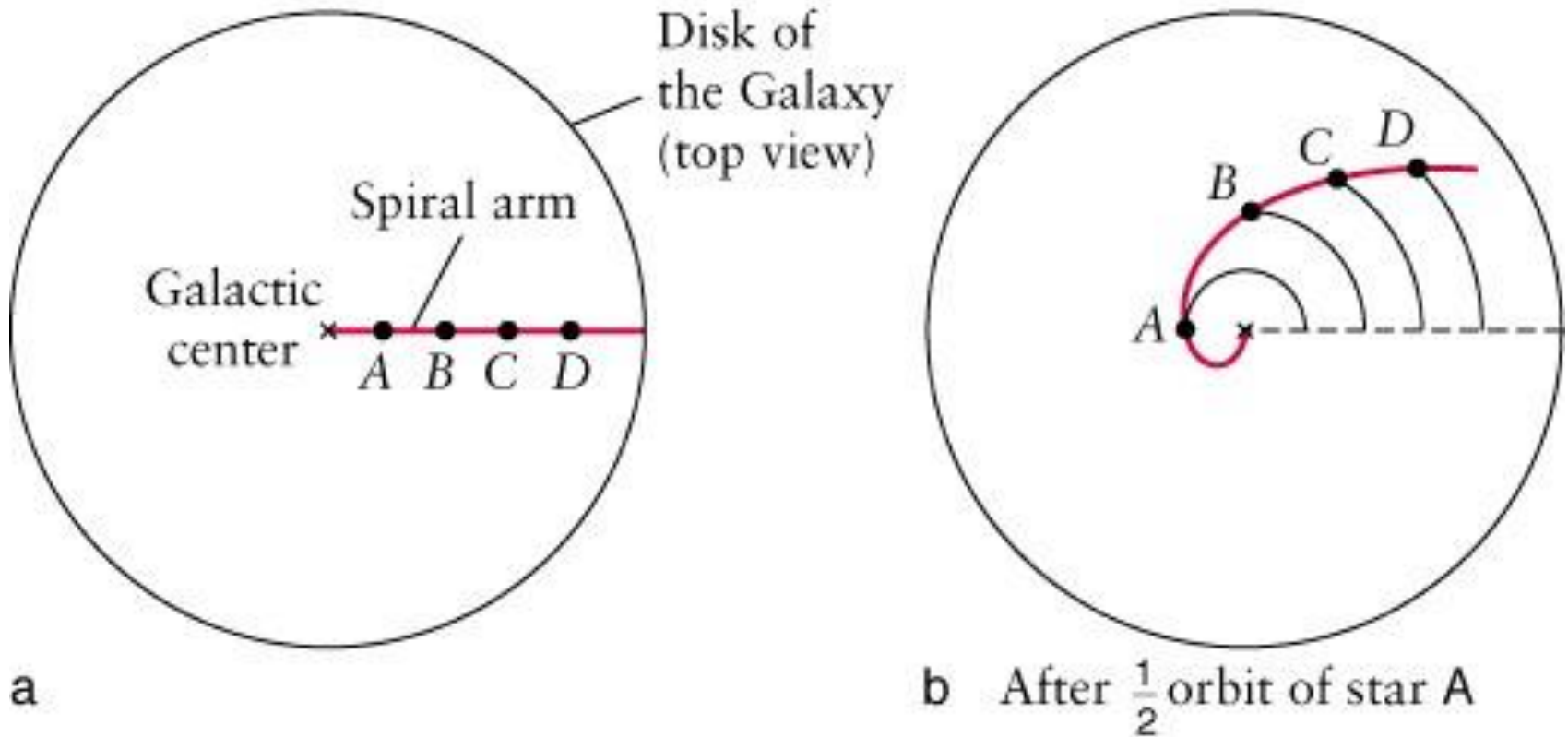
Differential rotation of the disk



In most spiral galaxies rotation curves are flat at larger distances

If the circular velocity $v_c = \text{const}$ then the circular frequency $\Omega = v_c / R$ must depend on radius. Disks with Ω dependent on R are said to show differential rotation.

The winding problem



Differential rotation of the disk causes the material arms to wind very tightly over a short time scale

Calculating the pitch angle

- The spiral arm can be described as a mathematical curve in the plane of the galaxy $\phi + g(R,t) = \text{const}$
or, for a galaxy with the m-fold symmetry
$$m \phi + f(R,t) = \text{const (modulo } 2\pi)$$
where $f = m g$ is called the shape function
- The pitch angle is given by $\cot \alpha = |R \partial\phi/\partial R|$
- For an initially radial arm with $\phi = \phi_0$, its position will evolve as $\phi = \phi_0 + \Omega(R) t$, so

$$\cot \alpha = R t |d\Omega/dR|, \quad \alpha = 0.14 \text{ deg}$$

for a galaxy with $v_c = 200$ km/s at $R = 5$ kpc after 10 Gyr (100 times too small!)

Solutions to the winding problem

- Spiral arms are quite young, after new stars form they are wound into spiral shape over a short time scale and then fade away (plausible for flocculent but not grand-design spirals)
- Spiral arms are not material features composed of the same stars but rather stationary density waves
- The spiral pattern may be temporary and result from a disturbance such as a close encounter with another galaxy (M51/NGC 5195)

The pattern speed

- The pattern speed for spirals is defined in a similar way as for bars, as the constant angular velocity of the spiral arms Ω_p
- It is not clear that the pattern speed indeed is a well-defined quantity for most spirals
- The pattern speed is difficult to measure and this has been achieved only for some spirals, e.g. for M100

$$\Omega_p = (28 \pm 5) \text{ km/s/kpc}$$



The anti-spiral theorem

Lynden-Bell & Ostriker 1967

- If spirals can be described by time-reversible Newtonian equations only and are stationary then the trailing arms should be as common as leading arms
- This is not the case which suggests that either spirals are not in steady state or are influenced by processes that are not time-reversible (e.g. gas dissipation)

Angular momentum transport

- The spiral pattern causes gravitational torques in the disk that result in the angular momentum transfer outside the disk
- Due to this phenomenon the angular momentum distribution in the disk changes significantly over the time scale of 1 Gyr
- This means that grand-design spirals probably do not survive for a longer period
- This is an example of **secular evolution** of galaxies, slow changes due to internal dynamical processes

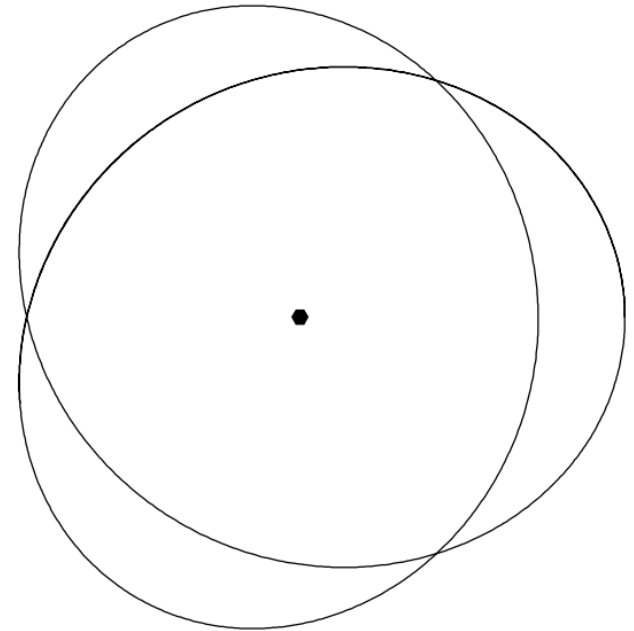
Orbits of stars

- If we view an orbit from a frame rotating at a constant angular speed Ω_p the azimuthal angle $\phi_p = \phi - \Omega_p t$, and the angle covered during the radial period

$$\Delta\phi_p = \Delta\phi - \Omega_p T_r$$

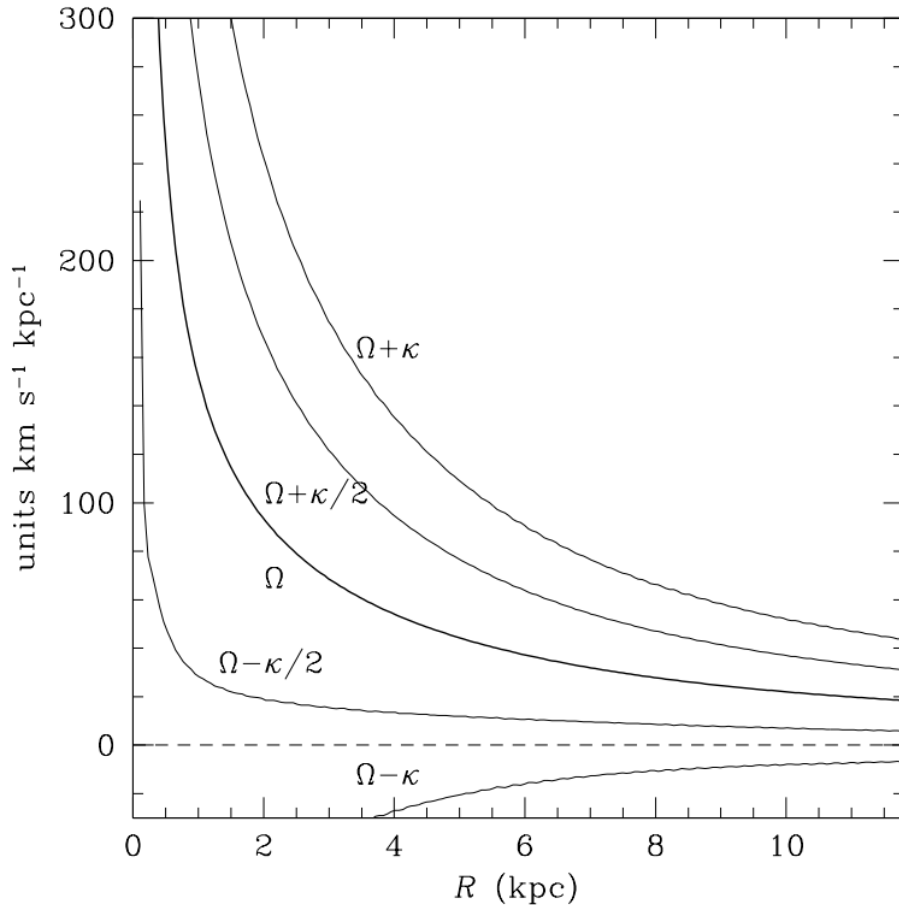
- The orbit is closed when $\Delta\phi_p = 2\pi n/m$ where n, m are integers
- For nearly circular orbits $\kappa = 2\pi/T_r$ and $\Omega = \Delta\phi/T_r$ so

$$\Omega_p = \Omega - n \kappa/m$$

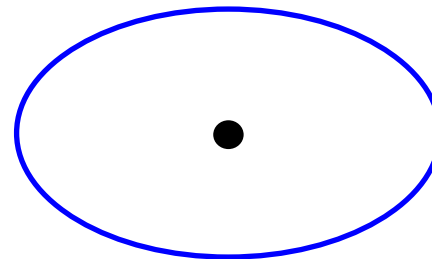


An orbit with $n=2$, $m=3$
The orbit closes after 3 radial oscillations and 2 azimuthal periods

Elliptical orbits

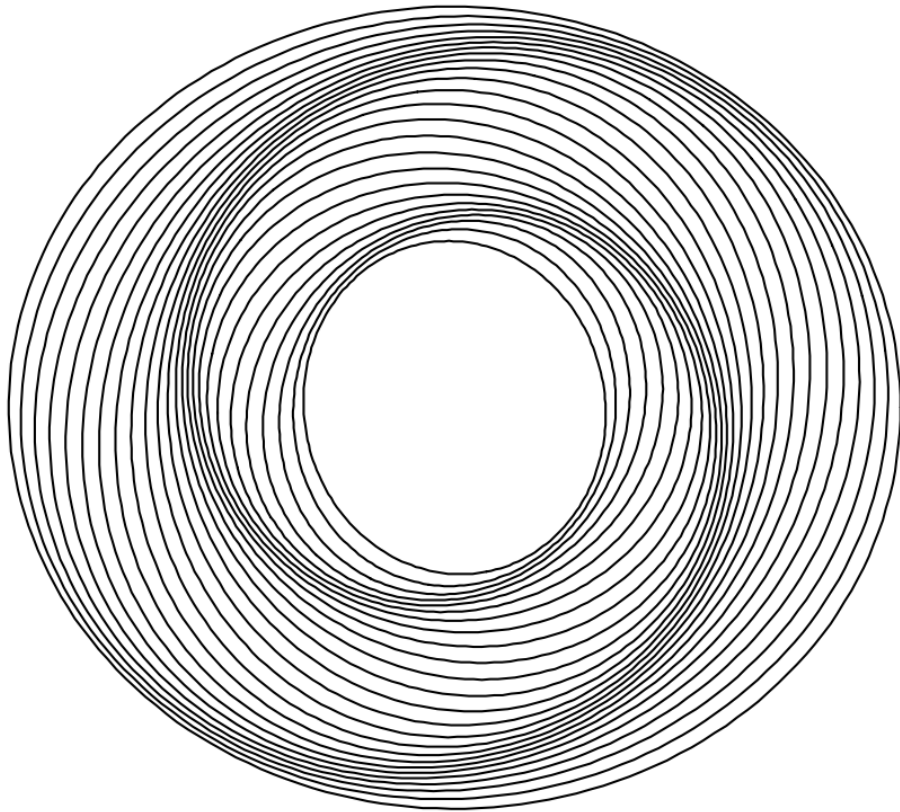


- The remarkable feature of the MW-like potentials is that only $\Omega - \kappa/2$ is approximately constant with radius
- Orbits with constant $\Omega_p = \Omega - \kappa/2$ would be closed at all radii



An orbit with $n=1, m=2$

Creating a spiral pattern



- By rotating the axes of the ellipses we can create spiral density waves
- This naturally explains the preference for two-armed spirals in nature

Winding the density wave

- Let the angle $\phi_p (R, t)$ mark the major axis of the pattern in the frame rotating at the pattern speed
- At the beginning all the major axes are aligned
 $\phi_p (R, 0) = \phi_0$
- The pattern will drift at a rate

$$\partial\phi_p/\partial t = \Omega - \kappa/2 - \Omega_p \quad \text{which gives}$$

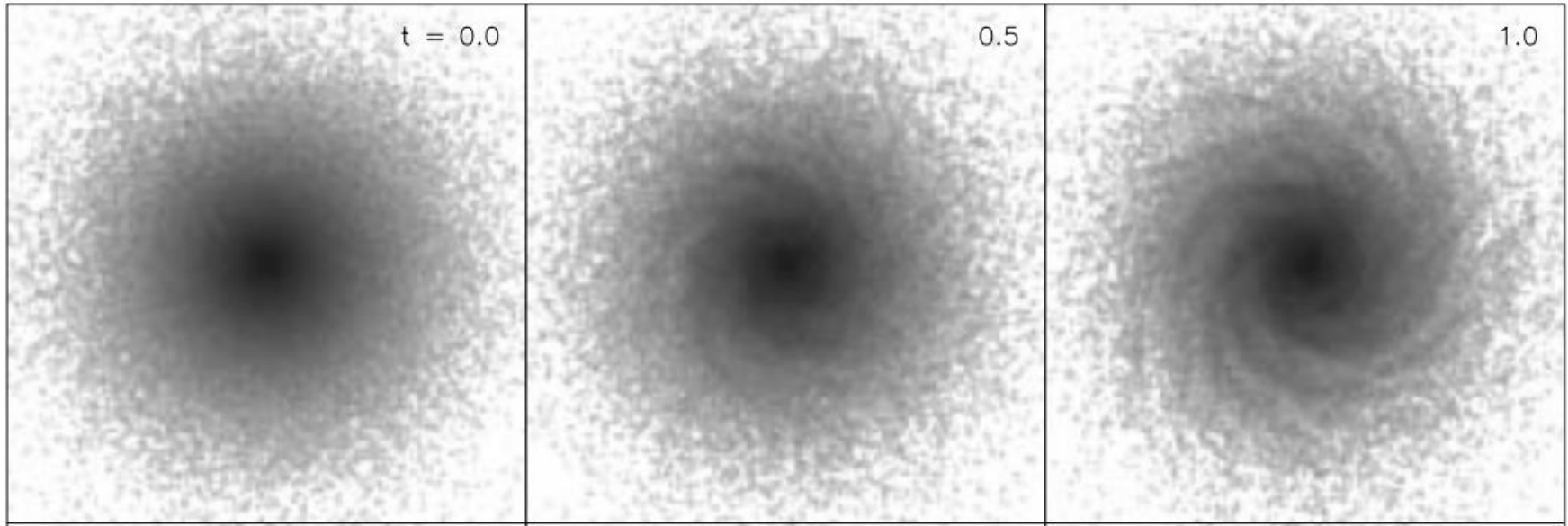
$$\phi_p(R, t) = \phi_0 + [\Omega(R) - \kappa(R)/2 - \Omega_p] t$$

- The pitch angle is then

$$\cot \alpha = |R \partial\phi_p/\partial R| = R t |d(\Omega - \kappa/2)/dR|, \quad \alpha = 0.8 \text{ deg}$$

for the MW at $R = 5-10$ kpc after 10 Gyr

Simulations of spirals



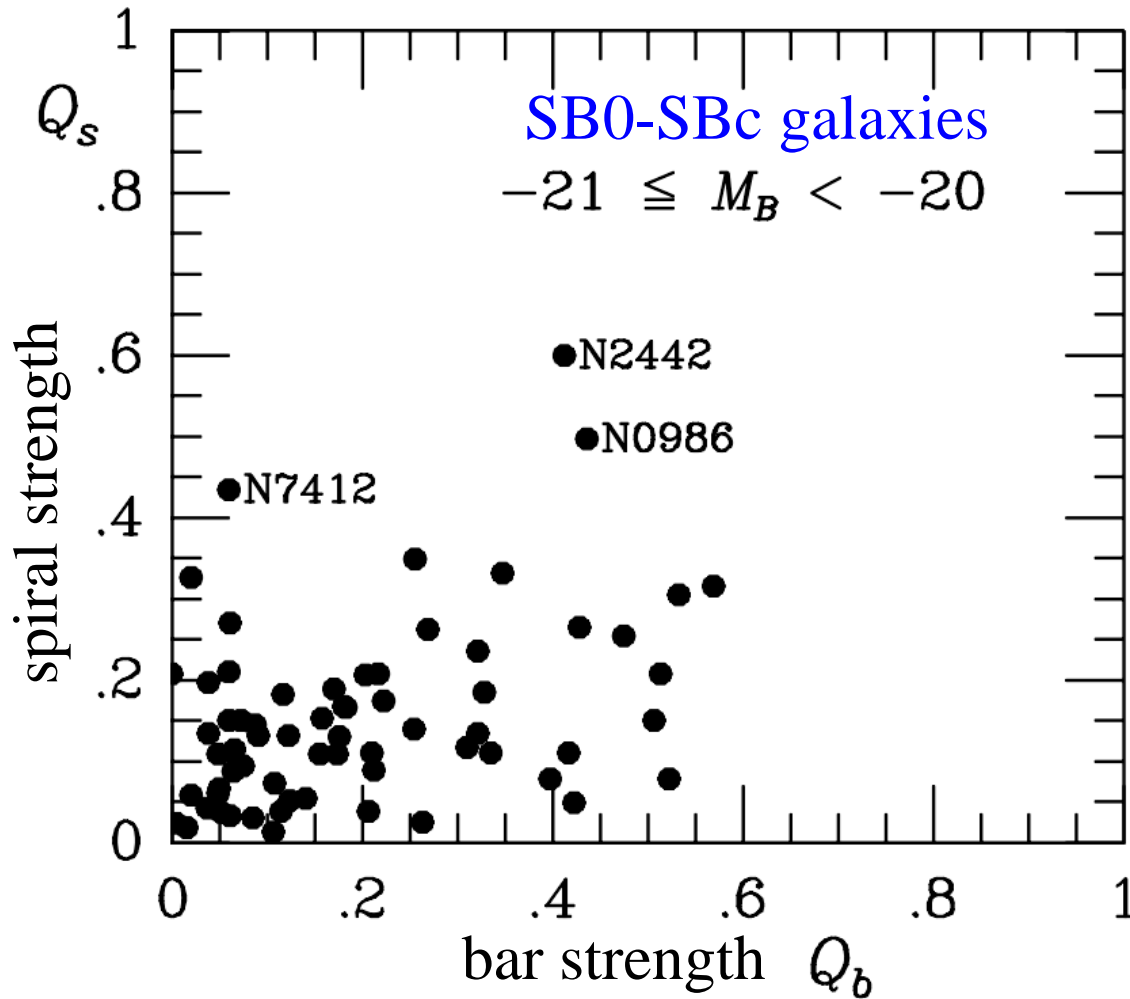
- N-body simulations of disk galaxies evolving in isolation fail to produce long-lasting grand-design spirals
- Spiral arms formed by amplification of initial fluctuations are multiple and transient

The bar/spiral connection

- The fraction of grand-design spirals is larger among barred than unbarred galaxies
- However, the pattern speed of the spiral structure is usually much lower than the pattern speed of the bar
- The two phenomena are probably related but the spiral arms cannot be directly driven by the bar



Bar-spiral correlation



There is very weak correlation between the strength of the bar and the strength of the spiral

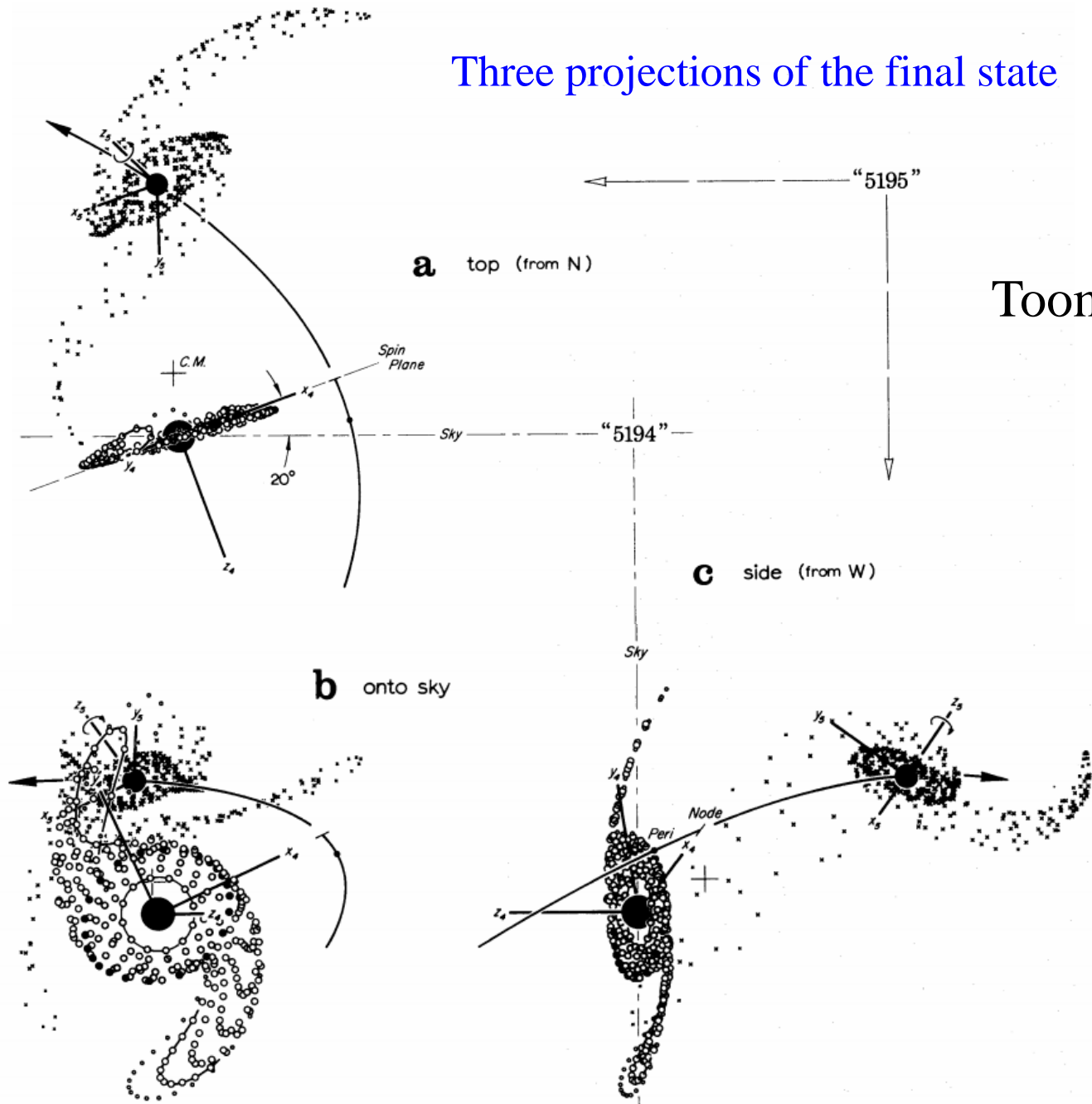
Formation of spiral structure

- Star formation causes irregularities in the distribution of stars that can be sheared by differential rotation into short spiral arm – this is the way to produce flocculent spirals
- Grand-design spirals with long arms extending over the whole galaxy are most probably produced by other mechanisms, e.g. by interactions with neighbouring galaxies
- The cases of best-studied spirals M51 and M81 support this hypothesis

Three projections of the final state

M51

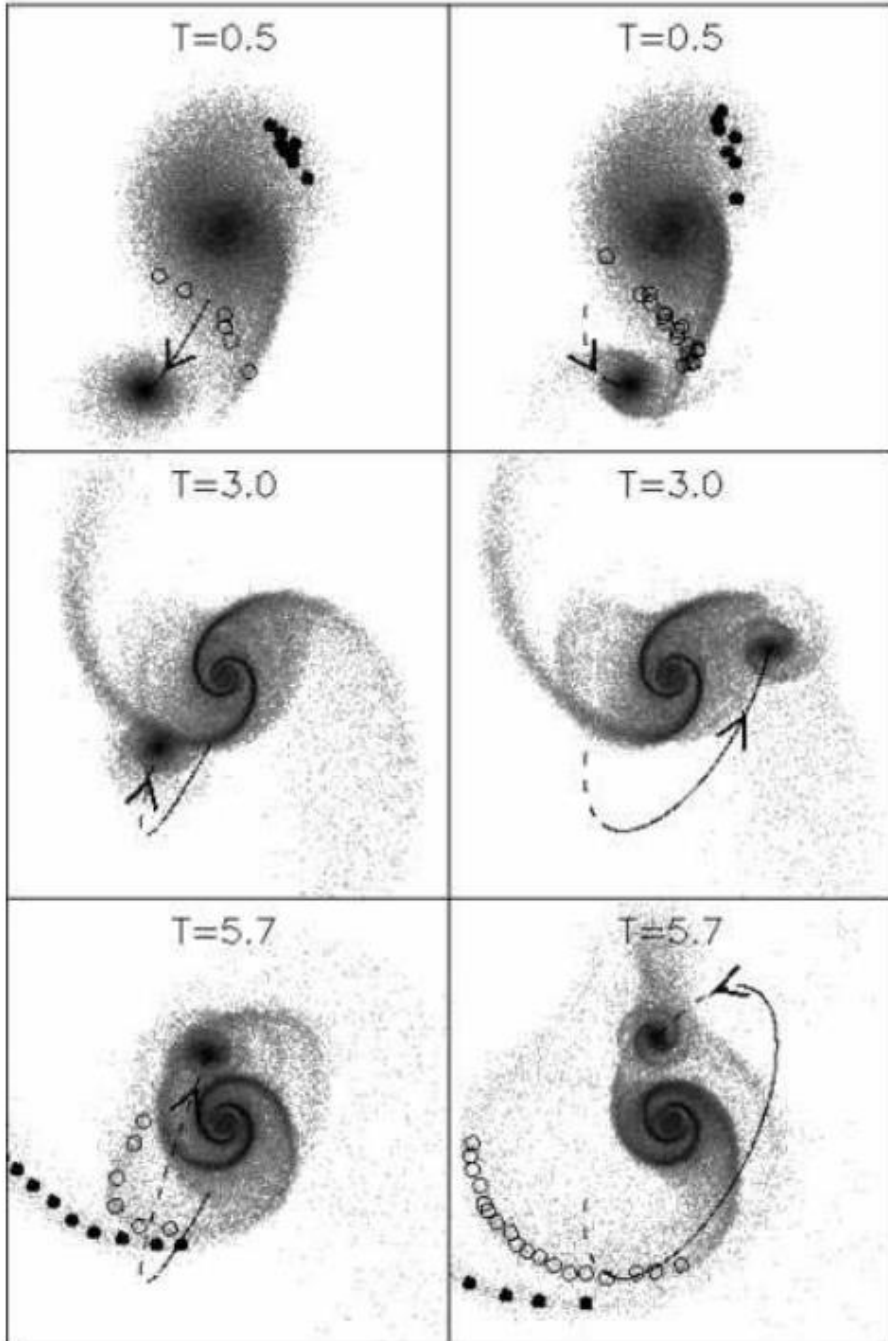
Toomre & Toomre 1972



(a) SINGLE PASSAGE

MULTIPLE PASSAGE

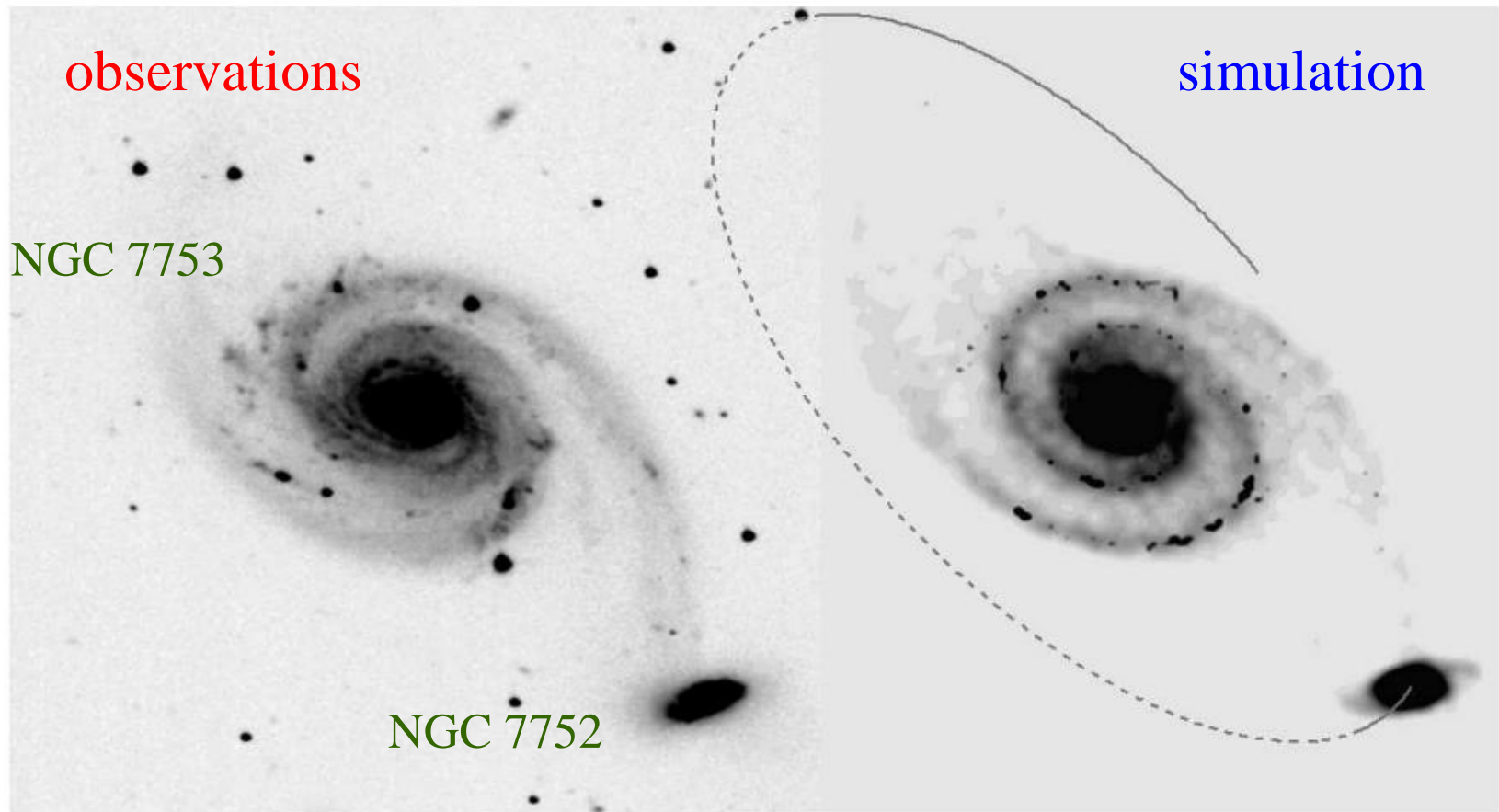
M51



- The spiral structure of M51 could be formed by a single or multiple passage of the companion
- Any preexisting spiral structure is erased
- A bar forms in the companion!

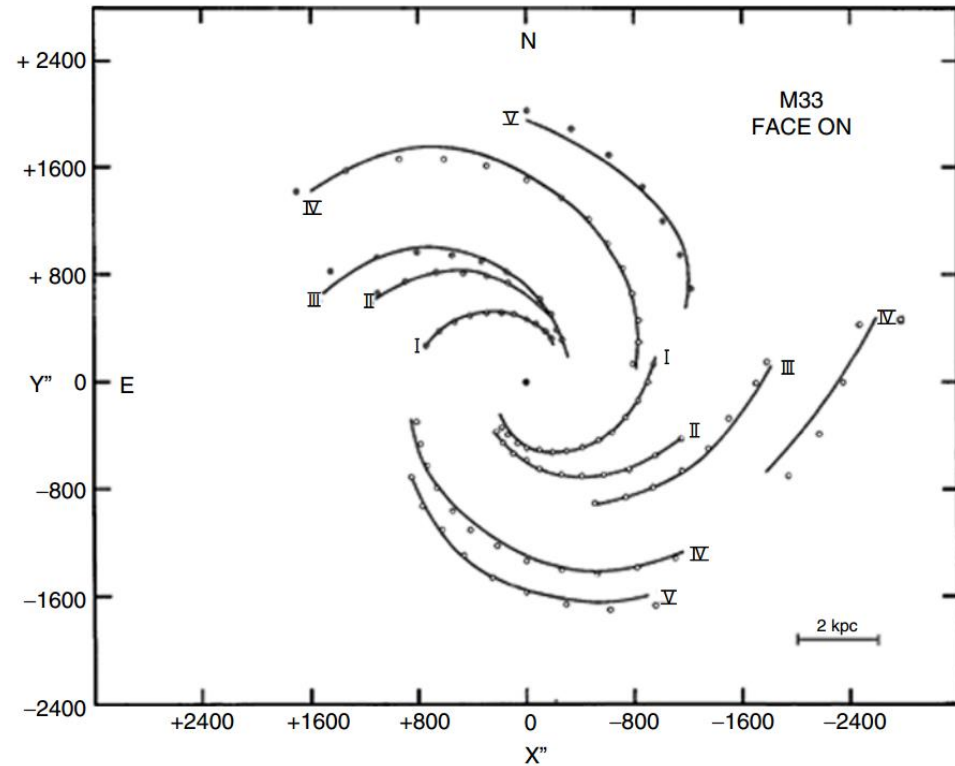
Salo & Laurikainen 2000

NGC 7753/7752



Spiral arms induced by interaction with a small companion

Spiral arms of M33

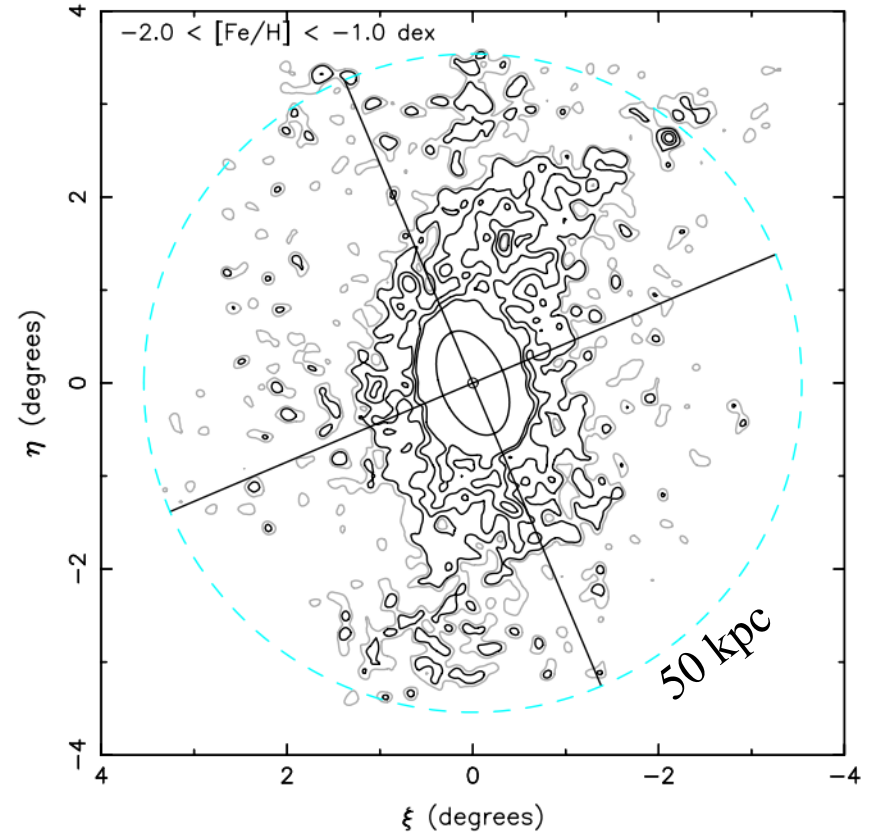
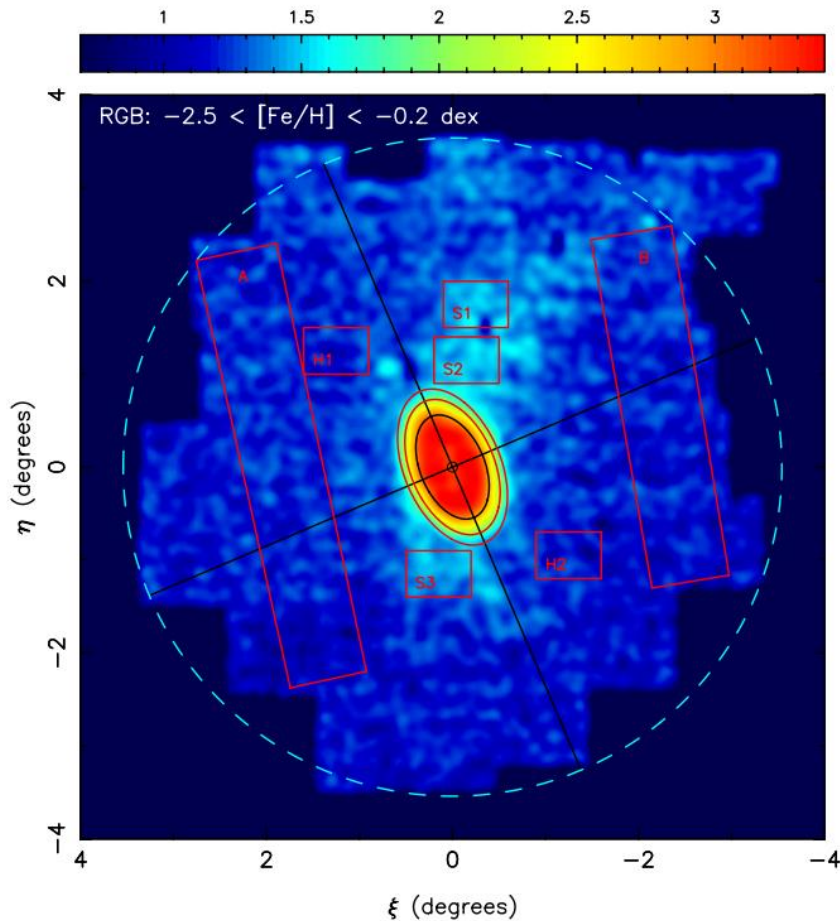


M33 has ten identified spiral arms, five on each side

Humphreys and Sandage (1980)

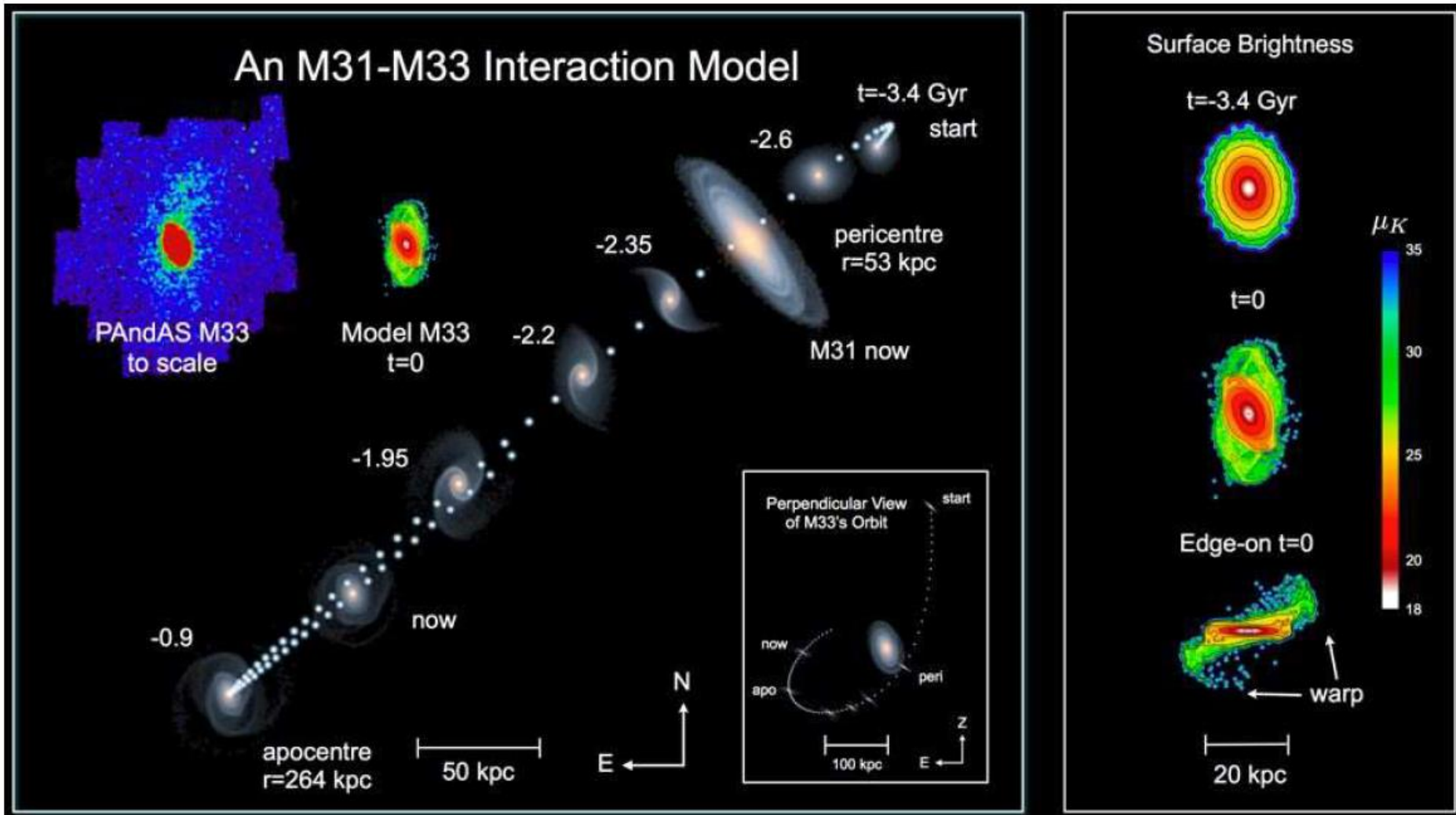
Outer structure in M33

McConnachie et al. 2010

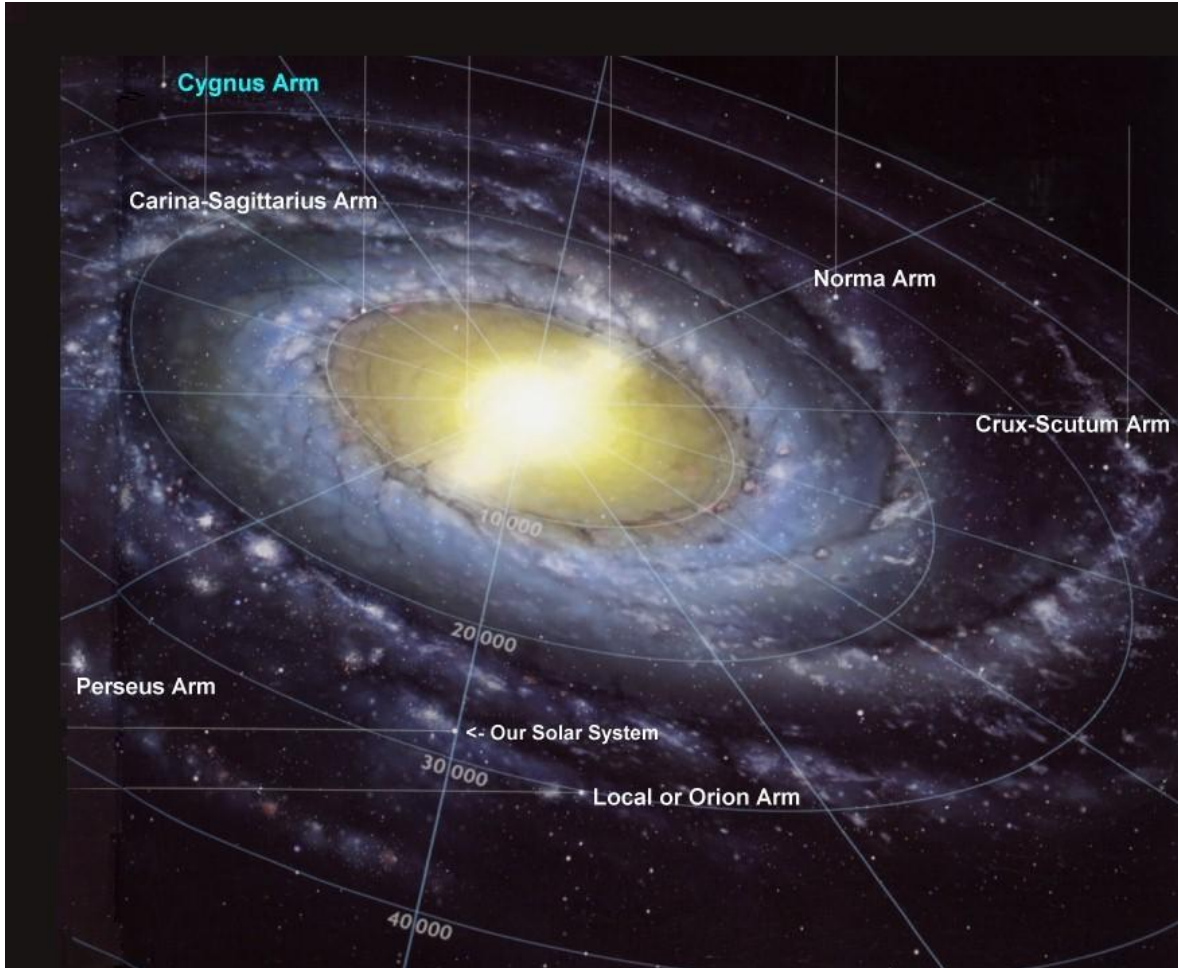


M33 has a vast S-shaped stellar substructure in the outskirts, out to 50 kpc in radius

Interaction M31-M33



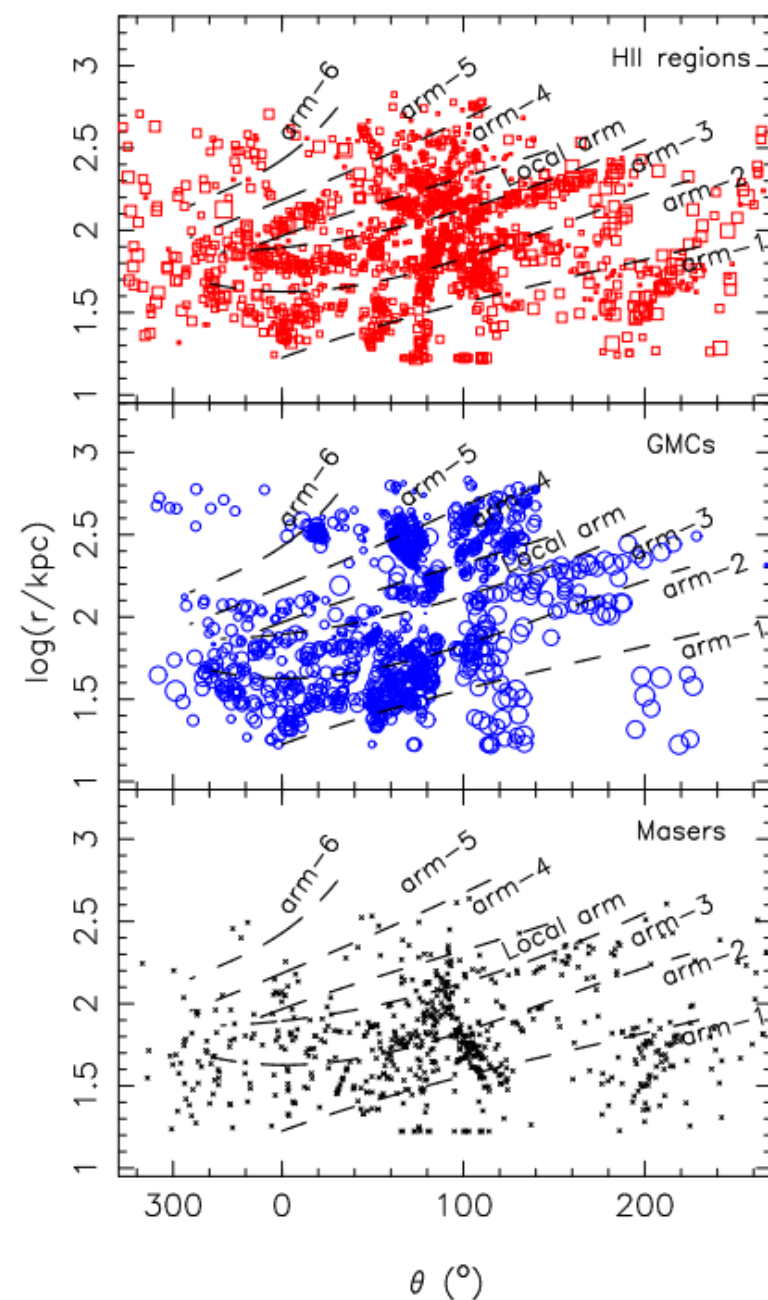
Spiral arms of the MW



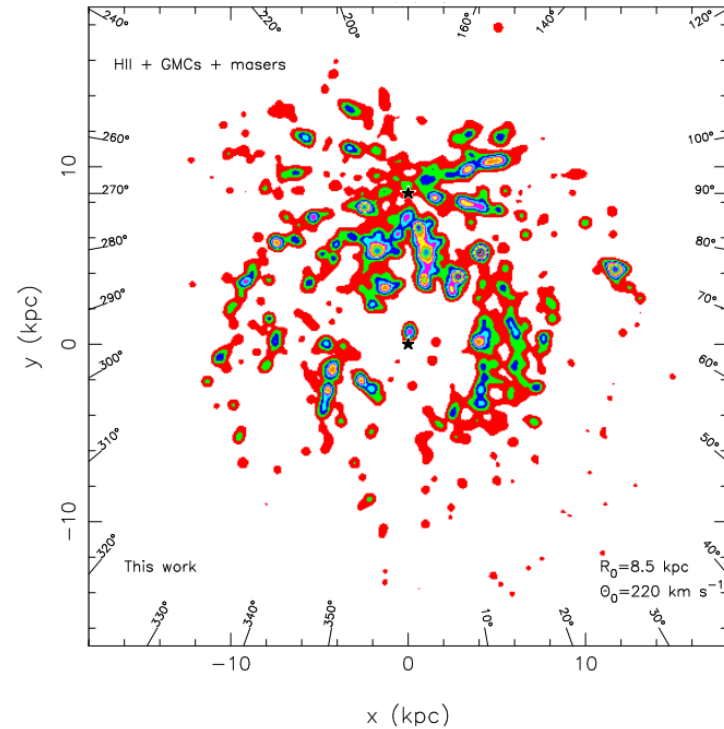
Milky Way has a number of well defined spiral arms

However, its spiral structure is not yet well determined

Mapping the arms



Hou & Han 2014



The spiral arms of the MW were mapped using distances to more than 2500 known HII regions, 1300 giant molecular clouds and 900 6.7 GHz methanol masers

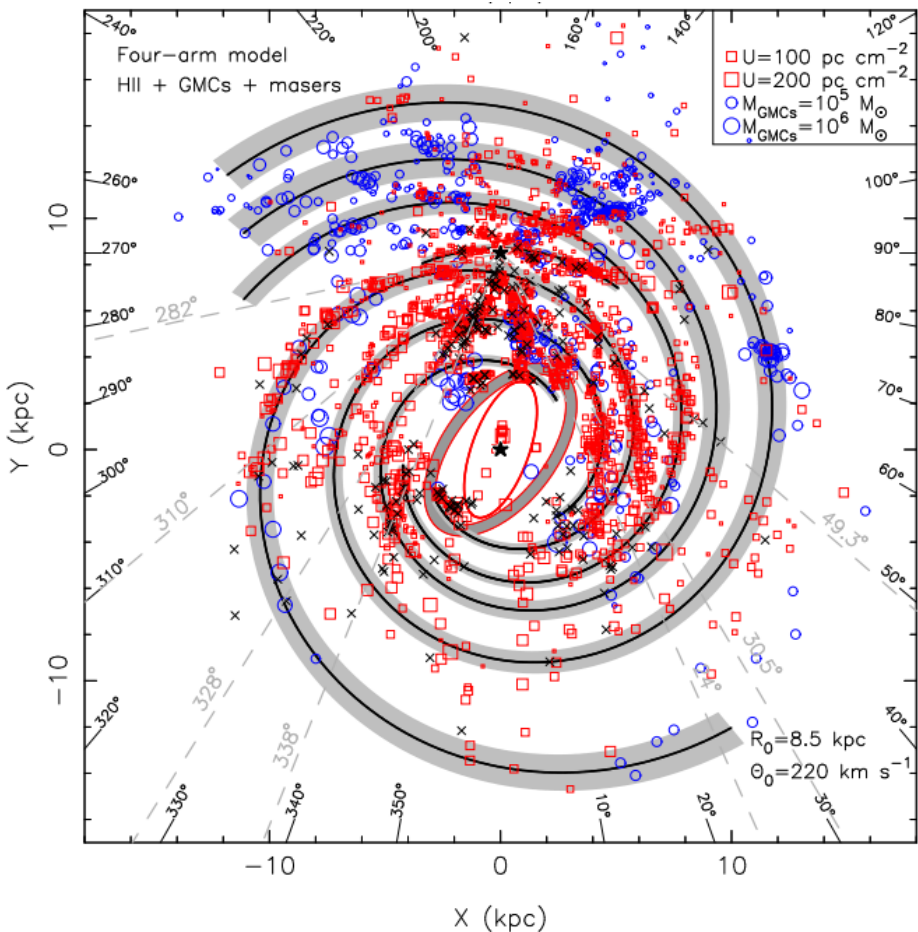
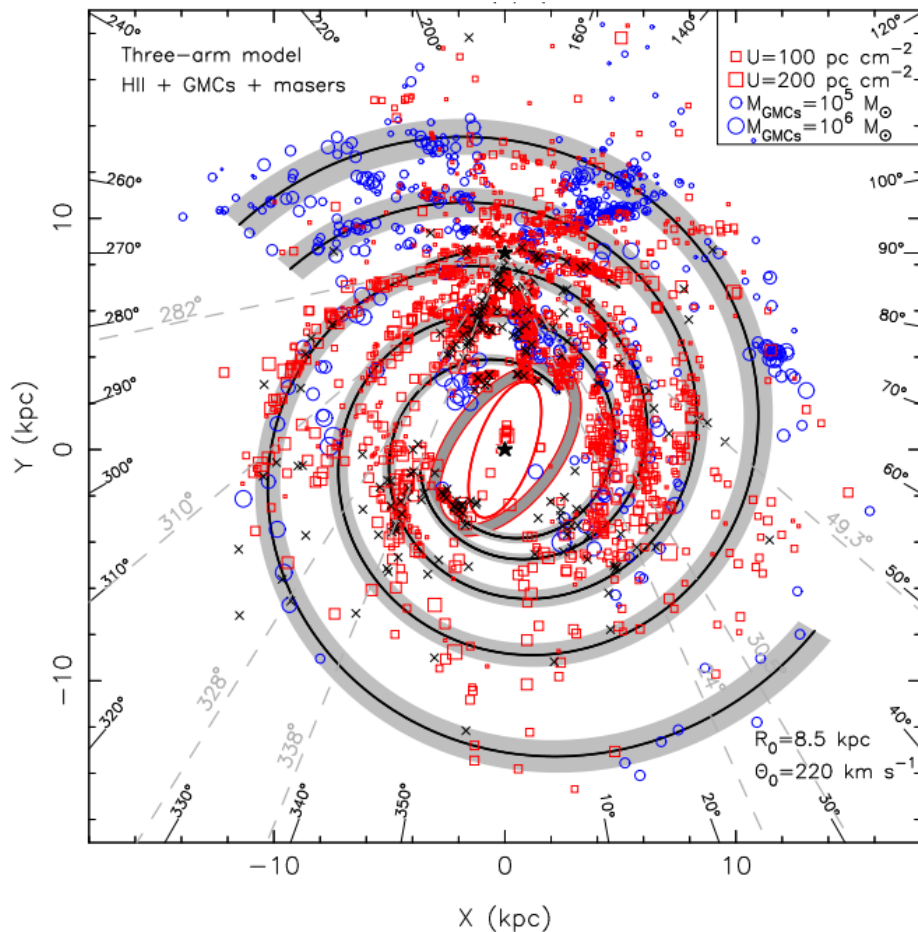
Model for MW spiral arms

- For the Milky Way, the two-arm logarithmic spirals can fit only stellar distribution
- Reproducing the distribution of star forming regions/GMCs requires more arms
- The arms can be described by a logarithmic spiral

$$\ln R/R_i = (\phi - \phi_i) \tan \alpha_i$$

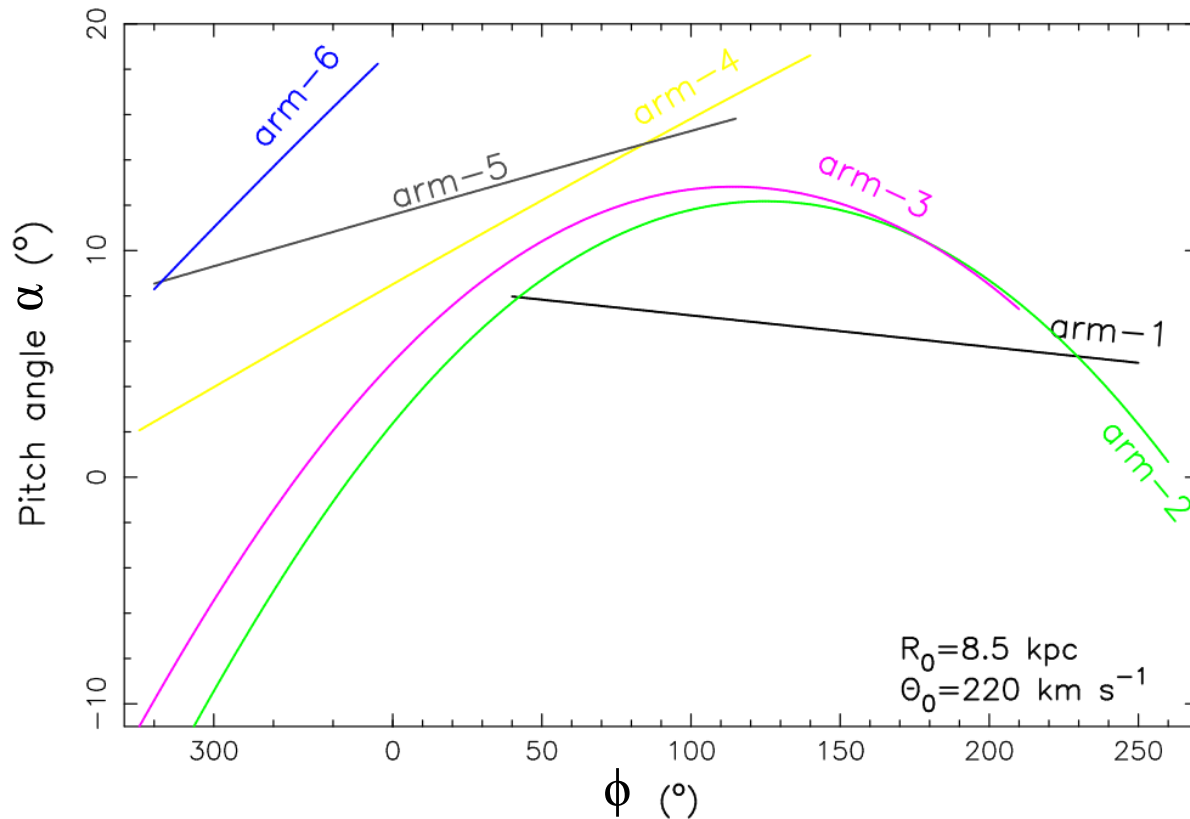
where R_i and ϕ_i are the initial values for the i th arm and α_i is the pitch angle for this arm

Models with 3 and 4 arms



The models of three- and four-arm spirals can fit data equally well

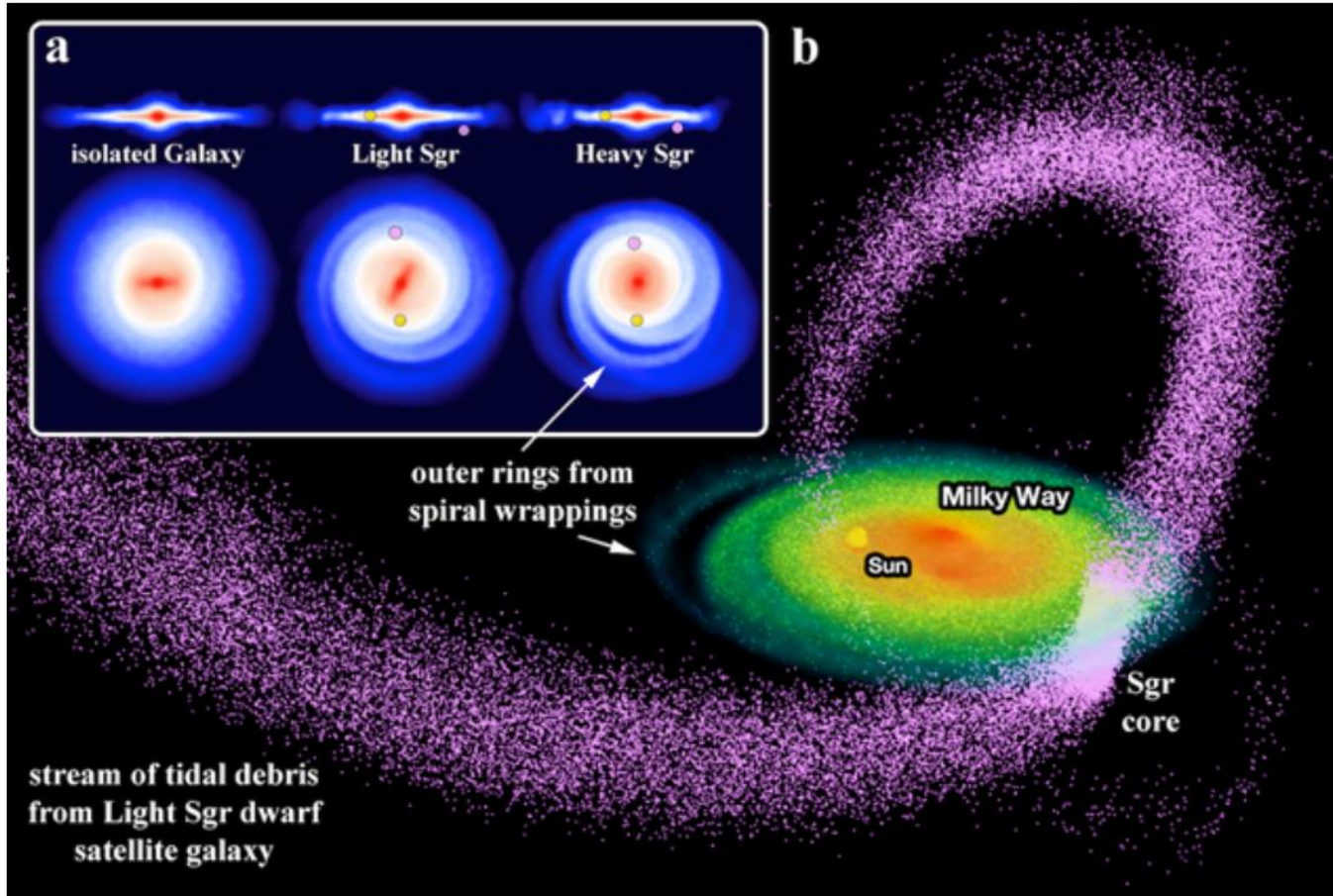
Pitch angle variation



In a more general polynomial-logarithmic spiral arm model the pitch angle can vary:

$$\ln R = a_i + b_i \phi + c_i \phi^2 + d_i \phi^3$$

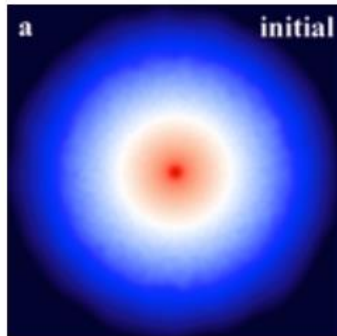
Tidally induced MW spiral arms



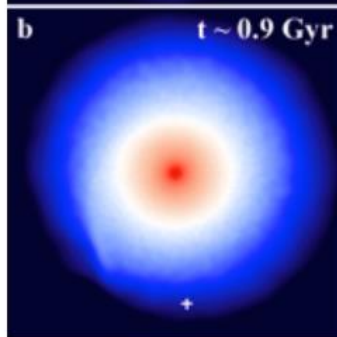
The spiral arms of the Milky Way could have been formed by interaction with Sagittarius

Tidally induced MW spiral arms

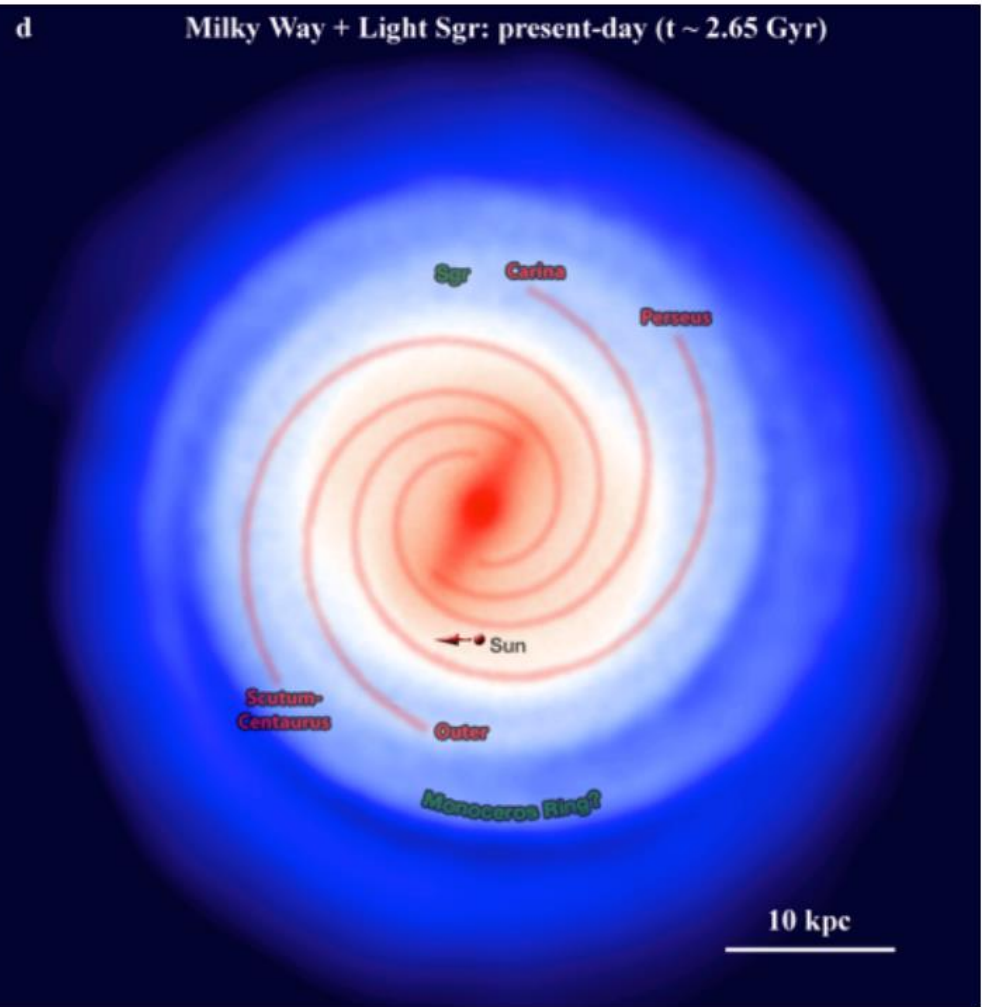
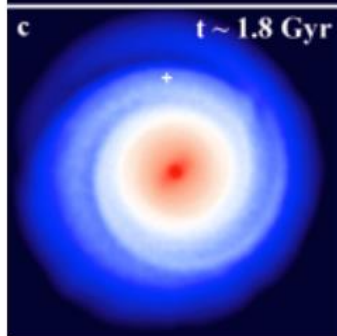
initial



first pericenter



second pericenter



Purcell et al. 2011